ABSTRACT

MICHEL, JOSHUA KLAUS. Identification, Characterization, and Physiologic Analysis of Proteolytic Enzymes in Hyperthermophilic Organisms. (Under the direction of Robert M. Kelly Ph.D.)

Capable of growth at or above 80°C, hyperthermophilic organisms encode a myriad of proteolytic enzymes, including a number of homo- and hetero-multimeric complexes. These large hyperthermophilic proteases are often comprised of fewer distinct subunits compared to the less thermophilic bacterial and archaeal homologs; thus they provide an attractive model system for study. Whole genome transcriptional response analysis was used to survey both previously characterized and putative proteases in the hyperthermophilic archaea *Pyrococcus furiosus* and *Sulfolobus solfataricus* and hyperthermophilic bacterium *Thermotoga maritima*. The proteolytic transcriptional response of these three organisms demonstrated a complex synergistic relationship between the ATP-dependent proteases (responsible for initial degradation of proteins) and the ATP-independent proteases that liberate free amino acids from smaller peptides. Additionally, all three proteolytic systems showed up-regulation of protease genes involved in the degradation of misfolded and regulatory proteins during cellular stress response to changes in environmental pH and temperature. To a lesser extent, the ATP-dependent proteases (e.g. Clp) were also involved in the response of *T. maritima* to increased levels of extracellular acetate; this was accompanied by decreased transcription of metabolic genes and entry into stationary-phase.

Thermal stress conditions also affected expression and multi-subunit composition in the *P. furiosus* proteosome, yielding a more thermostable complex. The *P. furiosus* genome encodes three proteasome component proteins: one α (PF1571) and two β

proteins (β1-PF1404; β2-PF0159), as well as an ATPase (PF0115), referred to as Proteasome-Activating Nucleosidase (PAN). Proteosome assembly and characteristics were found to be highly dependent on the environmental growth conditions. Increased growth temperature (shift from 90 to 105°C) resulted in a 2-fold up-regulation of β_1 mRNA within five minutes, suggesting a specific role during thermal stress. Consistent with this data, two-dimensional SDS PAGE revealed that incorporation of the β_1 protein relative to β_2 into the 20S proteasome (or core particle, CP) increased with increasing temperature for both native and recombinant versions. The recombinant form of PFα+PFβ_1+PFβ_2 CP assembled at 105°C was found to be more thermostable and have different catalytic rates and substrate specificities, when compared with a recombinant form of PFα+PFβ_1+PFβ_2 assembled at 90°C or the PFα+PFβ_2 version assembled at either 90°C or 105°C. These results indicate that the β_1 subunit in the *P. furiosus* 20S proteasome plays a thermostabilizing role in archaeal proteasome function during thermal stress when polypeptide turnover is essential to cell survival.

In contrast to *P. furiosus*, the hyperthermophilic archaeon *Archaeoglobus fulgidus* produces a 20S proteasome comprised of two distinct subunits, α (AF0490) and β (AF0481). Combination of *A. fulgidus* α and *P. furiosus* β_1 and/or β_2 yielded hybrid proteasome CPs that display characteristics different then the wild-type enzymes. Notably, *A. fulgidus* α was found to preferentially assemble with *P. furiosus* β_1, even in the presence of AFβ. The *A. fulgidus* recombinant proteasome exhibited comparable biochemical properties to the *P. furiosus* complex (α+β_2 or α+β_1+β_2), albeit with a reduced optimal temperature. However, the recombinant *A. fulgidus* 20S proteasome and hybrid CPs were not substrate-inhibited as was the case for the recombinant *P. furiosus*

20S proteasome. Taken together, these results demonstrate that proteasomes can be constructed with subunits from different hyperthermophiles, and that subunit composition influences biochemical and biophysical properties. The fact that hybrid inter-generic versions can be created *in vitro* also suggests that CPs in particular archaea may have arisen from common sources. Furthermore, the ability to interchange subunits and alter composition of the proteasome suggests that this system may provide a useful platform for designing proteases with unique activities or specific biophysical properties required for any biotechnological application.

Identification, Characterization, and Physiologic Analysis of Proteolytic Enzymes in Hyperthermophilic Organisms

by
Joshua K. Michel

A dissertation submitted to the Graduate Faculty of
North Carolina State University
In partial fulfillment of the
Requirement for the Degree of
Doctor of Philosophy

Chemical Engineering

Raleigh, North Carolina

2007

APPROVED BY:

_____	_____
Jason Haugh Ph.D	Todd R. Klaenhammer Ph.D.
_____	_____
David F. Ollis Ph.D.	Robert M. Kelly Ph.D. Chair of Advisory Committee

DEDICATION

This work is dedicated to:

Keith, Peggy & Nikki Michel

And

Klaus & Jeannine Kleeberg

BIOGRAPHY

Joshua K. Michel was born in San Francisco on February 26, 1977 and grew up on the east bay island of Alameda, California. After graduating from Bishop O'Dowd High School in Oakland, he attended the University of California at Davis where he majored in Biochemical and Chemical Engineering with a minor in English. While a student at U.C. Davis he worked as an undergraduate research assistant in both the Department of Anesthesiology and Department of Viticulture and Enology, which inspired him to pursue his graduate degree at North Carolina State University.

ACHKNOWLEDGEMENTS

I would first like to thank my advisor Robert M. Kelly for his support, ideas and guidance along the winding road of graduate research. Additionally, the entire faculty and staff of the Chemical and Biomolecular Engineering Department at North Carolina State University who show tremendous support and encouragement for the graduate students in their program. In particular I would like to thank the staff members Sandra Bailey and Kit Yeung for always being able to fix any problem that arises. I believe the chemical engineering graduate students at N.C. State rival any school, but I would like to single out those that spent their first year as graduate students in room 23 of the Riddick Engineering Building (they know who they are). I would like to express my sincere thanks to Don Ward, Keith Shockley, Dave Sehgal, Lara Madding, and Marybeth Pysz who welcomed me to their group and aided the start of my research, as well as the duo of Jason Nichols and Amy Vanfossen who helped me complete my thesis work. Finally I would like to Don Comfort, Matt Johnson, Brian Prevo, Sabrina Tachdjian, and Chung Jung (Hank) Chou for their help and advice as all of us worked our way through graduate school.

TABLE OF CONTENTS

LIST OF FIGURES

The Hyperthermophilic Proteolytic Machines: A Review of Large Multimeric Protease Function, Cellular Role, and transcriptional Response

The Archaeal 20S Proteasome. A Thermostable Model System for the Core Particle (CP)

Role of β1 subunit in the function and stability of the 20S proteasome in hyperthermophilic archaeon *Pyrococcus furiosus*

Intergenus compatibility of 20S proteasome alpha and beta subunits in hyperthermophilic archaea

Transcriptional analysis of the hyperthermophilic bacteria *Thermotoga maritima* in response to extracellular acetate and increased media acidity

LIST OF TABLES

The Hyperthermophilic Proteolytic Machines: A Review of Large Multimeric Protease Function, Cellular Role, and Transcriptional Response

The Archaeal 20S Proteasome. A Thermostable Model System for the Core Particle (CP)

Role of β1 subunit in the function and stability of the 20S proteasome in hyperthermophilic archaeon *Pyrococcus furiosus*

Intergenus compatibility of 20S proteasome alpha and beta subunits in hyperthermophilic archaea

Transcriptional analysis of the hyperthermophilic bacteria *Thermotoga maritima* in response to extracellular acetate and increased media acidity

Chapter 1

Proteolytic Machines in Hyperthermophiles:

A Review of Large Multimeric Protease Function, Cellular Role, and Transcriptional Response

Joshua K. Michel and Robert M. Kelly

Introduction

Proteases play a critical role in cell growth and survival in eukaryotes and bacteria. This is also true for hyperthermophiles. Integrated into the metabolic system, these enzymes are responsible for hydrolysis of internal and external peptides ultimately used as carbon and energy sources (1). Proteolytic enzymes also recognize and degrade intracellular proteins targeted for general turnover or those misfolded due to environmental stress (36). Additionally, proteases with tailored specificities are also involved in the breakdown of regulatory proteins and inhibitors in response to external factors, allowing for rapid adaptation to environmental alterations (111). Proteolytic structures cover a wide range of configurations, ranging from simple monomeric hydrolases to multi-subunit enzymes capable of forming complex quaternary structures with molecular masses in the range of 14 MDa (61). Through analysis of genome sequences, proteolytic inventories of a number of model hyperthermophilic organisms were previously examined (181), revealing among other things the prevalence of large multimeric proteases involved in a wide range of cellular functions (61); brief reviews of some of them are provided below. Also, we sought to reconcile what is known about the biochemical and biophysical properties of these proteases with transcriptomes from 130 growth conditions for the hyperthermophiles *Pyrococcus furiosus* (100, 154), *Thermotoga maritima* (28, 29, 32, 34, 80, 81, 134, 135, 153), and *Sulfolobus solfataricus* (168).

The ATP-Dependent Proteases in Hyperthermophiles

The Lon Protease: The Lon protease, initially discovered in *Escherichia coli*, was the among the first ATP-dependent proteases to be characterized and subsequently has been found in all three domains of life (166). Multiple Lon homologs have been found in a number of organisms (77). The active Lon enzyme is formed by identical subunits (~70-90 kDa) that contain an amino-terminal domain (LAN), ATPase domain (Walker motif) near the N-terminus, and a C-terminally located proteolytic domain (3, 48, 121). In bacteria and eukaryotes, these cytosolic homo-oligomeric proteases take either a ring-shaped hexamer or heptamer configuration with a Ser-Lys catalytic dyad active site sequestered within the inner chamber (19, 48, 144, 163). A similar Ser-Lys active site architecture was found for the *Archaeoglobus fulgidus* Lon-B homolog (18). However, Lon homologs in other archaea, such as *Methanococcus jannaschii*, appear to contain a Asp-Lys-Ser catalytic triad (74). The LAN domain found in bacterial and mitochondrial Lon homologs may play a role in substrate recognition (45), however this domain is absent in most archaeal Lon homologs. Two exceptions to this are the LonA homologs of *Methanosarcina acetivorans* (MA1862) and *Methanosarcina mazei* (MM3118), both of which contain a LAN region. The Lon structural configuration is similar to FtsH (described below), but differs from the other two main ATP dependent proteases (Clp and Proteasome) that are formed by multiple distinct subunits containing either an ATPase or proteolytic domain (108). In *E. coli*, Lon appears to work in conjunction with the heat shock chaperone system (DnaK) to prevent aggregation of misfolded proteins (21, 98, 161). Without Lon, *E. coli* generates 3 times more aggregated proteins compared to the wild type (143); Lon is also significantly involved in the cellular SOS response (50, 55).

Furthermore, *E. coli* lacking Lon are unable to adapt rapidly to nutritional downshifts (96, 122). While essential for stress response, the primary role of Lon may be the degradation of specific regulatory proteins.

The *E. coli* Lon protease is linked to stress response, based on its degradation of negative regulatory proteins, such as SulA and RcsA, that are responsible for UV light sensitivity and capsular polysaccharide production, respectively (2, 41, 57, 115, 145). The heat shock sigma factor σ^{32} is also degraded in a concerted manner by Lon, HflB, and Clp proteases (70, 82, 160). Lon plays a significant role in aggregated protein removal, but its overproduction results in many defects, such as the activation of the YoeB toxin that induces cleavage of mRNA (31). Two homologs of Lon are found in the hyperthermophilic bacterium *T. maritima*; the LonA (TM1633) protein contains both an ATPase and proteolytic domain, whereas LonB (TM1869) only contains an active site domain (181). Dynamic heat shock experiments (10°C temperature increase) with *T. maritima* showed that both LonA and LonB homologs were slightly down-regulated throughout the entire 90 minute stress response (135). Lon in *E. coli* is heat-induced, but the Lon induction during other types of stress is not universally observed (130, 176). Typically, the *lon* gene is within the heat shock regulon and rarely controlled by other regulators (176). However, LonA in *T. maritima* demonstrated a 3.4-fold increase when grown in co-culture with *P. furiosus*; LonB (TM1869) was largely unaffected. The *T. maritima lonA* up-regulation could be attributed to higher growth rates typically noted under co-culture conditions (81). The differences in transcription between the two *T. maritima lon* orthologs suggest that these enzymes may have developed distinct specialized functions similar that those noted in other organisms (176). Generally, *T.*

maritima Lon genes appear to be constitutively transcribed as no other significant changes were apparent in the other 72 conditions shown in Figure 1. Homologous Lon proteins are found in archaeal organisms as well (111, 181), but little is known about their role within the proteolytic system when compared to the data available in Bacteria and Eucarya.

Lon from the hyperthermophilic archaeon *Thermococcus kodakaraensis* showed a general structure similar to bacterial Lon (52). The enzyme was composed of identical subunits (~70 kDa) that contained both ATPase and proteolytic domains. In contrast to the bacterial and eukaryotic Lon, there were two transmembrane regions within the ATPase domain (52). Sequence comparisons of archaeal Lon homologs indicate that this membrane attachment region is a common feature (111). The cytosolic location of Lon in bacteria may be attributed to the presence of an additional ATP-dependent protease (FtsH) that is involved in membrane maintenance (6, 76, 165). The *P. furiosus* Lon homolog (PF0467) showed a -2.9 fold change after 1 hour in response to a 15°C increase in growth temperature (154). As Figure 2 shows, *P. furiosus* Lon was consistently transcribed during all growth phases at an above average level compared to the entire gene pool. It is interesting that the *M. jannaschii lon* gene (MJ1417) (15) and the *A. fulgidus* Lon homolog (141) demonstrated no transcriptional response to heat shock. However, MJ1417 was 3.7-fold higher in response to a 20°C temperature downshift (15). The disparity in Lon transcriptional changes between *P. furiosus*, *A. fulgidus*, and *M. jannaschii* may be indicative of underlying differences in the heat shock control mechanisms. The *M. jannaschii* Lon contains 4 transmembrane regions and has been suggested to aid in the degradation of non-native membrane proteins (15). However, the

increased transcription of Lon during cold shock may be related to a substrate preference for key regulatory proteins as seen in other organisms (106, 169). Furthermore, *M. jannaschii* Lon, along with other archaeal versions, may act to degrade damaged membrane-bound proteins in a similar fashion as the bacterial protease FtsH.

FtsH (or HflB) Protease: Filamentous temperature-sensitive H, FtsH (or HflB) is an ATP-dependent, self-compartmentalized, membrane-associated proteinase that is universally conserved in bacteria and eukaryotic organelles (76, 175). This enzyme class contains a zinc metalloprotease motif (147) and leucine-zipper sequence (156) located near the C-terminus, and is anchored to the cytoplasmic membrane by two transmembrane regions found near the N-terminus (175). Products of proteolysis range from 10 to 20 amino acid residues, with a possible preference of a hydrophobic residue at the N-terminal site of cleavage (5, 155). The *E. coli* homolog of FtsH is the only ATP-dependent protease essential for cellular growth under most conditions (68, 78, 162). This may be due to its role in degrading a deacetylase enzyme (LpxC) involved in the synthesis of lipopolysaccharide (LPS), thus allowing maintenance of a correct LPS to phospholipid ratio (75). Among the hyperthermophiles, an FtsH homologue is found in only the bacteria *T. martima* and *Aquifex aeolicus* (181). Studies on mesophilic organisms (*E. coli*, *Caulobacter crescentus*, and *Lactococcus lactis*) have found that FtsH is induced during stress response (44, 47, 69, 113). Dynamic transcriptional data for *T. maritima,* subjected to a 10°C heat shock, showed that the homolog to FtsH (TM0580) is immediately induced to a small extent (1.5-fold), with a maximal induction of 2.4-fold after 20 minutes (135). In *E. coli* FtsH has been implicated in the cytoplasmic degradation of σ^{32} (69, 174), the rapidly degraded transcription factor SoxS (59), as well

as the dislocation and proteolysis of membrane-bound proteins (92). However, in the case of *T. maritima*, there is no known σ^{32} homologue encoded in the genome (33). *Bacillus subtilis* also lacks a σ^{32} homologue and, while FtsH is up-regulated during stress, it is not heat shock-responsive; the *B. subtilis* FtsH is postulated to be directly involved in cell division and sporulation (39). Analysis of growth phase-related transcriptional changes showed that TM0580 is 4.6-fold reduced during stationary phase compared with mid-log cells. Yeast, higher order plants, and cyanobacteria encode multiple FtsH homologues that have been connected to the degradation of light damaged photosystem proteins (7, 105). Thus, TM0580 may also play a cellular role related to the degradation of misfolded or damaged membrane-bound proteins during stress.

The Clp family of Proteases: The caseinolytic protease (Clp) is a large multimeric barrel-shaped protease formed by four stacked rings of 6 or 7 subunits each (86, 87, 112). Present in both eukaryotic and bacterial organisms, including the hypthermophilic bacterium *T. maritima*, Clp is notably absent from the hyperthermophilic Archaea (111, 181); another ATP-dependent protease, the proteasome (discussed below), shares similar catalytic characteristics with Clp and may act as a functional homolog. The Clp catalytic core comprised of either ClpQ (HslV) or ClpP subunits, which form hexameric or heptameric rings, respectively (90, 112, 183). The ClpP proteolytic chamber, containing two 7-member rings, has an internal diameter of approximately 50Å and is accessible on either end by ~10Å axial openings (167, 180). Located within the chamber interior are 14 serine active sites responsible for proteolysis (180). The active site of ClpQ contains an N-terminal Thr residue, similar to that found in the 20S proteasome (142, 184). Some

ClpQ homologs have a Ser residue in place of the N-terminal Thr (83, 139). Inactive paralogs of ClpP, such as ClpR, have been found in certain bacteria and plants. In cyanobacteria, this catalytically inactive subunit associates with active ClpXP enzymes, but its specific function has yet to be fully elucidated (164). In some cases, ClpR has demonstrated the ability to regulate the transcription of ClpP (177). Due to the structural similarity of Clp and the proteasome, these inactive subunits could play a structural role similar to that found for the *P. furiosus* proteasome subunit β_1 or the non-active subunits of eukaryotic proteasomes (63, 65, 109). Multiple version of ClpP (e.g., ClpP1, ClpP2, ClpP3) are encoded in the genome of the cyanobacterium *Synechococcus elongates*; these form homo-multimeric proteolytic cores (ClpP3), as well as hetero-multimeric enzymes (ClpP1 & ClpP2) (164). Clp protease complexes with as many as 10 different isoforms have been found in the chloroplasts of *Arabidopsis thaliana* (128). In this case, the composition of the proteolytic core influences which ATPase version (ClpC or ClpX) will bind to the ends of the barrel structure (164). The genome of *T. maritima* encodes both ClpP (TM0695) and ClpQ (TM0521) proteolytic cores, along with the ATP-dependent subunits ClpX (TM0146), ClpC-1 (TM0198), ClpC-2 (TM0873), ClpC-3 (TM1391), and ClpY (TM0522). A similar inventory of Clp homologs is also found in the hyperthermophilic bacterium *Aquifex aeloicus* (38). Both ClpQ and ClpP are able to degrade small unfolded peptide substrates in the absence of ATP (73, 159). However, association with their respective ATPase subunits is required for full proteolytic activity.

The ATPase portion of Clp is formed by oligomeric rings comprised of 6 or 7 subunits (e.g. ClpA, ClpX, ClpY, ClpC), which in the presence of ATP self-assemble on either end of the proteolytic core (56, 85, 131). Both ClpA and ClpX form active

enzymes with ClpP, while ClpQ preferentially associates with ClpY (93, 114, 125). Differing ATPase configurations of Clp have been linked to altered substrate preferences and biochemical activities. Substrates targeted for degradation by Clp are identified by sequence motifs at either their amino or carboxyl-terminal ends (42). Internal recognition sites have also been noted, but to a lesser extent (72). For example, ClpAP preferentially degrades RepA, but removal of the 15 N-terminal amino acid residues of RepA results in a significant decrease in proteolysis (71). In contrast, Mu vir repressor, SSrA-tagged peptides, and MuA all have C-terminal recognition sites (58, 101, 102, 160). However, a recognition site is not always required for degradation, as demonstrated by ClpAP's ability to degrade unfolded proteins without a targeting motif (152). Conversely, ClpXP is unable to degrade peptides lacking a recognition site. Alternative targeting methods also exist; the specific degradation of the competence protein ComK requires binding to an adaptor protein (MecA) that facilitates ATPase attachment and unfolding (43, 129, 148). The limiting factor for protein proteolysis of folded proteins appears to be the rate of ATPase-facilitated unfolding. Protein unfolding mediated by Clp requires a large expenditure of energy (89); degradation of a dimeric 53 residue protein was found to require 150 ATP molecules (22). The products of Clp protein hydrolysis are small peptide fragments with a mean length of 8 to 10 residues. The consistency of product size may be due to activation/inactivation of the proteolytic core by the ATPase ring, as it shuttles the substrate peptide to the catalytic sites (30).

The Clp protease is involved in a variety of cellular functions central to survival under both normal and stress conditions. The Clp enzyme appears to play a role during cellular growth transitions and is required for the retention of cell viability during

stationary phase (26). Additionally, Clp has been implicated in sporulation, motility, cellular competence, and pathogenesis (117). During dynamic heat stress, *T. maritima* showed a slight transcriptional downshift (up to 1.8-fold) for ClpC-3 and ClpY. However, there was also increased transcription of the ATPase subunits ClpC-1 (up to 3.8-fold) and to a lesser extent ClpX (up to 2.0-fold) (135). In *E. coli*, ClpXP proteomic studies found a high substrate preference for the regulator RpoS as well as for the DnaK suppressor protein (DksA) (49). Thus, the increased transcription of ClpX in *T. maritima* may be related to the degradation of certain heat shock negative regulators; the *T. maritima* chaperone DnaK showed a maximum response of a 25-fold up-regulation after heat stress (135). Increased transcription of ClpC-1 is consistent with work showing that ClpC in *Staphylococcus aureus* is essential during stress response (24-26). The gene ClpC-2 demonstrated the highest transcriptional heat response, with a 43-fold increase 5 minutes after the 10°C step increase in temperature, decreasing to 8.6 fold after 60 minutes (135). This extremely high fold change for the *T. maritima* ClpC variant is similar to the 20- to 150-fold increase found for the *Bacillus subtilis* ClpC gene (95). The proteolytic subunits ClpQ and ClpP were up to 2.0-fold down-regulated during heat shock, indicating that the increased transcription of ClpC may be related to its independent chaperone function (4, 135). While the Clp complex plays a vital cellular role, changes in transcription of Clp-related genes has only been noted under stress conditions and during growth phase transitions.

In *Streptococcus pneumoniae* all Clp genes, except *clpX*, were down-regulated during late stationary phase (126, 140). Similarly, the *Oenococcus oeni* ClpX homolog is preferentially transcribed during exponential growth as opposed to stationary phase (79).

The transcription of ClpX in exponentially growing cells may be related to its broad substrate specificity; ClpX may have developed as an evolutionary compromise that optimized proteolysis of multiple substrates as opposed to a single target substrate (46). In comparison, during late-stationary phase, *T. maritima clpP* and *clpX* were 7-fold and 18-fold down-regulated, respectively, when compared to early stationary phase. However, proteolytic subunit *clpQ* gene was not changed; *clpC-2* was only slightly affected during the same time frame (80). Thus, ClpQ and ClpC-2 appear to be the primary *T. maritima* Clp homologues required during late stationary phase. Their transcriptional levels contrast with their homologs in *B. subtilis* where reduced amounts of ClpC, responsible for negative regulation of competence by inactivation of ComK, were noted (99, 123). The narrow proteolytic specificity of Clp may be related to its involvement in cellular control mechanisms. In contrast, the proteasome (discussed below) displays much broader substrate preferences.

The Proteasome: The 20S proteasome is a cylindrically-shaped protease ubiquitous to both Archaea and Eukarya (8, 13). In bacteria, the proteasome is found only in the actinomycetes *Rhodococcus erythropolis* (172), *Myobacterium tuberculosis* (35), *Streptomyces coelicolar* (119), and *Frankia* (10). This lack of the proteasome in other bacteria suggests that actinomycetes acquired this protease through lateral gene transfer (108); other bacteria contain a structurally related complex ClpQY (or HslVU) that shares a similar catalytic mechanism to the proteasome (14).

The proteasome from *Thermoplasma acidophilum* provided the original structure for this macromolecular complex, which subsequently has been found to be highly

conserved (8, 36, 60, 64, 107, 133). The 20S proteasome, or catalytic particle (CP), is composed of four stacked heptametrical rings that form a barrel-like structure with a hollow channel extending down the center (137). Each homomeric ring is composed entirely of either α or ß subunits, arranged in the order $\alpha_7\beta_7\beta_7\alpha_7$. To prevent undesirable protein degradation, all proteolytic activity is confined to the interior channel; the proteolytic active sites, typically an N-terminal Threonine, are located on the ß subunits (63, 67). As an additional safeguard to unwanted proteolysis, the ß proteins are expressed as precursors, which undergo self-processing (removal of ~10 N-terminal amino acid residues to expose the active Thr during assembly into the active proteasome structure (27, 62, 110, 151). The assembly of the proteasome is a complex process in which the α proteins self assemble into rings that act as scaffolds for the subsequent ß ring formation, resulting in a approximately 300 kDa half-proteasome. During the assembly of half-proteasomes into the final active 20S proteasome, the ß precursors are cleaved to expose the active site (120). While capable of degrading unfolded proteins into short 8-12 residue peptides, association with the proteasome activating nucleosidase (PAN) allows for the ATP-mediated degradation of folded proteins (138).

NOTE: *A detailed examination of hyperthermophilic proteasomes during stress and their potential use as model systems for studying eukaryotic proteasomes can be found in Chapter 2 entitled: "The Archaeal 20S Proteasome: A Thermostable Model System for the Core Particle (CP)."*)

ATP-Independent Proteases

Most heterotrophic hyperthermophiles can grow on proteinaceous substrates as primary carbon and energy sources. The hyperthermophilic archaea *Thermococcus celer*, *Pyrococcus woesei*, *Pyrococcus glycovorans*, and *P. furiosus* all exhibit the ability utilize peptides as a primary metabolites using a fermentation-based pathway (1, 9, 11). The

protein substrates must first be broken down by extracellular proteases, which may not be cell-associated (23, 157). The products of extracellular hydrolysis are transported into the cell, presumably by ABC-type transporters, where they are further broken down into individual amino acids by the concerted action proteases and peptidases (127). In addition to providing free amino acids from external sources for metabolism, the ATP-independent peptidases must break down peptides produced by ATP-dependent proteases during turnover of intracellular proteins (36).

Tricorn Peptidase: The self-compartmentalized tricorn protease is a hexmeric enzyme of 720 kDa, based on 120 kDa subunits (173). Quaternary association of the homohexamers results in an icosahedral capsid structure with a molecular mass of approximately 14.6 MDa (179). Possessing tryptic and chymotryptic specificities, this enzyme is capable of processive peptide degradation from the carboxal terminus resulting in di- and tri-peptides (20, 171). Within the proteolytic pathway, shown in Figure 4, evidence suggests that the Tricorn protease acts downstream of the proteasome (170). It has been suggested that the capsid structure of Tricorn allows for the efficient funneling of small peptide products to other associated proteases (173); combination of this enzyme with the interacting factors F1, F2, and F3 results in the complete degradation of peptides to free amino acids (170). The F1 enzyme is a prolyl iminopeptidase, similar to prolyl oligopeptidase (POP), and demonstrates wide substrate specificity (54, 124). Integrating factor F2 is an 89 kDa Zinc aminopeptidase that also exhibits broad activity for substrates with basic, neutral, and hydrophobic residues in the P1 position; with a 53% similarity to F2 (170), F3 displays a similar structure, but exhibits a clear preference for glutamate in the P1 location (97). While there is evidence for functional interaction between Tricorn

peptidase and the integrating factors, there is no direct documentation of an actual physical interaction between these proteases (170).

The Tricorn system is absent in *Pyroccoccus*, *Thermotoga*, and *Archaeoglobus*, but *S. solfataricus* encodes a Tricorn homolog (SSO2098), along with the three associated peptidases (SSO3115, SSO2154, & SSO2675) (181). As expected, the functional homolog of Tricorn, Tetrahedral aminopeptidase (TET), is not found in the *S. solfataricus* genome. Even though TET and Tricorn are assumed to fill similar roles, they exhibit significantly different transcriptional patterns. Subjecting *S. solfataricus* to heat shock, acid shock and base shock resulted in no significant differential transcription for SSO2098, the Tricorn peptidase (168). However, there was a slight (1.5-fold) increase in transcription during stationary phase compared to mid-log growth. This mirrored the proteasome complex transcriptional response and would be consistent with an enzyme co-regulated with the 20S proteasome. Similar to the Tricorn peptidase, the F1 *P. furiosus* homolog showed no response to shock conditions but was 2.0-fold up during stationary phase. In contrast, the interacting factors F2 and F3 demonstrated significant changes during heat shock conditions, as well as transcriptional response to changes in growth phase. As shown in Figure 3, SSO-F2 and SSO-F3 transcription was altered within 5 minutes of heat shock application and culminated in approximately 4-fold down-regulation after 60 minutes (168). Additionally, exposure of *S. solfataricus* to a step change in pH resulted in a significant down regulation of SSO-F2 and SSO-F3. Interestingly, SSO-F2 was immediately down-regulated 1.8-fold within 5 minutes after base shock, but returned to the baseline transcriptional level after 30 minutes. Conversely, SSO-F3 demonstrated no response to acid and base shock after 5 minutes;

after 30 minutes SSO-F3 transcription was reduced 3.3-fold and 2.2-fold for acid and base shock, respectively. This suggests that during long-term acid/base response the narrow specificity offered by the F3 homolog is dispensable when compared to the broad substrate activity offered by F2. An alternative to this multiple protease degradation pathway was identified in archaea in which TET aminopeptidase progressively hydrolyzes peptides to free amino acids (61).

Tetrahedral (TET) Aminopeptidase: The tetrahedral aminopeptidase (TET) is a large homomultimer capable of cleaving the N-terminal amino acid from a wide range of peptide substrates. Initially isolated from the archaeon *Haloarcula marimotui*, TET is comprised of twelve 42 kDa subunits, which form a tetrahedral-like structure with an approximate M_r of 400-500 kDa (51). Quaternary association between two TET enzymes results in an 800 kDa octahedral complex structurally reminiscent of viral capsid proteins (132, 149). Homologs of the TET aminopeptidase are found in the genomes of many archaea and bacteria, including a number of thermophilic and hyperthermophilic organisms (61, 181). Classified as a member of the M42 peptidase family, putative TET homologs are present in *P. horikoshii*, *P. furiosus*, *T. maritima*, *M. jannaschii*, and *A. fulgidus* and show a high level of primary sequence similarity as shown in Figure 5. The *T. maritima* M42 homologues (TM1048, TM1049, and TM1050), in contrast to those noted for the archaeal organisms, are encoded sequentially within the genome (136).

Crystal structures of both TET homologues characterized in *P. horikoshii* indicate that each subunit contains a single proteolytic domain, as well as two dimerization regions involved inter-subunit association (146). Substrate access to the interior of PhTET-2 (PH1527) is facilitated through 4 openings of 18Å diameter; a negative enzyme

surface potential forces the substrate peptides to enter with the N-terminus first (16). After proteolysis, amino acid residues are ejected from the central chamber through one of 12 separate openings which contain an electrostatic gradient that facilitates product movement out of the enzyme (16). The PhTET-2 enzyme exhibits a preference for Leu in the N-terminal position, in addition to lower activities towards other neutral residues (Met, Ile, and Ala). While displaying a similar overall shape to PhTET-2, PhTET-1 (PH0519) contains four sub-compartments with 3 active sites each, which are accessible through large openings (~13 Å) on each face of the tetrahedron (149). Additionally, this enzyme displays a broad aminopeptidase activity, along with the ability to remove N-terminal blocking groups; PhTET-2 does not possess de-blocking activity (149). Thus, significant difference in biochemical properties for these enzymes were noted, even though they have similar external structures and primary amino acid sequences (as much as 40% identitical).

As a possible alternative to the Tricorn peptidase degradation pathway, the TET aminopeptidase is able to hydrolyze small peptides generated by the proteasome, and other ATP-dependent proteases, into free amino acids (16). Hypertheromphilic genomes typically encode at least one M42 TET aminopeptidase or the Tricorn protease along with its complementary dipeptidases (181). It has been suggested that PhTET-1 is primarily involved in hydrolyzing imported peptides, whereas PhTET-2's principal role is the complementation of PhTET-1 during the breakdown of proteasome products (149). This hypothesis is based on structural differences between the enzymes and a 3.5-fold up-regulation of a TET-1 homolog (PF0369) in *P. furiosus* (149, 150). However, the increased transcription of all three *P. furiosus* homologs in cells grown on tryptone,

compared to maltose, seems to suggest that all TET homologs may be involved with imported peptide breakdown. As shown in Table 1, heat shock of *P. furiosus* growing on tryptone results in the down-regulation of all three genes. This is consistent with TET involvement in the nutritional pathway and a decreased requirement for amino acids during a cessation of growth in response to stress (91). However, the heat shock response of *P. furiosus* grown on maltose shows the TET-2 homolog (PF1547) is 2.2-fold down regulated after 60 minutes and seems unnecessary for the presumably higher production of proteasome products during heat-stress. As both PF0369 and PF1861 demonstrate no significant transcriptional changes in response to heat shock, the basal levels of PF0369 and PF1861 appear sufficient to hydrolyze proteasome peptides during normal and stress conditions (135); this is also supported by the relatively constant transcription of the proteasome complex (109, 135). The three TET similar genes in *T. maritima* exhibit little transcriptional change as shown in Figure 1. However, upon heat shock TM1048 and TM1049 were both 1.6-fold down-regulated after 60 minutes. In contrast, TM1050 reaches a maximum -1.8 fold decrease after only 5 minutes and rises slightly after 60 minutes. While the specificities and sizes of all three enzymes have yet to be determined, TM1050 appears to be a Leucine aminopeptidase based on a substrate preference for Leu-MCA (J.K. Michel and R.M. Kelly, unpublished). The homologs TM1049 and TM1050 exhibit average transcriptional levels for most conditions, whereas the transcription of TM1048 is below average. Additional biochemical characterization of these gene products is needed to ascertain whether they exhibit TET-like structure and what functional role they play.

Hyperthermophilic heterotrophs utilize exogenous peptides as a primary carbon source, facilitated through the reduction of elemental sulfur to hydrogen sulfide (88). However, in the presence of sulfur, *P. furiosus* can also ferment peptides as a primary growth substrate (1). When *P. furiosus* was grown on maltose or cellobiose in the presence of sulfur, both PF0369 and PF1547 were significantly up-regulated, as shown in Table 2. This increased transcription of TET-1 and TET-2 homologs indicate that they play a significant role under peptide-limiting growth conditions. The third TET homolog (PF1861) was unchanged on maltose + S^0, but slightly up-regulated on cellobiose + S^0 (Chou and Kelly, unpublished data). While not essential nor preferred, the third TET homolog may be involved in amino acid scavenging during extreme situations. Also of note, all three *P. furiosus* TET homologs are down-regulated in media containing tryptone + S^0, when compared to tryptone alone. This down-regulation in peptide-rich media with S° may also indicate that Pfu-TET is primarily associated with the breakdown of internally produced peptides, unless under metabolic duress. Several other putative peptidases (e.g., PF0366, PF0368, PF0370, and PF0477) have demonstrated high fold increases (>3.5-fold) in cells grown on peptides compared to carbohydrates (150). Additionally, the tri-lobed protease (TLP) has been suggested as alternative to the TET aminopeptidase in *P. furisosus* (17). However, no supporting documentation has been provided to support this claim.

Role of Smaller Multimeric and Monmeric Proteases

The proteolytic inventory of the sequenced model hyperthermophilic organisms is also populated by smaller multi-subunit proteases (<200kDa) and monomeric peptidases

typically smaller then 100 kDa (181, 185). These enzymes may play highly specific roles and display either narrow or broad substrate specificities. For example, the integrating factors (F1, F2, and F3) are purposed to play a complementary role to the proteasome and Tricorn protease by providing the final hydrolysis of small peptides produced during protein turnover (170). Several extracellular and membrane-associated proteases have been characterized from *Thermococcus* and *Pyrococcus* (40, 84, 94, 116, 158, 178). The proteases range in size from 40 to 68 kDa and are monomeric, except for the multimeric *P. abyssi* protease (116). The serine protease from *T. kodakaraensis* has broad substrate specifity for cleavage at the carboxy terminus. Serine proteases from *Thermococcus stetteri* and *P. abyssi* demonstrate narrow specificity for P1-located Arg/Phe and Aromatic/Leu, respectively (40, 94). Thermopsin, a 45 kDa caseinolytic proteases isolated from *S. acidocaldarius*, exhibits maximum activity between 75°C to 90°C, with an optimal pH of 2.0 (53, 103, 104). Isolated from the extracellular fractions of *Sulfolobus*, evidence also suggests that Thermopsin is tightly cell membrane-associated (104). Several Thermopsin homologs are found in *S. solfataricus* (SSO2045, SSO2037, and SSO1886) and are presumably involved in the degradation of extraceullular peptides prior to transport (185). Transcriptional data shows that all three homologs are consistently transcribed during mid-log, late-log, and early-stationary phase, as shown in Figure 3. The homolog SSO2045 shows the highest transcript presence of the three and exhibits significant down-regulation in response to stress conditions. Thirty minutes following either heat or base shock SSO2045 is down 2.4-fold and 1.8-fold, respectively (168). This down-regulation coincides with decreased growth rates during these shock periods, suggesting a primary role for SSO2045 under optimal growth conditions. As

discussed previously, heat-shock triggers an up-regulation of intracellular proteolysis and thus may limit the requirement for imported peptides produced by this protease. While Thermopsin homologs are not found in either *T. maritima* or *P. furiosus*, a number of other extracellular proteases appear as starting points for the peptide transport chain.

Pyrolysin is a cell envelope-associated proteases that has been linked to protein utilization during proteolytic growth (37). The *P. furiosus* pyrolysin homolog (PF0287) is a serine protease that displays broad endopeptidase activity (178). Formed by a single amino acid chain of 1398 residues that displays an approximate size of 130 kDa, Pyrolysin contains a pre-proenzyme region, catalytic domain (500 residues) and a long C-terminal extension (37, 178). As indicated by the heat plot in Figure 2, PF0287 is one of the most highly transcribed proteases in *P. furiosus* and is consistently transcribed during all phases of growth. During growth on maltose as a primary carbohydrate source, PF0287 is down-regulated about 5-fold during thermal stress response. This down-regulation is consistent with the lower transcription of Thermopsin in *S. solfataricus*; both responses may be explained by a shift in proteolytic prioties to intracellular protein hydrolysis. While this pyrolysin enzyme is not found in other archaeal genomes, *P. horikoshii* (PH0310) and *P. abyssi* (PAB1252) both encode thiol-proteases with conserved pro-enzyme and C-terminal regions. Thus, these other putative proteases may act as functional homologues for this extracellular enzyme.

Development of redundant proteolytic strategies has been evidenced by the ability of independent proteases to partially compensate for the loss of one or more proteolytic enzymes (118). In addition to the enzymes noted in Figure 4, the large repertoire of proteases encoded in hyperthermophilic genomes indicates the presence of such

redundant proteases. With suggested roles in the hydrolysis of peptides for metabolism, *Pyrococcus furiosus* proteases I (PfpI; PF1719) homologs are found in a number of archaeal genomes including *S. solfataricus* (SSO2098) (12). This intracellular multi-subunit enzyme forms a hexameric active enzyme of ~200 kDa with broad substrate activity (66). While PfpI is constantly transcribed during all growth phases, co-culture studies have shown that PfpI is 5.3-fold down-regulated during growth in the presence of *T. maritima*, compared to *P. furiosus* pure culture. This is significant due to the fact that under co-culture conditions increased extracellular Pyrolysin transcription was noted. If PfpI is primarily involved in the breakdown of imported peptides, this could indicate that peptides generated during co-culture conditions and imported to the cell do not require PfpI hydrolysis for further utilization; this could result from the production of shorter peptides by the combined action of *T. maritima* and *P. furiosus* extracellular proteases. During growth of *P. furiosus* in a chemostat on either maltose or sulfur, PfpI was up 1.8- and 2.3-fold respectively when sulfur was included in the growth media. However, in cells grown on tryptone, PfpI was down-regulated slightly in the presence of sulfur. SSO2098 was 1.5-fold down-regulated during stationary phase compared to mid-log cells, but did not respond to acid, base, or heat induced stress (168). The significant differences in transcriptional response between PfpI (PF1719) and SSO2098 suggest the presence of redundant PfpI-like proteases in *S. solfataricus*. However, evidence suggesting that *S. solfataricus* is unable to grow solely on peptides may offer one possible explanation for the transcriptional discrepancies.

Conclusion

While initially considered unique, the large multimeric proteases have shown to be ubiquitous in all domains of life. The reason for this conservation may be related to the functional advantages offered by self-compartmentalization. Additionally, the ability to form multiple sub-types of each protein, capable of dealing with a broad range of substrates under varying environmental conditions may provide another explanation for the inclusion of multiple subunits. As an example, the proteasome demonstrates the ability to alter both substrate specificity and biophysical stability by alteration in subunit composition (109). The mulimeric proteases in hyperthermophilic offer an attractive model of study due to a reduced number of possible configurations arising from a smaller pool of distinct subunits. The relevance of which may be shown by the potential use of large enzymes in biotechnological applications or as drug targets in treatment of cancer and neurological diseases (182).

References

1. **Adams, M. W. W., J. F. Holden, A. L. Menon, G. J. Schut, A. M. Grunden, C. Hou, A. M. Hutchins, F. E. Jenney, C. Kim, K. S. Ma, G. L. Pan, R. Roy, R. Sapra, S. V. Story, and M. Verhagen.** 2001. Key role for sulfur in peptide metabolism and in regulation of three hydrogenases in the hyperthermophilic archaeon *Pyrococcus furiosus*. J Bacteriol **183:**716-724.

2. **Aertsen, A., and C. W. Michiels.** 2005. SulA-dependent hypersensitivity to high pressure and hyperfilamentation after high-pressure treatment of *Escherichia coli* Lon mutants. Res Microbiol **156:**233-237.

3. **Amerik, A. Y., V. K. Antonov, A. E. Gorbalenya, S. A. Kotova, T. V. Rotanova, and E. V. Shimbarevich.** 1991. Site-directed mutagenesis of La protease - A catalytically active serine residue. FEBS Lett **287:**211-214.

4. **Andersson, F. I., R. Blakytny, J. Kirstein, K. Turgay, B. Bukau, A. Mogk, and A. K. Clarke.** 2006. Cyanobacterial ClpC/HSP100 protein displays intrinsic chaperone activity. J Biol Chem **281:**5468-5475.

5. **Asahara, Y., K. Atsuta, K. Motohashi, H. Taguchi, M. Yohda, and M. Yoshida.** 2000. FtsH recognizes proteins with unfolded structure and hydrolyzes the carboxyl side of hydrophobic residues. J. Biochem. (Tokyo) **127:**931.

6. **Bailey, S., P. Silva, P. Nixon, C. Mullineaux, C. Robinson, and N. Mann.** 2001. Auxiliary functions in photosynthesis: the role of the FtsH protease. Biochem Soc Trans **29:**455-459.

7. **Bailey, S., E. Thompson, P. J. Nixon, P. Horton, C. W. Mullineaux, C. Robinson, and N. H. Mann.** 2002. A critical role for the Var2 FtsH homologue

of *Arabidopsis thaliana* in the photosystem II repair cycle in vivo. J Biol Chem **277:**2006.

8. **Barber, R. D., and J. G. Ferry.** 2001. Archaeal proteasomes. Methods Enzymol **330:**413-24.

9. **Barbier, G., A. Godfroy, J. R. Meunier, J. Querellou, M. A. Cambon, F. Lesongeur, P. A. D. Grimont, and G. Raguenes.** 1999. *Pyrococcus glycovorans* sp nov., a hyperthermophilic archaeon isolated from the East Pacific Rise. Int. J. Syst. Bacteriol. **49:**1829-1837.

10. **Benoist, P., A. Muller, H. G. Diem, and J. Schwencke.** 1992. High-molecular-mass multicatalytic proteinase complexes produced by the nitrogen-fixing *Actinomycete frankia* Strain Br. J Bacteriol **174:**1495.

11. **Blamey, J., M. Chiong, C. Lopez, and E. Smith.** 1999. Optimization of the growth conditions of the extremely thermophilic microorganisms *Thermococcus celer* and *Pyrococcus woesei*. J Microbiol Methods **38:**169-175.

12. **Blumentals, I. I., A. S. Robinson, and R. M. Kelly.** 1990. Characterization of sodium dodecyl sulfate-resistant proteolytic activity in the hyperthermophilic Archaebacterium *Pyrococcus furiosus*. Appl Environ Microbiol **56:**1992-98.

13. **Bochtler, M., L. Ditzel, M. Groll, C. Hartmann, and R. Huber.** 1999. The proteasome. Annu Rev Biophys Biomol Struct **28:**295-317.

14. **Bochtler, M., L. Ditzel, M. Groll, and R. Huber.** 1997. Crystal structure of heat shock locus V (HslV) from *Escherichia coli*. Proc Natl Acad Sci U S A **94:**6070-4.

15. **Boonyaratanakornkit, B. B., A. J. Simpson, T. A. Whitehead, C. M. Fraser, N. M. A. El-Sayed, and D. S. Clark.** 2005. Transcriptional profiling of the hyperthermophilic methanarchaeon *Methanococcus jannaschii* in response to lethal heat and non-lethal cold shock. Environ. Microbiol. **7:**789.

16. **Borissenko, L., and M. Groll.** 2005. Crystal structure of TET protease reveals complementary protein degradation pathways in prokaryotes. J Mol Biol **346:**1207-1219.

17. **Bosch, J., T. Tamura, N. Tamura, W. Baumeister, and L. O. Essen.** 2007. The beta-propeller domain of the trilobed protease from *Pyrococcus furiosus* reveals an open Velcro topology. Acta Crystallogr., Sect. D: Biol. Crystallogr. **63:**179-187.

18. **Botos, I., E. E. Melnikov, S. Cherry, S. Kozov, O. V. Makhovskaya, J. E. Tropea, A. Gustchina, T. V. Rotanova, and A. Wlodawer.** 2005. Atomic-resolution crystal structure of the proteolytic domain of *Archaeoglobus fulgidus* Lon reveals the conformational variability in the active sites of Lon proteases. J Mol Biol **351:**144-157.

19. **Botos, I., E. E. Melnikov, S. Cherry, J. E. Tropea, A. G. Khalatova, F. Rasulova, Z. Dauter, M. R. Maurizi, T. V. Rotanova, A. Wlodawer, and A. Gustchina.** 2004. The catalytic domain of *Escherichia coli* Lon protease has a unique fold and a Ser-Lys dyad in the active site. J Biol Chem **279:**8140-8148.

20. **Brandstetter, H., J. S. Kim, M. Groll, P. Gottig, and R. Huber.** 2002. Structural basis for the processive protein degradation by tricorn protease. Biol Chem **383:**1157-1165.

21. **Bucca, G., A. M. E. Brassington, G. Hotchkiss, V. Mersinias, and C. P. Smith.** 2003. Negative feedback regulation of DnaK, ClpB and Lon expression by the DnaK chaperone machine in *Streptomyces coelicolor*, identified by transcriptome and *in vivo* DnaK-depletion analysis. Mol Microbiol **50:**153-166.

22. **Burton, R. E., S. M. Siddiqui, Y. I. Kim, T. A. Baker, and R. T. Sauer.** 2001. Effects of protein stability and structure on substrate processing by the ClpXP unfolding and degradation machine. EMBO J. **20:**3092-3100.

23. **Catara, G., G. Ruggiero, F. La Cara, F. A. Digilio, A. Capasso, and M. Rossi.** 2003. A novel extracellular subtilisin-like protease from the hyperthermophile *Aeropyrum pernix* K1: biochemical properties, cloning, and expression. Extremophiles **7:**391-399.

24. **Charpentier, E., R. Novak, and E. Tuomanen.** 2000. Regulation of growth inhibition at high temperature, autolysis, transformation and adherence in *Streptococcus pneumoniae* by ClpC. Mol Microbiol **37:**717-726.

25. **Chatterjee, I., P. Becker, M. Grundmeier, M. Bischoff, G. A. Somerville, G. Peters, B. Sinha, N. Harraghy, R. A. Proctor, and M. Herrmann.** 2005. *Staphylococcus aureus* ClpC is required for stress resistance, aconitase activity, growth recovery, and death. J Bacteriol **187:**4488-4496.

26. **Chatterjee, I., M. Herrmann, R. A. Proctor, G. Peters, and B. Kahl.** 2006. Enhanced post-stationary phase survival of a clinical thymidine-dependent small-colony variant of *Staphylococcus aureus* results from lack of functional TCA cycle. Int. J. Med. Microbiol. **296:**127-128.

27. **Chen, P., and M. Hochstrasser.** 1996. Autocatalytic subunit processing couples active site formation in the 20S proteasome to completion of assembly. Cell **86:**961.

28. **Chhabra, S. R., K. R. Shockley, S. B. Conners, K. L. Scott, R. D. Wolfinger, and R. M. Kelly.** 2003. Carbohydrate-induced differential gene expression patterns in the hyperthermophilic bacterium *Thermotoga maritima*. J Biol Chem **278:**7540-7552.

29. **Chhabra, S. R., K. R. Shockley, D. E. Ward, and R. M. Kelly.** 2002. Regulation of endo-acting glycosyl hydrolases in the hyperthermophilic bacterium *Thermotoga maritima* grown on glucan- and mannan-based polysaccharides. Appl Environ Microbiol **68:**545-554.

30. **Choi, K. H., and S. Licht.** 2005. Control of peptide product sizes by the energy-dependent protease ClpAP. Biochemistry **44:**13921-13931.

31. **Christensen, S. K., G. Maenhaut-Michel, N. Mine, S. Gottesman, K. Gerdes, and L. Van Melderen.** 2004. Overproduction of the Lon protease triggers inhibition of translation in *Escherichia coli*: involvement of the yefM-yoeB toxin-antitoxin system. Mol Microbiol **51:**1705-1717.

32. **Comfort, D. A., S. R. Chhabra, S. B. Conners, C. J. Chou, K. L. Epting, M. R. Johnson, K. L. Jones, A. C. Sehgal, and R. M. Kelly.** 2004. Strategic biocatalysis with hyperthermophilic enzymes. Green Chem. **6:**459-465.

33. **Conners, S. B., E. F. Mongodin, M. R. Johnson, C. I. Montero, K. E. Nelson, and R. M. Kelly.** 2006. Microbial biochemistry, physiology, and biotechnology of hyperthermophilic *Thermotoga* species. FEMS Microbiol Rev **30:**872-905.

34. **Conners, S. B., C. I. Montero, D. A. Comfort, K. R. Shockley, M. R. Johnson, S. R. Chhabra, and R. M. Kelly.** 2005. An expression-driven approach to the prediction of carbohydrate transport and utilization regulons in the hyperthermophilic bacterium *Thermotoga maritima*. J Bacteriol **187:**7267-7282.

35. **Darwin, K. H., S. Ehrt, J. C. Gutierrez-Ramos, N. Weich, and C. F. Nathan.** 2003. The proteasome of *Mycobacterium tuberculosis* is required for resistance to nitric oxide. Science **302:**1963.

36. **De Castro, R. E., J. A. Maupin-Furlow, M. I. Gimenez, M. K. H. Seitz, and J. J. Sanchez.** 2006. Haloarchaeal proteases and proteolytic systems. FEMS Microbiol Rev **30:**17.

37. **de Vos, W. M., W. G. B. Voorhorst, M. Dijkgraaf, L. D. Kluskens, J. Van der Oost, and R. J. Siezen.** 2001. Purification, characterization, and molecular modeling of pyrolysin and other extracellular thermostable serine proteases from hyperthermophilic microorganisms, p. 383-393, Hyperthermophilic Enzymes, Pt A, vol. 330.

38. **Deckert, G., P. V. Warren, T. Gaasterland, W. G. Young, A. L. Lenox, D. E. Graham, R. Overbeek, M. A. Snead, M. Keller, M. Aujay, R. Huber, R. A. Feldman, J. M. Short, G. J. Olsen, and R. V. Swanson.** 1998. The complete genome of the hyperthermophilic bacterium *Aquifex aeolicus*. Nature **392:**353-358.

39. **Deuerling, E., A. Mogk, C. Richter, M. Purucker, and W. Schumann.** 1997. The ftsH gene of *Bacillus subtilis* is involved in major cellular processes such as sporulation, stress adaptation and secretion. Mol Microbiol **23:**921.

40. **Dib, R., J. M. Chobert, M. Dalgalarrondo, G. Barbier, and T. Haertle.** 1998. Purification, molecular properties and specificity of a thermoactive and thermostable proteinase from *Pyrococcus abyssi*, strain st 549, hyperthermophilic archaea from deep-sea hydrothermal ecosystem. FEBS Lett **431:**279-284.

41. **Dierksen, K. P., and J. E. Trempy.** 1996. Identification of a second RcsA protein, a positive regulator of colanic acid capsular polysaccharide genes, in *Escherichia coli*. J Bacteriol **178:**5053-5056.

42. **Dougan, D. A., A. Mogk, and B. Bukau.** 2002. Protein folding and degradation in bacteria: To degrade or not to degrade? That is the question. Cell. Mol. Life Sci. **59:**1607-1616.

43. **Dougan, D. A., A. Mogk, K. Zeth, K. Turgay, and B. Bukau.** 2002. AAA plus proteins and substrate recognition, it all depends on their partner in crime. FEBS Lett **529:**6-10.

44. **Duwat, P., S. D. Ehrlich, and A. Gruss.** 1995. The Reca gene of *Lactococcus lactis* - characterization and involvement in oxidative and thermal stress. Mol Microbiol **17:**1121.

45. **Ebel, W., M. M. Skinner, K. P. Dierksen, J. M. Scott, and J. E. Trempy.** 1999. A conserved domain in *Escherichia coli* Lon protease is involved in substrate discriminator activity. J Bacteriol **181:**2236-2243.

46. **Farrell, C. M., T. A. Baker, and R. T. Sauer.** 2007. Altered specificity of a AAA plus protease. Mol Cell **25:**161-166.

47. **Fischer, B., G. Rummel, P. Aldridge, and U. Jenal.** 2002. The FtsH protease is involved in development, stress response and heat shock control in *Caulobacter crescentus*. Mol Microbiol **44:**461.

48. **Fischer, H., and R. Glockshuber.** 1994. A point mutation within the ATP-binding site inactivates both catalytic functions of the ATP-dependent protease La (Lon) from *Escherichia coli*. FEBS Lett **356:**101-103.

49. **Flynn, J. M., S. B. Neher, Y. I. Kim, R. T. Sauer, and T. A. Baker.** 2003. Proteomic discovery of cellular substrates of the ClpXP protease reveals five classes of ClpX-recognition signals. Mol Cell **11:**671-683.

50. **Frank, E. G., D. G. Ennis, M. Gonzalez, A. S. Levine, and R. Woodgate.** 1996. Regulation of SOS mutagenesis by proteolysis. Proc Natl Acad Sci U S A **93:**10291-10296.

51. **Franzetti, B., G. Schoehn, D. Garcia, R. W. Ruigrok, and G. Zaccai.** 2002. Characterization of the proteasome from the extremely halophilic archaeon *Haloarcula marismortui*. Archaea **1:**53-61.

52. **Fukui, T., T. Eguchi, H. Atomi, and T. Imanaka.** 2002. A membrane-bound archaeal lon protease displays ATP-independent proteolytic activity towards unfolded proteins and ATP-dependent activity for folded proteins. J Bacteriol **184:**3689-3698.

53. **Fusek, M., X. L. Lin, and J. Tang.** 1990. Enzymic Properties Of Thermopsin. J Biol Chem **265:**1496-1501.

54. **Goettig, P., M. Groll, J. S. Kim, R. Huber, and H. Brandstetter.** 2002. Structures of the tricorn-interacting aminopeptidase F1 with different ligands explain its catalytic mechanism. EMBO J. **21:**5343-5352.

55. **Gottesman, S.** 1996. Proteases and their targets in *Escherichia coli*. Annu Rev Genet **30:**465-506.

56. **Gottesman, S., W. P. Clark, V. Decrecylagard, and M. R. Maurizi.** 1993. Clpx, an alternative subunit for the ATP-dependent Clp protease of *Escherichia coli* - sequence and *in vivo* activities. J Biol Chem **268:**22618-22626.

57. **Gottesman, S., E. Halpern, and P. Trisler.** 1981. Role of SulA and SulB in filamentation by Lon mutants of *Escherichia coli* K-12. J Bacteriol **148:**265-273.

58. **Gottesman, S., E. Roche, Y. N. Zhou, and R. T. Sauer.** 1998. The ClpXP and ClpAP proteases degrade proteins with carboxy-terminal peptide tails added by the SsrA-tagging system. Genes Dev **12:**1338-1347.

59. **Griffith, K. L., I. M. Shah, and R. E. Wolf.** 2004. Proteolytic degradation of *Escherichia coli* transcription activators SoxS and MarA as the mechanism for reversing the induction of the superoxide (SoxRS) and multiple antibiotic resistance (Mar) regulons. Mol Microbiol **51:**1801.

60. **Groll, M., M. Bajorek, A. Kohler, L. Moroder, D. M. Rubin, R. Huber, M. H. Glickman, and D. Finley.** 2000. A gated channel into the proteasome core particle. Nat Struct Biol **7:**1062.

61. **Groll, M., M. Bochtler, H. Brandstetter, T. Clausen, and R. Huber.** 2005. Molecular machines for protein degradation. Chembiochem **6:**222-256.

62. **Groll, M., H. Brandstetter, H. Bartunik, G. Bourenkow, and R. Huber.** 2003. Investigations on the maturation and regulation of archaebacterial proteasomes. J Mol Biol **327:**75.

63. **Groll, M., L. Ditzel, J. Lowe, D. Stock, M. Bochtler, H. D. Bartunik, and R. Huber.** 1997. Structure of 20S proteasome from yeast at 2.4 angstrom resolution. Nature **386:**463.

64. **Groll, M., and R. Huber.** 2005. Purification, crystallization, and X-ray analysis of the yeast 20S proteasome, p. 329, Ubiquitin And Protein Degradation, Part A, vol. 398.

65. **Groll, M., and R. Huber.** 2003. Substrate access and processing by the 20S proteasome core particle. Int J Biochem Cell Biol **35:**606-616.

66. **Halio, S. B., Blumentals, II, S. A. Short, B. M. Merrill, and R. M. Kelly.** 1996. Sequence, expression in *Escherichia coli*, and analysis of the gene encoding a novel intracellular protease (PfpI) from the hyperthermophilic archaeon *Pyrococcus furiosus*. J Bacteriol **178:**2605-2612.

67. **Hegerl, R., G. Pfeifer, G. Puhler, B. Dahlmann, and W. Baumeister.** 1991. The 3-dimensional structure of proteasomes from *Thermoplasma acidophilum* as determined by electron-microscopy using random conical tilting. FEBS Lett **283:**117.

68. **Herman, C., T. Ogura, T. Tomoyasu, S. Hiraga, Y. Akiyama, K. Ito, R. Thomas, R. Dari, and P. Bouloc.** 1993. Cell-growth and lambda-phage development controlled by the same essential *Escherichia coli* gene, Ftsh Hflb. Proc Natl Acad Sci U S A **90:**10861-10865.

69. **Herman, C., D. Thevenet, R. Dari, and P. Bouloc.** 1995. Degradation Of σ(32), the heat-shock regulator in *Escherichia coli* is governed by Hflb. Proc Natl Acad Sci U S A **92:**3516.

70. **Herman, C., D. Thevenet, R. Dari, and P. Bouloc.** 1997. The HflB protease of *Escherichia coli* degrades its inhibitor lambda cIII. J Bacteriol **179:**358-363.

71. **Hoskins, J. R., S. Y. Kim, and S. Wickner.** 2000. Substrate recognition by the ClpA chaperone component of ClpAP protease. J Biol Chem **275:**35361-35367.

72. **Hoskins, J. R., and S. Wickner.** 2006. Two peptide sequences can function cooperatively to facilitate binding and unfolding by ClpA and degradation by ClpAP. Proc Natl Acad Sci U S A **103:**909-914.

73. **Huang, H. C., and A. L. Goldberg.** 1997. Proteolytic activity of the ATP-dependent protease HslVU can be uncoupled from ATP hydrolysis. J Biol Chem **272:**21364-21372.

74. **Im, Y. J., Y. Na, G. B. Kang, S. H. Rho, M. K. Kim, J. H. Lee, C. H. Chung, and S. H. Eom.** 2004. The active site of a Lon protease from *Methanococcus jannaschii* distinctly differs from the canonical catalytic dyad of Lon proteases. J Biol Chem **279:**53451-53457.

75. **Inagawa, T., J. Kato, H. Niki, K. Karata, and T. Ogura.** 2001. Defective plasmid partition in ftsH mutants of *Escherichia coli*. Mol. Genet. Genomics **265:**755.

76. **Ito, K., and Y. Akiyama.** 2005. Cellular functions, mechanism of action, and regulation of FtsH protease. Annu Rev Microbiol **59:**211.

77. **Iyer, L. M., D. D. Leipe, E. V. Koonin, and L. Aravind.** 2004. Evolutionary history and higher order classification of AAA plus ATPases. J Struct Biol **146:**11-31.

78. **Jayasekera, M. M. K., S. K. Foltin, E. R. Olson, and T. P. Holler.** 2000. *Escherichia coli* requires the protease activity of FtsH for growth. Arch Biochem Biophys **380:**103-107.

79. **Jobin, M. P., D. Garmyn, C. Divies, and J. Guzzo.** 1999. The *Oenococcus oeni* clpX homologue is a heat shock gene preferentially expressed in exponential growth phase. J Bacteriol **181:**6634-6641.

80. **Johnson, M. R., S. B. Conners, C. I. Montero, C. J. Chou, K. R. Shockley, and R. M. Kelly.** 2006. The *Thermotoga maritima* phenotype is impacted by syntrophic interaction with *Methanococcus jannaschii* in hyperthermophilic coculture. Appl Environ Microbiol **72:**811-818.

81. **Johnson, M. R., C. I. Montero, S. B. Conners, K. R. Shockley, M. A. Pysz, and R. M. Kelly.** 2004. Functional genomics-based studies of the microbial ecology of hyperthermophilic micro-organisms. Biochem Soc Trans **32:**188-192.

82. **Kanemori, M., K. Nishihara, H. Yanagi, and T. Yura.** 1997. Synergistic roles of Hs1VU and other ATP-dependent proteases in controlling in vivo turnover of sigma(32) and abnormal proteins in *Escherichia coli*. J Bacteriol **179:**7219-7225.

83. **Kang, M. S., S. R. Kim, P. Kwack, B. K. Lim, S. W. Ahn, Y. M. Rho, I. S. Seong, S. C. Park, S. H. Eom, G. W. Cheong, and C. H. Chung.** 2003. Molecular architecture of the ATP-dependent CodWX protease having an N-terminal serine active site. EMBO J. **22:**2893-2902.

84. **Kannan, Y., Y. Koga, Y. Inoue, M. Haruki, M. Takagi, T. Imanaka, M. Morikawa, and S. Kanaya.** 2001. Active subtilisin-like protease from a hyperthermophilic archaeon in a form with a putative prosequence. Appl Environ Microbiol **67:**2445-2452.

85. **Katayama, Y., S. Gottesman, J. Pumphrey, S. Rudikoff, W. P. Clark, and M. R. Maurizi.** 1988. The 2-Component, Atp-Dependent Clp Protease Of Escherichia-Coli - Purification, Cloning, And Mutational Analysis Of The Atp-Binding Component. J Biol Chem **263:**15226-15236.

86. **Katayama, Y., S. Gottesman, J. Pumphrey, S. Rudikoff, W. P. Clark, and M. R. Maurizi.** 1988. The 2-component, ATP dependent Clp protease of *Escherichia coli* - purification, cloning, and mutational analysis of the ATP-binding component. J Biol Chem **263:**15226-15236.

87. **Katayamafujimura, Y., S. Gottesman, and M. R. Maurizi.** 1987. A multiple-component, ATP-dependent protease from *Escherichia coli*. J Biol Chem **262:**4477-4485.

88. **Kelly, R. M., and M. W. W. Adams.** 1994. Metabolism in hyperthermophilic microorganisms. Antonie Van Leeuwenhoek International Journal Of General And Molecular Microbiology **66:**247-270.

89. **Kenniston, J. A., T. A. Baker, J. M. Fernandez, and R. T. Sauer.** 2003. Linkage between ATP consumption and mechanical unfolding during the protein processing reactions of an AAA(+) degradation machine. Cell **114:**511-520.

90. **Kessel, M., W. F. Wu, S. Gottesman, E. Kocsis, A. C. Steven, and M. R. Maurizi.** 1996. Six-fold rotational symmetry of ClpQ, the *E. coli* homolog of the 20S proteasome, and its ATP-dependent activator, ClpY. FEBS Lett **398:**274-278.

91. **Khmel, I. A.** 2005. Regulation of expression of bacterial genes in the absence of active cell growth. Russ J Genet **41:**968-984.

92. **Kihara, A., Y. Akiyama, and K. Ito.** 1999. Dislocation of membrane proteins in FtsH-mediated proteolysis. EMBO J. **18:**2970.

93. **Kim, Y. I., I. Levchenko, K. Fraczkowska, R. V. Woodruff, R. T. Sauer, and T. A. Baker.** 2001. Molecular determinants of complex formation between Clp/Hsp100 ATPases and the ClpP peptidase. Nat Struct Biol **8:**230-233.

94. **Klingeberg, M., B. Galunsky, C. Sjoholm, V. Kasche, and G. Antranikian.** 1995. Purification and properties of a highly thermostable, sodium dodecyl sulfate-resistant and stereospecific proteinase from the extremely thermophilic Archaeon *Thermococcus stetteri*. Appl Environ Microbiol **61:**3098-3104.

95. **Kruger, E., U. Volker, and M. Hecker.** 1994. Stress induction of clpC in *Bacillus subtilis* and its involvement in stress tolerance. J. Bacteriol. **176:**3360-3367.

96. **Kuroda, A.** 2006. A polyphosphate-Lon protease complex in the adaptation of *Escherichia coli* to amino acid starvation. Biosci Biotechnol Biochem **70:**325-331.

97. **Kyrieleis, O. J. P., P. Goettig, R. Kiefersauer, R. Huber, and H. Brandstetter.** 2005. Crystal structures of the tricorn interacting factor F3 from *Thermoplasma*

acidophilum, a zinc aminopeptidase in three different conformations. J Mol Biol **349:**787-800.

98. **Laskowska, E., D. KuczynskaWisnik, J. SkorkoGlonek, and A. Taylor.** 1996. Degradation by proteases Lon, Clp and HtrA, of *Escherichia coli* proteins aggregated *in vivo* by heat shock; HtrA protease action *in vivo* and *in vitro*. Mol Microbiol **22:**555-571.

99. **Lee, A. Y., S. G. Park, C. W. Kho, S. Y. Park, S. Cho, S. C. Lee, D. H. Lee, P. K. Myung, and B. C. Park.** 2004. Identification of the degradome of Isp-1, a major intracellular serine protease of *Bacillus subtilis*, by two-dimensional gel electrophoresis and matrix-assisted laser desorption/ionization-time of flight analysis. Proteomics **4:**3437-3445.

100. **Lee, H. S., K. R. Shockley, G. J. Schut, S. B. Conners, C. I. Montero, M. R. Johnson, C. J. Chou, S. L. Bridger, N. Wigner, S. D. Brehm, F. E. Jenney, D. A. Comfort, R. M. Kelly, and M. W. W. Adams.** 2006. Transcriptional and biochemical analysis of starch metabolism in the hyperthermophilic archaeon *Pyrococcus furiosus*. J Bacteriol **188:**2115-2125.

101. **Levchenko, I., L. Luo, and T. A. Baker.** 1995. Disassembly Of The Mu-Transposase Tetramer By The Clpx Chaperone. Genes Dev **9:**2399-2408.

102. **Levchenko, I., M. Yamauchi, and T. A. Baker.** 1997. ClpX and MuB interact with overlapping regions of Mu transposase: Implications for control of the transposition pathway. Genes Dev **11:**1561-1572.

103. **Lin, X. L., M. T. Liu, and J. Tang.** 1992. Heterologous expression of Thermopsin, a heat-stable acid proteinase. Enzyme Microb Technol **14:**696-701.

104. **Lin, X. L., and J. Tang.** 1990. Purification, characterization, and gene cloning of Thermopsin, a thermostable acid protease from *Sulfolobus acidocaldarius*. J Biol Chem **265:**1490-1495.

105. **Lindahl, M., C. Spetea, T. Hundal, A. B. Oppenheim, Z. Adam, and B. Andersson.** 2000. The thylakoid FtsH protease plays a role in the light-induced turnover of the Photosystem II D1 protein. Plant Cell Environ **12:**419-432.

106. **Liu, J. J., W. M. Cosby, and P. Zuber.** 1999. Role of Lon and ClpX in the post-translational regulation of a sigma subunit of RNA polymerase required for cellular differentiation in *Bacillus subtilis*. Mol Microbiol **33:**415-428.

107. **Lowe, J., D. Stock, B. Jap, P. Zwickl, W. Baumeister, and R. Huber.** 1995. Crystal structure of the 20S proteasome from the archaeon *T. acidophilum* at 3.4 A resolution. Science **268:**533-9.

108. **Lupas, A., J. M. Flanagan, T. Tamura, and W. Baumeister.** 1997. Self-compartmentalizing proteases. Trends Biochem Sci **22:**399.

109. **Madding, L. S., K. R. Shockley, S. B. Conners, K. L. Epting, M. R. Johnson, and R. M. Kelly.** 2007. Role of β1 subunit in function and stability of the 20S proteasome from the hyperthermophilic archaeon *Pyrococcus furiosus*. J Bacteriol **189:**583-590.

110. **Maupin-Furlow, J. A., H. C. Aldrich, and J. G. Ferry.** 1998. Biochemical characterization of the 20S proteasome from the methanoarchaeon *Methanosarcina thermophila*. J Bacteriol **180:**1480.

111. **Maupin-Furlow, J. A., M. A. Gil, M. A. Humbard, P. A. Kirkland, W. Li, C. J. Reuter, and A. J. Wright.** 2005. Archaeal proteasomes and other regulatory proteases. Curr Opin Microbiol **8:**720-728.

112. **Maurizi, M. R., W. P. Clark, Y. Katayama, S. Rudikoff, J. Pumphrey, B. Bowers, and S. Gottesman.** 1990. Sequence and structure of Clp-P, the proteolytic component of the ATP-dependent Clp protease of *Escherichia coli*. J Biol Chem **265:**12536-12545.

113. **Melchers, K., T. Wiegert, A. Buhmann, S. Postius, K. P. Schafer, and W. Schumann.** 1998. The Helicobacter felis ftsH gene encoding an ATP-dependent metalloprotease can replace the Escherichia coli homologue for growth and phage lambda lysogenization. Arch Microbiol **169:**393.

114. **Missiakas, D., F. Schwager, J. M. Betton, C. Georgopoulos, and S. Raina.** 1996. Identification and characterization of HsIV HsIU (ClpQ ClpY) proteins involved in overall proteolysis of misfolded proteins in *Escherichia coli*. EMBO J. **15:**6899-6909.

115. **Mizusawa, S., and S. Gottesman.** 1983. Protein-degradation in *Escherichia coli* - The Lon gene controls the stability of SulA protein. Proc Natl Acad Sci U S A **80:**358-362.

116. **Morikawa, M., Y. Izawa, N. Rashid, T. Hoaki, and T. Imanaka.** 1994. Purification and characterization of a thermostable thiol protease from a newly isolated hyperthermophilic *Pyrococcus Sp.* Appl Environ Microbiol **60:**4559-4566.

117. **Msadek, T., V. Dartois, F. Kunst, M. L. Herbaud, F. Denizot, and G. Rapoport.** 1998. ClpP of Bacillus subtilis is required for competence development, motility, degradative enzyme synthesis, growth at high temperature and sporulation. Mol Microbiol **27:**899-914.

118. **Nagler, D. K., and R. Menard.** 2003. Family C1 cysteine proteases: Biological diversity or redundancy? Biol Chem **384:**837-843.

119. **Nagy, I., T. Tamura, J. Vanderleyden, W. Baumeister, and R. De Mot.** 1998. The 20S proteasome of *Streptomyces coelicolor*. J Bacteriol **180:**5448.

120. **Nandi, D., E. Woodward, D. B. Ginsburg, and J. J. Monaco.** 1997. Intermediates in the formation of mouse 20S proteasomes: Implications for the assembly of precursor beta subunits. EMBO J. **16:**5363.

121. **Neuwald, A. F., L. Aravind, J. L. Spouge, and E. V. Koonin.** 1999. AAA(+): A class of chaperone-like ATPases associated with the assembly, operation, and disassembly of protein complexes. Genome Res **9:**27-43.

122. **Nomura, K., J. Kato, N. Takiguchi, H. Ohtake, and A. Kuroda.** 2004. Effects of inorganic polyphosphate on the proteolytic and DNA-binding activities of Lon in *Escherichia coli*. J Biol Chem **279:**34406-34410.

123. **Ogura, M., L. Liu, M. LaCelle, M. M. Nakano, and P. Zuber.** 1999. Mutational analysis of ComS: evidence for the interaction of ComS and MecA in the regulation of competence development in *Bacillus subtilis*. Mol Microbiol **32:**799-812.

124. **Ollis, D. L., E. Cheah, M. Cygler, B. Dijkstra, F. Frolow, S. M. Franken, M. Harel, S. J. Remington, I. Silman, J. Schrag, J. L. Sussman, K. H. G.**

Verschueren, and A. Goldman. 1992. The alpha/beta-hydrolase fold. Protein Eng **5:**197-211.

125. **Ortega, J., H. S. Lee, M. R. Maurizi, and A. C. Steven.** 2004. ClpA and ClpX ATPases bind simultaneously to opposite ends of ClpP peptidase to form active hybrid complexes. J Struct Biol **146:**217-226.

126. **Osteras, M., A. Stotz, S. S. Nuoffer, and U. Jenal.** 1999. Identification and transcriptional control of the genes encoding the *Caulobacter crescentus* ClpXP protease. J Bacteriol **181:**3039-3050.

127. **Palmieri, G., A. Casbarra, I. Fiume, G. Catara, A. Capasso, G. Marino, S. Onesti, and M. Rossi.** 2006. Identification of the first archaeal oligopeptide-binding protein from the hyperthermophile *Aeropyrum pernix*. Extremophiles **10:**393-402.

128. **Peltier, J. B., J. Ytterberg, D. A. Liberles, P. Roepstorff, and K. J. van Wijk.** 2001. Identification of a 350-kDa ClpP protease complex with 10 different Clp isoforms in chloroplasts of *Arabidopsis thaliana*. J Biol Chem **276:**16318-16327.

129. **Persuh, M., I. Mandic-Mulec, and D. Dubnau.** 2002. A MecA paralog, YpbH, binds ClpC, affecting both competence and sporulation. J. Bacteriol. **184:**2310-2313.

130. **Phillips, T. A., R. A. VanBogelen, and F. C. Neidhardt.** 1984. Lon gene product of *Escherichia coli* is a heat-shock protein. J. Bacteriol. **159:**283-287.

131. **Porankiewicz, J., J. M. Wang, and A. K. Clarke.** 1999. New insights into the ATP-dependent Clp protease: *Escherichia coli* and beyond. Mol Microbiol **32:**449-458.

132. **Porciero, S., V. Receveur-Brechot, K. Mori, B. Franzetti, and A. Roussel.** 2005. Expression, purification, crystallization and preliminary crystallographic analysis of a deblocking aminopeptidase from *Pyrococcus horikoshii*. Acta Crystallograph. Sect. F Struct. Biol. Cryst. Commun. **61:**239-242.

133. **Puhler, G., F. Pitzer, P. Zwickl, and W. Baumeister.** 1994. Proteasomes - multisubunit proteinases common to *Thermoplasma* and Eukaryotes. Syst Appl Microbiol **16:**734.

134. **Pysz, M. A., S. B. Conners, C. I. Montero, K. R. Shockley, M. R. Johnson, D. E. Ward, and R. A. Kelly.** 2004. Transcriptional analysis of biofilm formation processes in the anaerobic, hyperthermophilic bacterium *Thermotoga maritima*. Appl Environ Microbiol **70:**6098-6112.

135. **Pysz, M. A., D. E. Ward, K. R. Shockley, C. I. Montero, S. B. Conners, M. R. Johnson, and R. M. Kelly.** 2004. Transcriptional analysis of dynamic heat-shock response by the hyperthermophilic bacterium *Thermotoga maritima*. Extremophiles **8:**209-17.

136. **Rawlings, N. D., F. R. Morton, and A. J. Barrett.** 2006. MEROPS: the peptidase database. Nucleic Acids Res **34:**D270-D272.

137. **Rechsteiner, M., L. Hoffman, and W. Dubiel.** 1993. The Multicatalytic And 26S Proteases. J Biol Chem **268:**6065.

138. **Reuter, C. J., S. J. Kaczowka, and J. A. Maupin-Furlow.** 2004. Differential regulation of the PanA and PanB proteasome-activating nucleotidase and 20S proteasomal proteins of the haloarchaeon *Haloferax volcanii*. J Bacteriol **186:**7763-72.

139. **Rho, Y. M., M. S. Kang, S. R. Kim, I. S. Seong, S. H. Eom, G. W. Jeong, and C. H. Chung.** 2003. Characterization of the ATP-dependent CodWX protease that has N-terminal Ser active site for proteolysis. FASEB J **17:**A1331-A1331.

140. **Robertson, G. T., W. L. Ng, J. Foley, R. Gilmour, and M. E. Winkler.** 2002. Global transcriptional analysis of clpP mutations of type 2 *Streptococcus pneumoniae* and their effects on physiology and virulence. J Bacteriol **184:**3508-3520.

141. **Rohlin, L., J. D. Trent, K. Salmon, U. Kim, R. P. Gunsalus, and J. C. Liao.** 2005. Heat shock response of *Archaeoglobus fulgidus*. J Bacteriol **187:**6046.

142. **Rohrwild, M., G. Pfeifer, U. Santarius, S. A. Muller, H. C. Huang, A. Engel, W. Baumeister, and A. L. Goldberg.** 1997. The ATP-dependent HsIVU protease from *Escherichia coli* is a four-ring structure resembling the proteasome. Nat Struct Biol **4:**133-139.

143. **Rosen, R., D. Biran, E. Gur, D. Becher, M. Hecker, and E. Z. Ron.** 2002. Protein aggregation in *Escherichia coli*: role of proteases. FEMS Microbiol Lett **207:**9-12.

144. **Rotanova, T. V., E. E. Melnikov, A. G. Khalatova, O. V. Makhovskaya, I. Botos, A. Wlodawer, and A. Gustchina.** 2004. Classification of ATP-dependent proteases Lon and comparison of the active sites of their proteolytic domains. Eur J Biochem **271:**4865-4871.

145. **Roudiak, S. G., A. Seth, N. Knipfer, and T. E. Shrader.** 1998. The Lon protease from *Mycobacterium smegmatis*: Molecular cloning, sequence analysis, functional expression, and enzymatic characterization. Biochemistry **37:**377-386.

146. **Russo, S., and U. Baumann.** 2004. Crystal structure of a dodecameric tetrahedral-shaped aminopeptidase. J Biol Chem **279:**51275-51281.

147. **Saikawa, N., K. Ito, and Y. Akiyama.** 2002. Identification glutamic acid 479 as the gluzincin coordinator of zinc in FtsH (HflB). Biochemistry **41:**1861.

148. **Schlothauer, T., A. Mogk, D. A. Dougan, B. Bukau, and K. Turgay.** 2003. MecA, an adaptor protein necessary for ClpC chaperone activity. Proc Natl Acad Sci U S A **100:**2306-2311.

149. **Schoehn, G., F. M. D. Vellieux, M. A. Dura, V. Receveur-Brechot, C. M. S. Fabry, R. W. H. Ruigrok, C. Ebel, A. Roussel, and B. Franzetti.** 2006. An archaeal peptidase assembles into two different quaternary structures - A tetrahedron and a giant octahedron. J Biol Chem **281:**36327-36337.

150. **Schut, G. J., S. D. Brehm, S. Datta, and M. W. W. Adams.** 2003. Whole-genome DNA microarray analysis of a hyperthermophile and an archaeon: *Pyrococcus furiosus* grown on carbohydrates or peptides. J Bacteriol **185:**3935-3947.

151. **Seemuller, E., A. Lupas, and W. Baumeister.** 1996. Autocatalytic processing of the 20S proteasome. Nature **382:**468.

152. **Sharma, S., J. R. Hoskins, and S. Wickner.** 2005. Binding and degradation of heterodimeric substrates by ClpAP and ClpXP. J Biol Chem **280:**5449-5455.

153. **Shockley, K. R., K. L. Scott, M. A. Pysz, S. B. Conners, M. R. Johnson, C. I. Montero, R. D. Wolfinger, and R. M. Kelly.** 2005. Genorne-wide transcriptional variation within and between steady states for continuous growth

of the hyperthermophile *Thermotoga maritima*. Appl Environ Microbiol **71:**5572-5576.

154. **Shockley, K. R., D. E. Ward, S. R. Chhabra, S. B. Conners, C. I. Montero, and R. M. Kelly.** 2003. Heat shock response by the hyperthermophilic archaeon *Pyrococcus furiosus*. Appl Environ Microbiol **69:**2365-71.

155. **Shotland, Y., A. Shifrin, T. Ziv, D. Teff, S. Koby, O. Kobiler, and A. B. Oppenheim.** 2000. Proteolysis of bacteriophage lambda CII by *Escherichia coli* FtsH (HflB). J Bacteriol **182:**3111.

156. **Shotland, Y., D. Teff, S. Koby, O. Kobiler, and A. B. Oppenheim.** 2000. Characterization of a conserved alpha-helical, coiled-coil motif at the C-terminal domain of the ATP-dependent FtsH (HfIB) protease of *Escherichia coli*. J Mol Biol **299:**953.

157. **Siezen, R. J., and J. A. M. Leunissen.** 1997. Subtilases: The superfamily of subtilisin-like serine proteases. Protein Sci **6:**501-523.

158. **Siezen, R. J., W. G. B. Voorhorst, A. Warner, and W. M. deVos.** 1997. Homology modelling of subtilases from the hyperthermophilic archaea *Pyrococcus furiosus* and *Thermococcus stetteri*. Protein Eng **10:**53-53.

159. **Singh, S. K., R. Grimaud, J. R. Hoskins, S. Wickner, and M. R. Maurizi.** 2000. Unfolding and internalization of proteins by the ATP-dependent proteases ClpXP and ClpAP. Proc Natl Acad Sci U S A **97:**8898-8903.

160. **Smith, C. K., T. A. Baker, and R. T. Sauer.** 1999. Lon and Clp family proteases and chaperones share homologous substrate-recognition domains. Proc Natl Acad Sci U S A **96:**6678-6682.

161. **Sobczyk, A., A. Bellier, J. Viala, and P. Mazodier.** 2002. The Lon gene, encoding an ATP-dependent protease, is a novel member of the HAIR/HspR stress-response regulon in *actinomycetes*. Microbiology-Sgm **148:**1931-1937.

162. **Srinivasan, R., G. Anilkumar, H. Rajeswari, and P. Ajitkumar.** 2006. Functional characterization of AAA family FtsH protease of *Mycobacterium tuberculosis*. FEMS Microbiol Lett **259:**97-105.

163. **Stahlberg, H., E. Kutejova, K. Suda, B. Wolpensinger, A. Lustig, G. Schatz, A. Engel, and C. K. Suzuki.** 1999. Mitochondrial Lon of *Saccharomyces cerevisiae* is a ring-shaped protease with seven flexible subunits. Proc Natl Acad Sci U S A **96:**6787-6790.

164. **Stanne, T. M., E. Pojidaeva, F. I. Andersson, and A. K. Clarke.** 2007. Distinctive types of ATP-dependent Clp proteases in cyanobacteria. J. Biol. Chem. **282:**14394-14402.

165. **Stirnberg, M., S. Fulda, J. Huckauf, M. Hagemann, R. Kramer, and K. Marin.** 2007. A membrane-bound FtsH protease is involved in osmoregulation in *Synechocystis sp* PCC 6803: the compatible solute synthesizing enzyme GgpS is one of the targets for proteolysis. Mol Microbiol **63:**86-102.

166. **Swamy, K. H. S., and A. L. Goldberg.** 1981. *Escherichia coli* contains 8 soluble proteolytic activities, one being ATP dependent. Nature **292:**652-654.

167. **Szyk, A., and M. R. Maurizi.** 2006. Crystal structure at 1.9 angstrom of *E. coli* ClpP with a peptide covalently bound at the active site. J Struct Biol **156:**165-174.

168. **Tachdjian, S., and R. M. Kelly.** 2006. Dynamic metabolic adjustments and genome plasticity are implicated in the heat shock response of the extremely thermoacidophilic Archaeon *Sulfolobus solfataricus*. J Bacteriol **188:**4553-4559.

169. **Takaya, A., Y. Kubota, E. Isogai, and T. Yamamoto.** 2005. Degradation of the HilC and HilD regulator proteins by ATP-dependent Lon protease leads to downregulation of *Salmonella pathogenicity* island 1 gene expression. Mol Microbiol **55:**839-852.

170. **Tamura, N., F. Lottspeich, W. Baumeister, and T. Tamura.** 1998. The role of Tricorn protease and its aminopeptidase-interacting factors in cellular protein degradation. Cell **95:**637-648.

171. **Tamura, N., G. Pfeifer, W. Baumeister, and T. Tamura.** 2001. Tricorn protease in bacteria: Characterization of the enzyme from *Streptomyces coelicolor*. Biol Chem **382:**449-458.

172. **Tamura, T., I. Nagy, A. Lupas, F. Lottspeich, Z. Cejka, G. Schoofs, K. Tanaka, R. Demot, and W. Baumeister.** 1995. The first characterization of a eubacterial proteasome - The 2os complex of *Rhodococcus*. Curr Biol **5:**766.

173. **Tamura, T., N. Tamura, Z. Cejka, R. Hegerl, F. Lottspeich, and W. Baumeister.** 1996. Tricorn protease - The core of a modular proteolytic system. Science **274:**1385-1389.

174. **Tomoyasu, T., J. Gamer, B. Bukau, M. Kanemori, H. Mori, A. J. Rutman, A. B. Oppenheim, T. Yura, K. Yamanaka, H. Niki, S. Hiraga, and T. Ogura.** 1995. *Escherichia coli* Ftsh is a membrane-bound, ATP-dependent protease which degrades the heat-shock transcription factor σ(32). EMBO J. **14:**2551.

175. **Tomoyasu, T., K. Yamanaka, K. Murata, T. Suzaki, P. Bouloc, A. Kato, H. Niki, S. Hiraga, and T. Ogura.** 1993. Topology And subcellular localization of Ftsh protein in *Escherichia Coli*. J Bacteriol **175:**1352.

176. **Tsilibaris, V., G. Maenhaut-Michel, and L. Van Melderen.** 2006. Biological roles of the Lon ATP-dependent protease. Res Microbiol **157:**701-713.

177. **Ventura, M., Z. D. Zhang, M. Cronin, C. Canchaya, J. G. Kenny, G. F. Fitzgerald, and D. van Sinderen.** 2005. The ClgR protein regulates transcription of the clpP operon in *Bifidobacterium breve* UCC 2003. J Bacteriol **187:**8411-8426.

178. **Voorhorst, W. G. B., R. I. L. Eggen, A. C. M. Geerling, C. Platteeuw, R. J. Siezen, and W. M. deVos.** 1996. Isolation and characterization of the hyperthermostable serine protease, pyrolysin, and its gene from the hyperthermophilic archaeon *Pyrococcus furiosus*. J Biol Chem **271:**20426-20431.

179. **Walz, J., T. Tamura, N. Tamura, R. Grimm, W. Baumeister, and A. J. Koster.** 1997. Tricorn protease exists as an icosahedral supermolecule *in vivo*. Mol Cell **1:**59-65.

180. **Wang, J. M., J. A. Hartling, and J. M. Flanagan.** 1997. The structure of ClpP at 2.3 angstrom resolution suggests a model for ATP-dependent proteolysis. Cell **91:**447-456.

181. **Ward, D. E., K. R. Shockley, L. S. Chang, R. D. Levy, J. K. Michel, S. B. Conners, and R. M. Kelly.** 2002. Proteolysis in hyperthermophilic microorganisms. Archaea **1:**63-74.

182. **Yamada, S. I., J. I. Niwa, S. Ishigaki, M. Takahashi, T. Ito, J. Sone, M. Doyu, and G. Sobue.** 2006. Archaeal proteasomes effectively degrade aggregation-prone proteins and reduce cellular toxicities in mammalian cells. J Biol Chem.

183. **Yoo, S. J., J. H. Seol, D. H. Shin, M. Rohrwild, M. S. Kang, K. Tanaka, A. L. Goldberg, and C. H. Chung.** 1996. Purification and characterization of the heat shock proteins HslV and HslU that form a new ATP-dependent protease in *Escherichia coli*. J Biol Chem **271:**14035-14040.

184. **Yoo, S. J., Y. K. Shim, I. S. Seong, J. H. Seol, M. S. Kang, and C. H. Chung.** 1997. Mutagenesis of two N-terminal Thr and five Ser residues in Hs1V, the proteolytic component of the ATP-dependent Hs1VU protease. FEBS Lett **412:**57-60.

185. **Zwickl, P., E. Seemuller, B. Kapelari, and W. Baumeister.** 2002. The proteasome: A supramolecular assembly designed for controlled proteolysis, p. 187-222, Protein Folding In The Cell, vol. 59.

Table 1. Fold changes of *P. furiosus* TET aminopeptidase homologs for selected growth conditions.

	Heat Shock* (Maltose)	Heat Shock* (Tryptone)	Maltose + Tryptone vs. Maltose	Tryptone + S^0 vs. Tryptone	Maltose + S^0 vs. Maltose	Cellobiose + S^0 vs. Cellobiose
PF0369	N.C.	-3.1	+3.6	-1.4	+1.4	+2.4
PF1547	-2.2	-1.8	+2.7	-1.7	+2.6	+4.2
PF1861	N.C.	-1.9	+1.7	-1.7	N.C.	+1.8

N.C. – No significant fold changed noted.
* - Heat shock fold change is after 60 min following 10°C step increase and fold change is shown relative to baseline (t=0).

Figure 1 – Heat plot representation of transcriptional changes in *T. maritima* as determined be cDNA microarray analysis. Red coloring represents higher log square mean transcription compared to the average gene. Green denotes lower average transcription , while black is an average transcriptional level within +/- 1.0 fold. Grey cells indicate that there are no data available for that particular condition. Along the vertical axis are the protease found in *T. maritima* and each column represent a separate experimental condition.

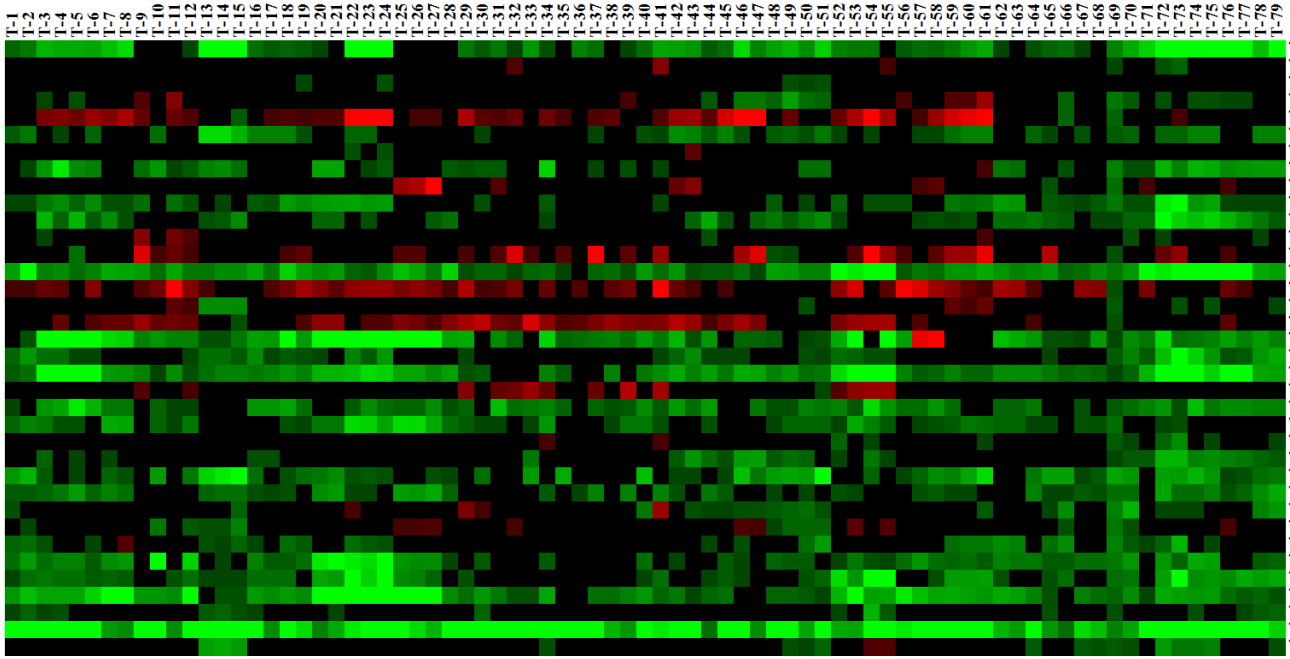
T-1 T-2 T-3 T-4 T-5 T-6 T-7 T-8 T-9 T-10 T-11 T-12 T-13 T-14 T-15 T-16 T-17 T-18 T-19 T-20 T-21 T-22 T-23 T-24 T-25 T-26 T-27 T-28 T-29 T-30 T-31 T-32 T-33 T-34 T-35 T-36 T-37 T-38 T-39 T-40 T-41 T-42 T-43 T-44 T-45 T-46 T-47 T-48 T-49 T-50 T-51 T-52 T-53 T-54 T-55 T-56 T-57 T-58 T-59 T-60 T-61 T-62 T-63 T-64 T-65 T-66 T-67 T-68 T-69 T-70 T-71 T-72 T-73 T-74 T-75 T-76 T-77 T-78 T-79
TM0042 Leucine Aminopeptidase (putative)
TM0129 Carboxypeptidase (putative)
TM0145 Endopeptidase (putative)
TM0146 Clp ATPase Subunit (putative)
TM0198 Clp ATPase Subunit (putative)
TM0365 Aspartyl aminopeptidase (putative)
TM0409 Metallo Peptidase (putative)
TM0445 Predicted GTPases
TM0463 Signal peptidase II (putative)
TM0516 Clostripain-related protein (putative)
TM0521 CodW subunit of CodWX peptidase (putative)
TM0522 HslVU ATPase (putative)
TM0571 Serine Peptidase (putative)
TM0643 Peptidase (putative)
TM0695 ClpP Protease Subunit
TM0747 Carboxypeptidase (putative)
TM0785 Protease (putative)
TM0873 Clp protease, ATPase subunit (putative)
TM0874 Inactive homolog of Metallo-peptidase (putative)
TM0890 RseP Peptidase (putative)
TM0916 Serine Protease
TM0963 Oligoendopeptidase F (#)
TM1048 M42 Aminopeptidase (putative*)
TM1049 M42 Aminopeptidase (putative*)
TM1050 M42 Aminopeptidase (#)
TM1346 Metallo-peptidases (putative)
TM1391 Clp protease, ATPase (putative)
TM1478 Methionine aminopeptidase
TM1572 Signal peptidase I (putative)
TM1589 Peptidase (putative)
TM1633 Lon protease (putative*)
TM1696 Prepilin Peptidase (putative)
TM1713 Proline dipeptidase (putative)
TM1822 FtsH Protease Activity Modulator (putative)
TM1823 FtsH Protease Activity Modulator (putative)
TM1869 ATP-dependent protease (putative)

Figure 1 continued.

Key of Conditions Tested

T-1	**Acetate Shock Baseline**
T-2	**Acetate Shock after 10 min**
T-3	**pH 5.6 BSM**
T-4	**pH 5.6 BSM with 40mM Acetate**
T-5	**pH 6.8 BSM**
T-6	**pH 6.8 BSM with 40mM Acetate**
T-7	**Sample Cooling with Coil Heat Exchanger**
T-8	**Sample Cooling on Ice**
T-9	**Co-Culture M. jannaschii/T. maritima**
T-10	**Co-Culture M. jannaschii/T. maritima (Pressurized)**
T-11	**Pure T. maritima**
T-12	**Pure T. maritima with Sparged N2**
T-13	**Early Log Growth Phase**
T-14	**Mid-Log Growth Phase**
T-15	**Early Stationary Growth Phase**
T-16	**Osmotic Shock Baseline**
T-17	**Osmotic Shock 5 min**
T-18	**Osmotic Shock 30 min**
T-19	**Osmotic Shock 180 min**
T-20	**BSM**
T-21	**BSM with Small Peptide**
T-22	**Small Peptide Dynamic Response Baseline (1)**
T-23	**Small Peptide Dynamic Response 10 min (1)**
T-24	**Small Peptide Dynamic Response 30 min (1)**
T-25	**Small Peptide Dynamic Response Baseline (2)**
T-26	**Small Peptide Dynamic Response 10 min (2)**
T-27	**Small Peptide Dynamic Response 30 min (2)**
T-28	**Arabinose**
T-29	**Barley**
T-30	**Chitin**
T-31	**Galactomannan**
T-32	**Glucose**
T-33	**Glucomannan**
T-34	**Laminatin**
T-35	**Mannose**
T-36	**Pustulan**
T-37	**Rhamnose**
T-38	**Ribose**
T-39	**Starch**
T-40	**Xylan**
T-41	**Xylose**
T-42	**Chl^+ Mutant Challenge Baseline**
T-43	**Chl^+ Mutant Challenge 5 min**
T-44	**Chl^+ Mutant Challenge 30 min**
T-45	**Wild Type Chl Challenge Baseline**
T-46	**Wild Type Chl Challenge 5 min**
T-47	**Wild Type Chl Challenge 30 min**
T-48	**Mid-Log Phase in BSM Media**
T-49	**Mid-Log BSM with Salmon DNA**
T-50	**Sationary Phase in BSM Media**
T-51	**Stationary Phase in BSM media with Salmon DNA**
T-52	**Mid-Log Phase in BSM Media**
T-53	**Mid-Log Phase in BSM Media with T. maritima & P. furiosus DNA**
T-54	**Sationary Phase in BSM Media**
T-55	**Stationary Phase in BSM Media with T. maritima & P. furiosus DNA**
T-56	**Heat Shock Baseline**
T-57	**Heat Shock 1 min**
T-58	**Heat Shock 5 min**
T-59	**Heat Shock 30 min**
T-60	**Heat Shock 60 min**
T-61	**Heat Shock 90 min**
T-62	**Small Peptide High Dose (Control)**
T-63	**Small Peptide High Dose**
T-64	**Mix M. jannaschii/T. maritima Mid-Log Phase**
T-65	**Mix M. jannaschii/T. maritima Early Stationary Phase**
T-66	**Mix M. jannaschii/T. maritima Late Stationary Phase**
T-67	**Pure T. maritima Mid-Log Phase**
T-68	**Pure T. maritima Early Stationary Phase**
T-69	**Pure T. maritima Late Stationary Phase**
T-70	**T. maritima Pure Culture**
T-71	**Mix T. maritima/Pfu Culture**
T-72	**Chemostat Cellobiose**
T-73	**Chemostat Celobiose and Maltose**
T-74	**Chemostat Maltose**
T-75	**Chemostat Celobiose and Maltose**
T-76	**Cellobiose Batch**
T-77	**Cellobiose and Sulfur Batch**
T-78	**Maltose Batch**
T-79	**Maltose and Sufur Batch**

Figure 2. Heat plot representation of transcriptional changes in *P. furiosus* as determined be cDNA microarray analysis. Red coloring represents higher log square mean transcription compared to the average gene. Green denotes lower average transcription , while black is an average transcriptional level within +/- 1 fold. Grey cells indicate that there is no data available for that particular condition. Along the vertical axis are the protease found in *P. furiosus* and each column represent a separate experimental condition.

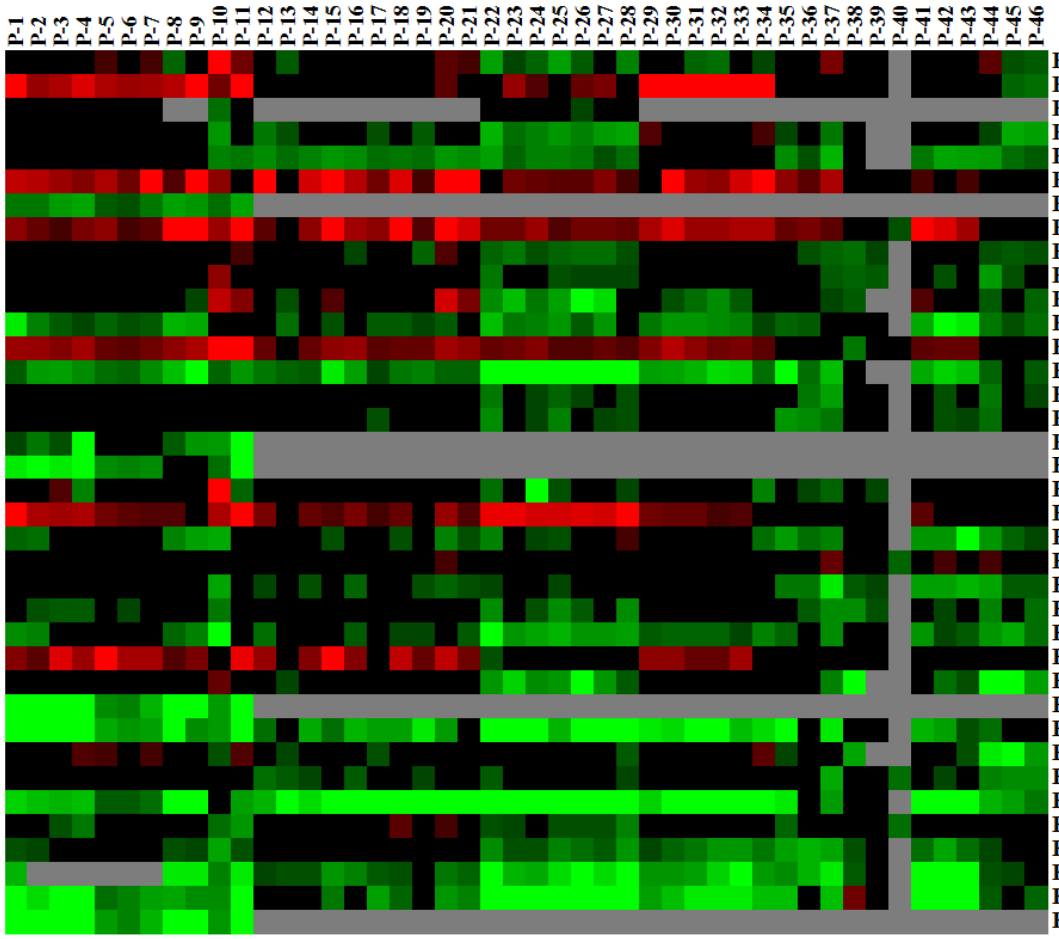

PF0115	ATP-dependent 26S proteasome ATPase
PF0159	20S proteasome, β2 protein
PF0167	Membrane-associated protease (putative)
PF0172	Metal-dependent proteases (putative)
PF0240	Periplasmic serine proteases (putative*)
PF0287	Pyrolysin
PF0313	Signal peptidase I (putative)
PF0318	Aminopeptidases/acylpeptide hydrolase (putative*)
PF0369	TET Aminopeptidase
PF0392	Membrane-associated protease (putative)
PF0456	Metallo carboxypeptidase
PF0457	Membrane-associated protease (putative)
PF0467	Lon protease (putative*)
PF0473	Endopeptidase (putative)
PF0541	Methionine aminopeptidase (putative*)
PF0617	Hydrogenase-processing endopeptidase (putative)
PF0688	Subtilisin-like serine protease (putative)
PF0702	Proline dipeptidase (putative)
PF0747	Proline dipeptidase (putative)
PF0825	Prolyl oligopeptidase
PF0874	Zn-dependent dipeptidase (putative)
PF1185	Acetylornithine deacetylase (putative)
PF1299	Pyroglutamyl peptidase (putative)
PF1343	Proline Aminopeptidase (putative)
PF1404	20S proteasome, β1 protein
PF1547	TET Aminopeptidase
PF1571	20S proteasome, α Protein
PF1583	Serine-like signal peptide peptidase (putative*)
PF1670	Subtilisin-like serine proteases (putative*)
PF1719	Intracellular protease (putative)
PF1861	Lysine Specific Aminopeptidase
PF1905	Serine protease (putative)
PF1924	Aminopeptidase DmpA (putative)
PF2048	Succinyl-diaminopimelate desuccinylase (putative)
PF2059	Aminopeptidase N (putative)
PF2063	Aminopeptidase N (putative)
PF2065	Aminopeptidase N (putative)

Figure 2 continued

Key of Conditions Tested

P-1	Maltose Chemostat m=0.45	P-24	Maltose
P-2	Cellobiose Chemostat m=0.45	P-25	Maltose/Cellobiose Mix
P-3	Cellobiose/Sulfur Chemostat m=0.45	P-26	Pullulan
P-4	Maltose/Sulfur Chemostat m=0.45	P-27	Starch
P-5	Maltose 5 hr	P-28	Trehalose
P-6	Maltose 8 hr	P-29	Growth Phase 6 hr
P-7	Maltose 16 hr	P-30	Growth Phase 8 hr
P-8	Cellobiose	P-31	Growth Phase 10 hr
P-9	Cellobiose/Sulfur	P-32	Growth Phase 12 hr
P-10	Mix Tma/Pfu Culture in BSM Media	P-33	Growth Phase 16 hr
P-11	Pure Pfu Culture in BSM Media	P-34	Chemostat Biofilm vs. Plantonic Cells (150 hr)
P-12	Barley	P-35	Dynamic Heat Shock on Maltose (Baseline)
P-13	Cellobiose	P-36	Dynamic Heat Shock on Maltose (0 min)
P-14	Chitin	P-37	Dynamic Heat Shock on Maltose (5 min)
P-15	Cellobiose/Sulfur	P-38	Dynamic Heat Shock on Maltose (30 min)
P-16	Laminarin	P-39	Dynamic Heat Shock on Maltose (60 min)
P-17	Maltose	P-40	Dynamic Heat Shock on Maltose (90 min)
P-18	Maltose/Sulfur	P-41	Dynamic Heat Shock on Tryptone (Baseline)
P-19	Starch	P-42	Dynamic Heat Shock on Tryptone (0 min)
P-20	Tryptone (no yeast extract or sulfur)	P-43	Dynamic Heat Shock on Tryptone (5 min)
P-21	Tryptone with Sulfur	P-44	Dynamic Heat Shock on Tryptone (30 min)
P-22	Cellobiose	P-45	Dynamic Heat Shock on Tryptone (60 min)
P-23	Glycogen	P-46	Dynamic Heat Shock on Tryptone (90 min)

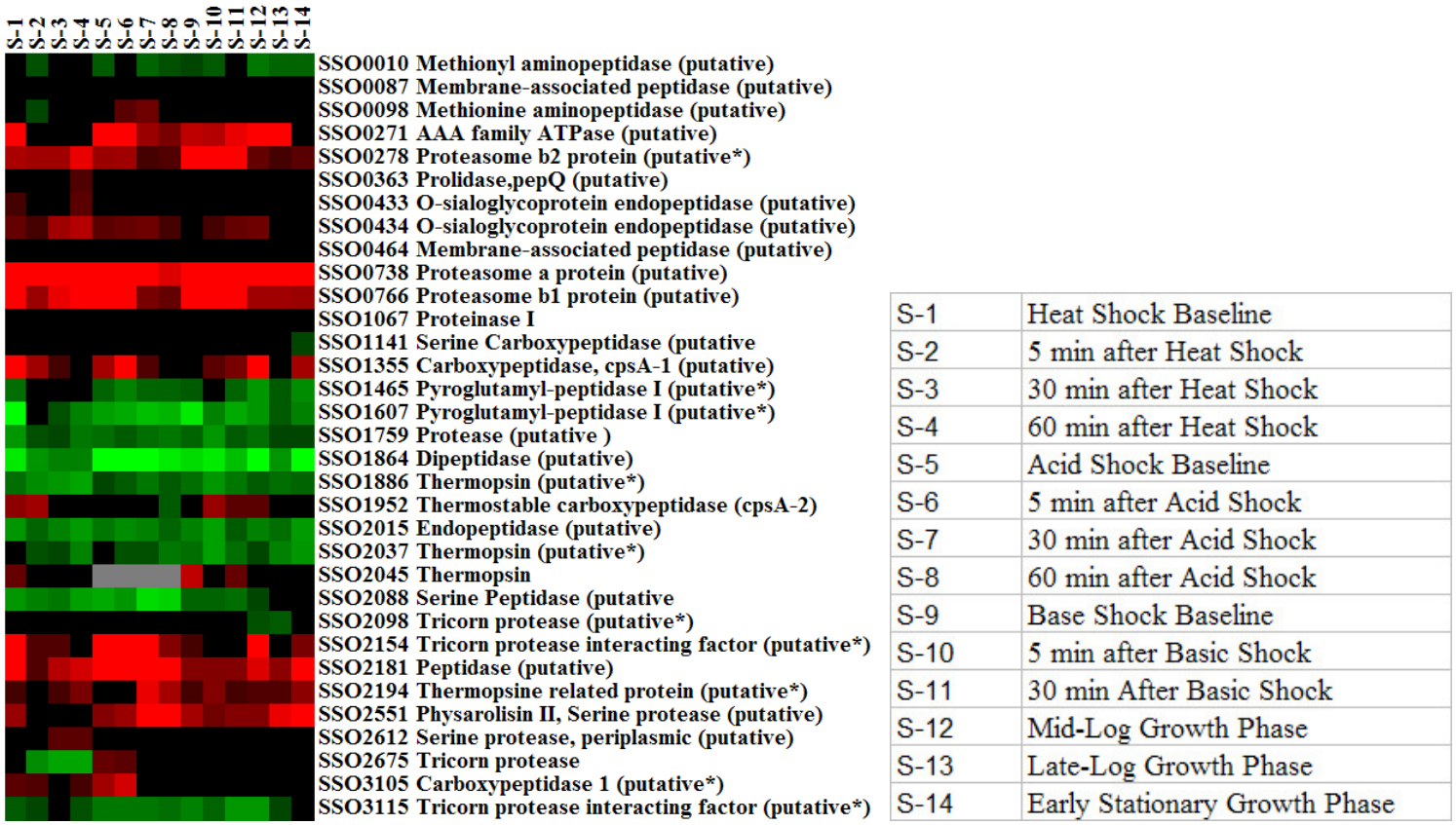

S-1	Heat Shock Baseline
S-2	5 min after Heat Shock
S-3	30 min after Heat Shock
S-4	60 min after Heat Shock
S-5	Acid Shock Baseline
S-6	5 min after Acid Shock
S-7	30 min after Acid Shock
S-8	60 min after Acid Shock
S-9	Base Shock Baseline
S-10	5 min after Basic Shock
S-11	30 min After Basic Shock
S-12	Mid-Log Growth Phase
S-13	Late-Log Growth Phase
S-14	Early Stationary Growth Phase

Figure 3.Heat plot representation of transcriptional changes in *S. solfataricus* as determined be microarray analysis. Red coloring represents higher log square mean transcription compared to the average gene. Green denotes lower average transcription , while black is an average transcriptional level within +/- 1 fold. Grey cells indicate that there is no data available for that particular condition. Along the vertical axis are the protease found in *S. solfataricus* and each column represent a separate experimental condition. The key describing the conditions listed in each column is shown to the right.

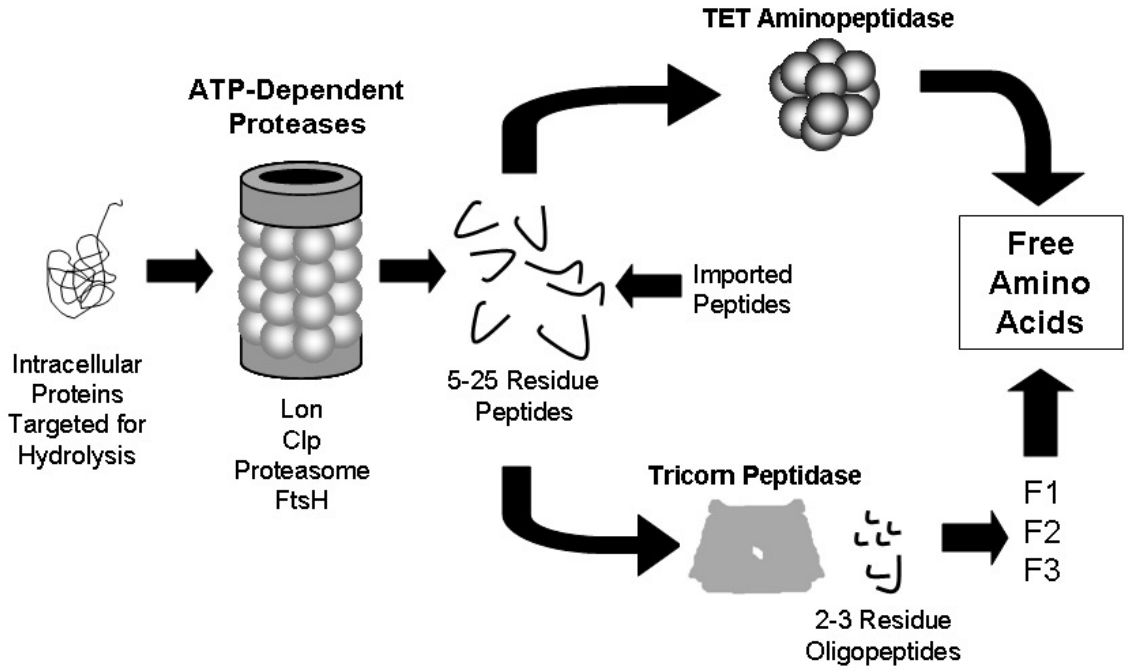

Figure 4. Proposed proteolytic system for degradation of intracellular proteins and imported peptides in which ATP-dependent protease products are degraded by either the TET Aminopeptidase or Tricorn Peptidase pathway.

Figure 5. Alignment of M42 family aminopeptidases from the hyperthermophilic organisms *P. horikoshii*, *P. furiosus*, *T. maritima*, *M. jannaschii*, and *A. fulgidus*.

```
PH0519 -------MMSMIEKLKKFTQIPGISGYEER-IREEIIREIKDFAD-YKVDAIGNLIVELG 51
PH1527 ---MEVRNMVDYELLKKVVEAPGVSGYEFLGIRDVVIEEIKDYVDEVKVDKLGNVIAHKK 57
PH0737 -------MERIVKILREILEIPSPTGYTKE-VMSYLEKFLKENEVNFYYTNKG---ALIA 49
PH1821 MDLKGGESMVDWKLMQEIIEAPGVSGYEHLGIRDIVVDVLKEVADEVKVDKLGNVIAHFK 60
TM1048 ------MKMETGKLLMELSNLDGPSGYETN-VVSYIKSVIEPFVDEAKTTRHGSLIGYKK 53
TM1049 ------------MYLKELSMMPGVSGDEGK-VRDFIKSKIEGLVDNLYTDVLGNLIALKR 47
TM1050 ----------MKELIRKLTEAFGPSGREEE-VRSIILEELEGHIDGHRIDGLGNLIVWK- 48
PF0369 --------MKLIEMLKEITQVPGISGYEER-VREKIIEWIKDYAD-YKVDEIGNLIVELG 50
PF1547 --------MVDYELLKKVVEAPGVSGYEFMGIRDVVIEEIKDYVDEVNVDKLGNVIAHKK 52
PF1861 --------MVDWELMKKIIESPGVSGYEHLGIRDLVVDILKDVADEVKIDKLGNVIAHFK 52
AF1795 -------------------------------------------------MGNLICTKN 9
MJ0555 --------MSVVEYLKKLSKLHGISGREDS-VREFMKKELEKYCDSVEIDNFGNLIAKRG 51
                                                          *

PH0519 EGEER--ILFMAHMDEIGLLITGITDEGKLRFRKVGGIDDRLLYGRHVNVVTEKGI-LDG 108
PH1527 GEGPK--VMIAAHMDQIGLMVTHIEKNGFLRVAPIGGVDPKTLIAQRFKVWIDKGKFIYG 115
PH0737 GNHPKPELVVIAHVDTLGAMVKEILPDGHLAFSRIGGLVLPTFEGEYCTIITRKGKKFRG 109
PH1821 GSSPR--IMVAAHMDKIGVMVNHIDKDGYLHIVPIGGVLPETLVAQRIRFFTEKGE-RYG 117
TM1048 GKGIG-KLAFFAHVDEIGFVVSKVEG-QFARLEPVGGVDPKVVYASKVRIYT-----KNG 106
TM1049 GRDSSKKLLVSAHMDEVGFVVSKIEKDGKVSFLPVGGVDPRILPGKVVQVKN-----LKG 102
TM1050 GSGEK-KVILDAHIDEIGVVVTNVDDKGFLTIEPVGGVSPYMLLGKRIRFENG----TIG 103
PF0369 EGEVK--AVFMAHMDEIGLLITGITQDGKLRFRKVGGIDDRLLYGRHVDVITENGK-LDG 107
PF1547 GEGPK--VMIAAHMDQIGLMVTHIEKNGFLRVAPIGGIDPRTLIAQRFKVWIDKGKFIYG 110
PF1861 GSAPK--VMVAAHMDKIGLMVNHIDKDGYLRVVPIGGVLPETLIAQKIRFFTEKGE-RYG 109
AF1795 GGEPE--IMVAAHMDEIGFAVKYIDDKGFIRIAPIGGWFSQIALAQRVVLYGKK-K-VYG 65
MJ0555 NKGKK--IMIAAHMDEIGLMVKYIDDNGFLKFTKIGGIYDPTILNQKVVVHGSKGD-LIG 108
                . **:* :*  :. :       .  :**           .         *

PH0519 VIGATPP--HLSL--ERDKSVIPWYDLVIDIGAESKEEALEL-VKPLDFAVFKKHFSVLN 163
PH1527 VGASVPP--HIQK-PEDRKKAPDWDQIFIDIGAESKEEAEDMGVKIGTVITWDGRLERLG 172
PH0737 TLLLRNPSAHVNREVGKKERKEENMYIRLDELVEKREDTEKLGIRPGDFIAFDPKFEYV- 168
PH1821 VVGVLPP--HLRRGQEDKGSKIDWDQIVVDVGASSKEEAEEMGFRVGTVGEFAPNFTRLN 175
TM1048 IERGVIG--MLAP-HLQDS-ESRKKVLTYDEIFVDLSLCERD-VRVGDIAVIDQTAFET- 160
TM1049 VIGYRPI--HLQR-DEENT-PPRFENLRIDFGFSSADEAKKY-VSIGDYVSFVSDYIEK- 156
TM1050 VVGMEGE--TTEE-RQENVRKLSFDKLFIDIGANSREEAQKM-CPIGSFGVYDSGFVEV- 158
PF0369 VIGALPP--HLNV--KGVKDVVPWYQLTIDIGAESKEEALSLGVKPLDYAVFKKHFSVLN 163
PF1547 VGGSVPP--HIQK-PEDRKKAPDWDQIFIDIGAESKEEAEELGVKIGTIVTWDGRLERLG 167
PF1861 VVGVLPP--HLRREAKDQGGKIDWDSIIVDVGASSREEAEEMGFRIGTIGEFAPNFTRLS 167
AF1795 VIGCKPP--HLMK-DEERKKGIEIKDMFVDIGASSKEEVLEMGINVGTPVALDREIVELA 122
MJ0555 VLGSKPP--HRMK-EEEKTKIIKYEDMFIDIGAESREEAIEMGVNIGTWVSFLSEVYDLG 165
                              :  *    . .

PH0519 GKYVSTRGLDDRFGVVALIEAIKDLVDHELEGKVIFAFTVQEEVGLKGAKFLANHYYPQY 223
PH1527 KHRFVSIAFDDRIAVYTILEVAKQLK--DAKADVYFVATVQEEVGLRGARTSAFGIEPDY 230
PH0737 NGFVKSHFLDDKASVAAILDLIIDMKDELEKYPVAFFFSPYEEVGHGGS--AGYPPTTKE 226
PH1821 EHRFATPYLDDRICLYAMIEAARQLG--DHEADIYIVGSVQEEVGLRGARVASYAINPEV 233
TM1048 NGKVVGKALDNRASCGVLVKVLEFLKRYDHPWDVYVVFSVQEETGCLGALTGAYEINPDA 220
TM1049 NGRAVGKAFDDRAGCSVLIDVLESG--VSPAYDTYFVFTVQEETGLRGSAVVVEQLKPTC 214
TM1050 SGKYVSKAMDDRIGCAVIVEVFKRIK---PAVTLYGVFSVQEEVGLVGASVAGYGVPADE 215
PF0369 NKIVSTRSLDDRFGVVALVQAIRNLVDHELSGKFIFAFTVQEEIGLKGAKFLAEKYSPEY 223
PF1547 KHRFVSIAFDDRIAVYTLIETARQLQ--DTKADIYFVATVQEEVGLRGARTSAFGINPDY 225
PF1861 EHRFATPYLDDRICLYAMIEAARQLG--EHEADIYIVASVQEEIGLRGARVASFAIDPEV 225
AF1795 NGRITGKAFDNRVGVAVMIEAVRRAK---ADITIHAVATVQEEVGLKGARTSAFAIEPTA 179
MJ0555 KNRLTGKAFDDRVGCAVLLEVMKRLSEEDIDCQVYAVGTVQEEVGLKGARVSAFKINPDV 225
              :*::    .:::.                 :  ** *  *:        .
```

```
PH0519 AFAIDSFACCSPLTGDVK-----LGKG---PVIRAVDNSAIYSRDLARKVWSIAEKNGIE 275
PH1527 GFAIDVTIAADIPGTPEHKQVTHLGKGTAIKIMDRS---VICHPTIVRWLEELAKKHEIP 287
PH0737 LLVVDMGVVGEGVSGKET-----------AVSIAAKDTTGPYDYDMTNRLIELAEENNIP 275
PH1821 GIAMDVTFAKQP--HDKGKIVPELGKG---PVMDVG---PNINPKLRAFADEVAKKYEIP 285
TM1048 AIVMDVTFASEPPFSDH----IELGKG---PVIG---LGPVVDRNLVQKIIEIAKKHNVS 270
TM1049 AIVVETTTAGDNPELEERKWATHLGDG---PAITFYHRGYVIPKEIFQTIVDTAKNNDIP 271
TM1050 AIAIDVTDSADTPKAIKR-HAMRLSGG---PALKVKDRASISSKRILENLIEIAEKFDIK 271
PF0369 AFAIDSFACCSELTGDVR-----LGGG---AVIRAVDNSAIYSRDLARKVWEIAEKNNIP 275
PF1547 GFAIDVTIAADVPGTPEHKQVTQLGKGTAIKIMDRS---VICHPTIVRWMEELAKKYEIP 282
PF1861 GIAMDVTFAKQP--NDKGKIVPELGKG---PVMDVG---PNINPKLRQFADEVAKKYEIP 277
AF1795 AIAVDTCVAADFPGSESAHMDVKLGKGAAITVIDASGRGLIASPKVLRWLTETAEKYGIP 239
MJ0555 AIALDVTIAGDHPGIKKEDAPVDLGKGPVVGIVDASGRGLIAHPKVLDMIKAVSEKYKID 285
        :.::     .                     :           :       :::  :

PH0519 IQIGVTGG--GTDASAFQDRSK---TLALSVPIKYLHSEVETLHLNDLEKLVKLIEALAF 330
PH1527 YQLEILLG-GGTDAGAIHLTKAGVPTGALSVPARYIHSNTEVVDERDVDATVELMTKALE 346
PH0737 YVVDVFPY-YGSDGSAALRAGWDFRVALIGPGVHASHG-MERTHVKGLLATKELIRAYIK 333
PH1821 LQVEPSPRPTGTDANVMQINREGVATAVLSIPIRYMHSQVELADARDVDNTIKLAKALLE 345
TM1048 LQEEAVGGRSGTETDFVQLVRNGVRTSLISIPLKYMHTPVEMVDPRDVEELARLLSLVAV 330
TM1049 FQMKRRTAG-GTDAGRYARTAYGVPAGVISTPARYIHSPNSIIDLNDYENTKKLIKVLVE 330
TM1050 YQMEVLTFG-GTNAMGYQRTREGIPSATVSIPTRYVHSPSEMIAPDDVEATVDLLIRYLG 330
PF0369 IQIGVTGG--GTDASVFQHKSK---VLALSVPMKYLHSEVEMLNVKDLEALIALIEAITF 330
PF1547 YQWDILLG-GGTDAGAIHLTRAGVPTGAVSIPARYIHSNAEVVDERDVDASVKLMVKVLE 341
PF1861 LQVEPSPRPTGTDANVMQINREGVATAVLSIPIRYMHSQVELADARDVDNTIKLAKALLE 337
AF1795 YQLEVAEG-GTTDATAIHLTKAGIPAGVVSVPARYIHSPVEVVDLKDVESAVEIVARAIE 298
MJ0555 VQWEVGEG-GTTDATAIHLTREGIPTGVISVPARYIHTPVEVIDKRDLEKTVELVYNCIK 344
                ::              :.   :  *   .     .     :

PH0519 EL------- 332
PH1527 NIHELKI-- 353
PH0737 WKG------ 336
PH1821 ELKPMDFTP 354
TM1048 ELEV----- 334
TM1049 EGKIVEVVS 339
TM1050 A-------- 331
PF0369 EI------- 332
PF1547 HIHELKI-- 348
PF1861 ELKPMDFTP 346
AF1795 NAKNYF--- 304
MJ0555 EVNNFF--- 350
```

Chapter 2

The Archaeal 20S Proteasome

A Thermostable Model System for the Core Particle (CP)

Joshua K. Michel and Robert M. Kelly

In Press: Chapter 20 of Thermophiles: Biology and Technology at High Temperatures

Introduction

The 20S proteasome (also referred to as the core particle, CP) is a cylindrically shaped protease ubiquitous to both Archaea and Eukarya.[1,2] The 20S proteasome has also been found in the actinomycetes *Rhodococcus erythropoli*[3], *Myobacterium tuberculosis*[4], *Streptomyces coelicolar*[5], and *Frankia*.[6] The lack of proteasome genes encoded in other bacterial genomes suggests that the actinomycetes acquired the proteasome by lateral gene transfer.[7] Most bacteria contain a related complex, ClpQY (or HslVU), that shares a similar catalytic mechanism to the proteasome and apparently plays a similar functional role.[8]

The eukaryotic and archaeal 20S proteasomes share a similar overall size and structure, but differ in complexity – the archaeal proteasome is based on fewer unique proteins (which may be processed prior to being incorporated into the macromolecular complex as subunits). As such, the 20S archaeal proteasome serves as a simpler model system for examining the significance of subunit composition on biochemical, biophysical and functional properties of the multimeric protease. In addition, the archaeal proteasome, presumably related to the ancestral eukaryotic proteasome precursor, may provide insight into how eukaryotic proteasomes developed into the complex proteases that now exist.

20S Proteasome Structure

The 20S proteasome from the thermophilic archaeon *Thermoplasma acidophilum* was the first archaeal proteasome structure resolved and subsequently has been found to be closely related to all archaeal proteasomes examined to date.[2,9-13] Like its eukaryotic

counterpart, the 20S archaeal proteasome is composed of four stacked heptametric rings that form a barrel-like structure with a hollow channel extending down the center.[14] The hollow channel is comprised of three cavities consisting of two antechambers formed by the α rings and a central channel formed by the β rings.[9] To prevent undesirable protein degradation in the cytosol, active sites are compartmentalized within the interior channel of the 20S proteasome. The overall length of the cylindrical enzyme is 148 Å with maximum and minimum diameters of 113 Å and 75 Å, respectively.[9] Each homomeric ring is composed entirely of either α or β subunits, arranged in the order $\alpha_7\beta_7\beta_7\alpha_7$, as shown in Figure 1. The catalytic core consists of 6 to 14 active sites (typically involving a Threonine [Thr] residue) located on the N-terminal regions of the β subunits.[15,16] Access to the central chamber of the archeal 20S proteasome is facilitated through 13 Å openings on either end of the cylinder.[17] Comparatively, the eukarotic 20S proteasome core is inaccessible through the ends, except by major rearrangement of the α subunit N-termini that creates an opening of 10 Å.[15] Unlike eukaryotic genomes that have been found to encode up to 23 unique proteasome α/β subunit proteins, the *T. acidophilum* proteasome is comprised of only two different subunits (one α and one β) with molecular weights of 20 and 35 kDa, respectively.[17,18] This simple basis for 20S proteasome structure is typical among all archaea, whose genomes encode between 2 and 4 different α/β subunit proteins.[19-21]

20S Proteasome Assembly

The creation of the 20S proteasome is a complex process in which α proteins self-assemble into rings that then act as scaffolds for the subsequent ß ring formation.[22,23] The

result is a half-proteasome complex, with an approximate size of 300 kDa. These ring-dimers in turn associate and cleave the β pro-pepide to form the complete and functional 600-700 kDa enzyme.[24] As one of several measures to prevent to unwanted proteolysis, the β proteins cannot form ring structures in the absence of α proteins.[25] For *Archaeoglobus fulgidus*, there is no major conformational change of contact areas after formation of the α-β complex, suggesting that these regions are complementary prior to assembly.[26] This assembly process appears to be conserved across all archaea, but as structural complexity increases (more than one α and/or β subunit type) so do the assembly mechanisms.[24]

For many thermophilic archaea*, in vitro* combination of the α and β proteins leads to spontaneous self-directing assembly of the 20S proteasome, without need for chaperones or other accessory proteins.[20,27] However, this process can be extremely inefficient, such as is the case for the *Methanosarcina thermophila* 20S proteasome in which only 50% of the β proteins were processed and incorporated into a fully active 20S CP.[25] Likewise, the assembly of the *Pyrococcus furiosus* 20S proteasome at physiologically relevant temperatures yielded a substantial amount of unincorporated β proteins.[28] The recombinant 20S proteasome from *Methanococcus jannaschii* required denaturation of α and β subunits with urea, followed by their combination at high temperature and subsequent refolding by removal of the denaturant using dialysis. Without unfolding-refolding of the *M. jannaschii* proteasome, an active enzyme was produced, but with a markedly decreased optimal temperature (95ºC) compared to the native version

(119ºC).[29] Presumably, the native intracellular assembly environment increases the folding efficiency of 20S proteasomes.

As a safeguard to unwanted proteolysis prior to assembly, β proteins are expressed as precursors that undergo self-processing (removal of ~10 N-terminal amino acid residues to expose the active site Thr) during assembly into the active structure.[25,26,30,31] The precursor N-terminal region in yeast is essential for proper incorporation of the β subunit into the proteasome[32], thus acting as an intramolecular chaperone. Conversely, β proteasome incorporation in *T. acidophilum,* showed no dependence on the pro-peptide region[22], indicating that the archaeal β pro-peptide functions solely as a temporary inhibitor of proteolysis. The pro-peptide also acts to protect the active site; premature processing of the β protein results in acetylation of Thr residues, yielding an inactive enzyme.[32] Cleavage of the pro-peptide occurs during combination of dimer rings into a fully functional 20S proteasomes.[33] The processing of the β-pro-peptide appears to be intramolecular and autocatalytic in nature, while the α protein is not subject to any cleavage.[31]

The N-terminal region of the α subunit contains an α-helix that is required for proper ring formation.[22] While the α proteins do not contain a pro-peptide sequence, it has been suggested that the archaeal α subunits may be subjected to post-translational modification, such as phosphorylation.[34,35] The influence and purpose of α protein modifications on the 20S proteasome's interaction with regulatory proteins such as PAN (proteasome-activating nucleotidase) have yet to be fully elucidated.

Role of α Subunits

Access to the 20S proteasome interior is regulated by the α subunits, which in eukaryotes form a stable plug on each end of the cylinder.[15] In yeast, extension of the N-termini from $\alpha_{1,2,3,6,7}$ prevents access of proteins to the center chamber; multiple hydrogen bonds are formed between the overlapping α subunit N-termini, contributing significantly to the stability of the "gates".[15,36] Opening of the 20S eukaryotic proteasome axial channel is facilitated by attachment of the 19S regulatory component.[37-39] Combination of the 19S and 20S proteasomes, into the 26S complex, creates an enzymatic machine cable of selectively degrading ubiquitin-tagged proteins.[40-43] Conversely, 20S proteasome structures from *T. thermophila* and *A. fulgidus* show disorder among the α N-termini with the presence of only 1 hydrogen bond between the Asp9 and Tyr8 residues of adjacent α subunits.[9,17,26] Lack of α subunit interaction contributes to N-terminal flexibility of archaeal proteasomes, which allows entry of unfolded proteins and peptides without need for the ATP-dependent protein PAN.[44,45]

Hyperthermophilic archaea encode both single and multiple homologs of α and ß proteasome components, as shown in Table 1. The rarity of archaeal genomes encoding multiple α proteins supports genome sequence data suggesting β differentiation evolutionarily predated that of the α-subunits.[46] One example of α differentiation is found in the native proteasome from *Methanosarcina thermophila*, which contain multiple α subunits differing in length by 4 amino acids, but encoded by the same gene.[47] The difference in α subunit length has been attributed to three potential translation start sites within the α gene.[25] Alternatively, multiple native 20S proteasome sub-types have

also been found in the haloarchaea; *Haloferax volcanii* produces at least 2 distinct proteasome sub-types resulting from 2 unique α genes.[48] Immunoanalysis of the *H. volcanii* proteasome shows the α_1 subunit represented 60% of incorporated α protein, while α_2 comprised the other 40%.[48] However, α_2 has exhibited a 7-fold transcriptional increase during the transition from exponential growth to stationary phase,[49] indicating the involvement of post-translational mechanisms to regulate subunit levels.[49] While noted for a limited number of archaeal proteins,[50-52] α_1 and α_2 proteins have been found subject to N-terminal acetylation.[34] Alternatively, *H. volcanii* may alter proteasome composition to better adapt to certain growth phase conditions. With the limited data available for multiple α proteins in Archaea, the impact of different α subunits on structure and activity is largely unknown.

In eukaryotic organisms, the 20S proteasome is distributed throughout the cellular space,[53] but during mitosis there is an increased movement of proteasomes to the nucleus.[54] In solid tumor cells, cellular stress (e.g., hypoxia and starvation) causes nuclear localization of the proteasome, which subsequently induces drug resistance.[55] Nuclear localization signals (NLS), found on the α subunits, facilitate intracellular proteasome transport; a highly similar sequence to the NLS is also found on the *T. acidophilum* α-subunit.[56] The production of a recombinant version of this archaeal proteasome in mouse cells results in active import of the *T. acidophilum* proteasome into the nucleus.[57] Since *T. acidophilum* does not contain a nucleus, this NLS-similar sequence may represent an alternative signal that later developed into the NLS of eukaryotic organisms. Observations that *T. acidophilum* cell-lysate facilitates the nuclear import of both human

and *Thermoplasma* proteasome[58] supports the use of the archaeal system as a model for NLS-mediated relocation.

Role of β Subunits

Eukaryotic organisms ubiquitously encode a highly diversified set of subunit proteins: the yeast proteasomes consist of 7 α and 7 β subunits, while mammalian cells encode for 7 α and 10 β proteins.[10] The 14 different subunits encoded by yeast are essential for cellular survival under standard growth conditions.[32,59,60] Other efforts with eukaryotic organisms demonstrated significant cellular changes from loss of proteasome subunit function.[61,62] The presence of three γ–inducible, mammalian proteasome β subunits has been linked to production of alternative degradation products for antigenic presentation on cellular surfaces.[63] Similarly, *Drosophila melanogaster* produces 6 male-specific 20S proteasome subunit isoforms only during late spermatogenesis.[64] Functional requirement for proteasome activity varies by organism, and may depend on the availability of complementary proteases to compensate for proteasome loss.[21] Mutation of the 20S proteasome in *Mycobacterium smegmatis* showed no effect on cellular growth or degradation of peptides, but in *Mycobacterium tuberculosis* the proteasome was required for growth during oxidative or nitrosactive stress.[4,65] For eukaryotes, the large number of proteases encoded in their genomes makes determination of proteasome-specific functions difficult.

Native versions of the archaeal proteasome have been isolated and characterized from *P. furiosus,*[66] *M. jannaschii,*[67] *M. thermophila,*[47] *H. volcanii,*[35] and *Haloarcula*

marismortui.[68] Inhibition of the entire *T. acidophilum* 20S proteasome impacted cellular survival during heat stress.[69] Proteasome inhibition studies carried out in *H. volcanii* demonstrated that the lack of an active 20S proteasome led to a 30% decrease in growth rate under otherwise optimal conditions.[70] The necessity of proteasome function during stress conditions most likely stems from this protease's ability to degrade large unfolded, misfolded, and damaged proteins.

The genomes of *M. thermophila*, *H. volcanii*, *M. jannaschii* and *A. fulgidus* encode only single versions of α and β proteins.[71] On the other hand, the genomes of *Sulfolobus solfataricus* and *P. furiosus* contain a single α protein gene and two distinct β protein genes.[21] The purpose and function of these additional β subunit homologs in archaeal proteasomes is not known, although this simple model could offer insight into the maturation of the diverse set of homologous β subunits found in eukaryotes.

Transcriptional response studies on hyperthermophilic archaea containing proteasomes comprised of single α and ß subunits show a consistent tendency for higher transcription of β during stress conditions. The *A. fulgidus* proteasome exhibited a 2.7-fold decrease in transcription of the α gene after heat shock, while transcripts for β exhibited a slight increase.[72] *M. jannaschii* showed no significant change in transcription of 20S proteasome genes in response to a 10ºC temperature increase.[73] But, *M. jannaschii* did respond to a 20ºC decease in temperature with a 2.3-fold increase in β transcription, while α remained unchanged.[73] The increased *M. jannaschii* β transcription during cold shock may be related to the difficulty of proteasome formation at sub-optimal

conditions.[29,74] In addition, the α protein of *M. jannaschii* is unique because of the conservation of amino acid residues associated with the active site of β, which may result in transcriptional trends differing from other archaea. These conserved residues in the *M. jannaschii* α protein are likely a remnant from times before differentiation of α and β.

Unlike the case in eukaryotes, in which some multiple versions of α and β proteins have been observed to share 90% identical protein sequences,[75] the two *P. furiosus* β proteins are only 48% identical at the amino acid level.[28] This suggests that the β subunits can play distinct roles in *P. furiosus* CP structure and function. Transcriptional analysis of the three subunits from *P. furiosus* showed that, under heat shock conditions, the α gene was down-regulated 2.0-fold, β_1 increased 2-fold, and β_2 remained relatively constant. The decreased transcription of the *P. furiosus* α subunit is consistent with results for heat shocked *A. fulgidus,*[72] and may relate to the inherent thermal stability of α proteins compared with β. The *P. furiosus* β_1 and β_2 proteins exhibit melting temperatures of 104.4ºC and 93.1ºC respectively[28], while the α protein is estimated to melt at approximately 135ºC.[76]

For *P. furiosus*, active recombinant enzymes can be formed from combinations of α and β_2, as well as $\alpha+\beta_1+\beta_2$.[28] When these enzymes were assembled at 90ºC, the version with β_1 demonstrated a slightly higher activity. However, versions containing $\alpha+\beta_1+\beta_2$ assembled at 105°C demonstrated significantly higher activity and thermostability. Two-dimensional gel electrophoresis showed a greater amount of β_1, compared to β_2, incorporated into the recombinant *P. furiosus* proteasome at higher assembly

temperatures.[28] Native proteasomes isolated from *P. furiosus* cells grown under heat shock conditions demonstrated a ratio of β_1 to β_2 similar to the ratio noted for the recombinant enzymes assembled at higher temperatures; native proteasomes from non-stressed cells contained a lower amount of β_1, as shown in Figure 2. This suggests that the β_1 subunit, while not essential for catalytic activity, plays a role in stabilizing and activating the *P. furiosus* CP assembly, particularly at supraoptimal temperatures such as those encountered during thermal stress events. Furthermore, the response of *P. furiosus* to produce proteasomes with higher β_1 content was controlled at both the transcriptional level and during enzyme assembly.

For the hyperthermophilic archaea, it is not clear whether CPs with 2 β subunits create any special physiological or ecological advantages during thermal stress response. Perhaps hyperthermophiles whose genomes encode 2 β proteins experience frequent temperature excursions in their natural habitats. Recent results from our laboratory showed that when *S. solfataricus* was shifted from optimal (80°C) to supraoptimal (90°C) temperatures, the transcription of ORFs encoding CP proteins (α, β_1, β_2) were unaffected throughout the 60 min period following the temperature shift.[77] However, it was also noted that the transcriptional level of CP proteins in *S. solfataricus* were much higher than in *P. furiosus* under both normal and stressed conditions. In any case, these data suggest that the impact of CP β subunit content on function at suboptimal, optimal and supraoptimal temperatures merits further examination.

The relative conservation of proteasome constituent proteins across all domains of life is a primary reason that archaeal proteasomes can serve as model systems for investigating structure and function issues of this complex protease. In fact, recombinant 20S proteasome proteins form active proteases when combined with pro-subunits from different organisms. The possibility to form a hybrid proteasome, consisting of subunits from different organisms was first noted for *Aeropyrum pernix* and *A. fulgidus*.[26] The α protein from *A. fulgidus* has recently demonstrated the ability to form active proteasome CPs when combined with either *P. furiosus* β_1, β_2, or the combination of both β_1 and β_2.[76] In addition to the creation of a hybrid CP, the formation of an active enzyme by *A. fulgidus* α + *P. furiosus* β_1 was interesting since *P. furiosus* β_1 does not from an active CP when combined with *P. furiosus* α.[28] While intra-domain hybrid 20S proteasomes are fully assembled and active, the creation of inter-domain hybrids has yet to be demonstrated. Formation of such hybrids might be biotechnologically relevant in light of reports demonstrating the *in vivo* degradation of aggregation-prone proteins by a mesophilic archaeal proteasome expressed in mammalian cells.[78]

Proteasome Biocatalysis

The 20S proteasome is a member of the T1 peptidase family[71] characterized by an N-terminal Thr nucleophile.[79] While initial observations noted that a Ser residue could be substituted in place of Thr without modifying hydrolysis of LLVY-Amc[80], it was subsequently shown that the cleavage pattern was impacted as a result of the residue change.[81] The hydroxyl group of Thr apparently initiates hydrolysis of the peptide bond, followed by nucleophilic attack from a water molecule resulting in peptide bond

cleavage.[81,82] Even though the substrate specificity of 20S proteasomes may vary, the N-terminal Thr residue is conserved in all known active β subunits.[1,19,20,27,43]

Individual β proteins comprising eukaryotic proteasome are associated with certain substrate specificities.[32] Yeast proteasome subunits β_1, β_2, and β_5 are linked to chymotrypsin-like, trypsin-like, and post-glutamyl peptide hydrolase-like activities, respectively.[15,59,83,84] The β_1 and β_2 active sites prefer cleavage after acidic and basic residues on the substrate protein or peptide.[85,86] However, while the three active sites differ in their cleavage preference, all contribute significantly to protein degradation.[87] The limited number of active sites (i.e., 3) in eukaryotic proteasomes differs significantly from the 14 active sites present in the archaeal CP that exhibit only chymotrypsin-like activity.

The increased number of active sites present in the archaeal proteasome has yet to be connected to a physiological role or advantage. In part, this is due to a lack of understanding of which factors influence activity and substrate specificity. A prime example is the *M. jannaschii* proteasome that consists of two unique subunits (α+β) with 14 active sites distributed in β chamber. The *M. jannaschii* native proteasome exhibits an optimal activity at 119ºC,[67] although recombinant versions showed optimal temperatures of 95ºC and 110ºC, depending on assembly conditions.[74] The recombinant *M. jannaschii* 20S proteasome with an optimal temperature closest to the native organism was subjected to chemical denaturation followed by refolding at elevated temperatures, thus demonstrating the importance of assembly conditions on enzyme function. In addition,

recombinant *M. jannaschii* proteasomes have demonstrated decreased enzymatic activity in response to high osmotic pressure, while the native enzyme exhibited increased protease activity under these conditions.[29] Most studies on native proteasomes have focused on structure, size, and substrate preferences. Table 2 summarizes the biochemical data available for several of the native archaeal proteasomes characterized to date; note that detailed kinetics are typically carried out only on recombinant versions such that information from such studies may not reflect *in vivo* properties (as shown in Table 3). The range of activities presented in Table 2 may indicate diversity within the archaeal 20S proteasome family; however, the complete picture remains unclear without detailed kinetics and cleavage patterns for the native enzymes. Inconsistencies in extents of protein purification make direct biocatalytic comparisons between specific proteasomes intractable. Differences between protocols and purification levels for native and recombinant proteasomes represent an obstacle to the more widespread use of archaeal 20S proteasomes as model systems.

The impact of multiple α or β proteins on archaeal proteasome biocatalysis has not been studied to any extent as yet. The 20S proteasome from *P. furiosus* has been examined along these lines and the presence of 2 alternative β pro-subunits impacted biocatalytic and biophysical properties.[66] For the *P. furiosus* CP, both the β_1 and β_2 proteins contain the conserved active site Thr residue, implying that 14 active sites are present in this enzyme. However, the increased incorporation of β_1 at 105ºC assembly (shown in Table 2) altered the substrate preference by increasing the degradation of LLVY-MCA compared to AAF-MCA [28]. Alternatively, a preference was shown for AAF-MCA by the

P. furiosus proteasome assembled at 90ºC (lower ratio of β_1). Furthermore, increased incorporation of β_1 into the CP yielded an enzyme with almost twice the V_{max} of the version with less β_1.[28] These results support a role for β_1 in both biocatalysis as well as structural integrity at elevated temperatures. It is worth noting that the kinetic properties of the recombinant *P. furiosus* 20S proteasome were consistent with previously reported values for the native CP in terms of both V_{max} (2200 pmol/min-μg) and K_m (0.46 mM) .[66]

Concluding Remarks

Archaeal 20S proteasomes have the potential to serve as simpler model systems for core particles from eukaryotic sources, especially in determining the role of α/β subunit composition in biochemical and physiological function. This is primarily due to the homogeneity of β subunits found within a single archaeal organism's proteasome. As more becomes known about the mechanisms of assembly, biochemical and biophysical characteristics, and cellular roles for archaeal 20S proteasomes, such information can be used as a basis to examine aspects of the complex heteromultimeric proteasome in eukaryotic systems. Additionally, the ease of recombinant production, assembly, and purification of thermophilic and hyperthermophilic proteasomes makes them attractive systems for study from a logistical perspective. One of the current disadvantages of using hyperthermophilic proteasomes as model systems is the lack of data regarding the enzyme's *in vivo* function. However, as genetic systems become more widely available for archaea, such as in the hyperthermophilic organisms *Thermococcus* KOD and *Sulfolobus* spp (see Chapters 11 and 13), the contribution of the 20S proteasome to cellular function can be scrutinized.[88-90] Furthermore, intriguing possibilities using

archaeal proteasomes for novel therapeutic strategies exist and merit further examination in their own right.[78]

ACKNOWLEDGMENTS

This work was supported in part by grants from the Biotechnology Program of the US National Science Foundation and the Energy Biosciences Program of the US Department of Energy. JK Michel acknowledges support from an NIH Biotechnology Traineeship.

References

1. Bochtler, M. et al., The proteasome, *Annu. Rev. Biophys. Biomol. Struct.*, 28, 295, 1999.
2. Barber, R.D. and Ferry, J.G., Archaeal proteasomes, *Methods Enzymol.*, 330, 413, 2001.
3. Tamura, T. et al., The first characterization of a eubacterial proteasome - The 2os complex of *Rhodococcus*, *Curr. Biol.*, 5, 766, 1995.
4. Darwin, K.H. et al., The proteasome of *Mycobacterium tuberculosis* is required for resistance to nitric oxide, *Science*, 302, 1963, 2003.
5. Nagy, I. et al., The 20S proteasome of *Streptomyces coelicolor*, *J. Bacteriol.*, 180, 5448, 1998.
6. Benoist, P. et al., High-molecular-mass multicatalytic proteinase complexes produced by the nitrogen-fixing *Actinomycete frankia* Strain Br, *J. Bacteriol.*, 174, 1495, 1992.
7. Lupas, A. et al., Self-compartmentalizing proteases, *Trends Biochem. Sci.*, 22, 399, 1997.
8. Bochtler, M. et al., Crystal structure of heat shock locus V (HslV) from *Escherichia coli*, *Proc. Natl. Acad. Sci. U. S. A.*, 94, 6070, 1997.
9. Lowe, J. et al., Crystal structure of the 20S proteasome from the archaeon *T. acidophilum* at 3.4 A resolution, *Science*, 268, 533, 1995.
10. Groll, M. and Huber, R. in *Ubiquitin And Protein Degradation, Part A* 329 (2005).

11. Groll, M. et al., A gated channel into the proteasome core particle, *Nat. Struct. Biol.*, 7, 1062, 2000.

12. De Castro, R.E. et al., Haloarchaeal proteases and proteolytic systems, *FEMS Microbiol. Rev.*, 30, 17, 2006.

13. Puhler, G. et al., Proteasomes - multisubunit proteinases common to Thermoplasma and Eukaryotes, *Syst. Appl. Microbiol.*, 16, 734, 1994.

14. Rechsteiner, M., Hoffman, L. and Dubiel, W., The Multicatalytic And 26S Proteases, *J. Biol. Chem.*, 268, 6065, 1993.

15. Groll, M. et al., Structure of 20S proteasome from yeast at 2.4 angstrom resolution, *Nature*, 386, 463, 1997.

16. Hegerl, R. et al., The 3-dimensional structure of proteasomes from *Thermoplasma acidophilum* as determined by electron-microscopy using random conical tilting, *FEBS Lett.*, 283, 117, 1991.

17. Zwickl, P. et al., Primary structure of the *Thermoplasma* proteasome and its implications for the structure, function, and evolution of the multicatalytic proteinase, *Biochemistry (Mosc).* 31, 964, 1992.

18. Puhler, G. et al., Subunit stoichiometry and 3-dimensional arrangement in proteasomes from *Thermoplasma acidophilum*, *EMBO J.*, 11, 1607, 1992.

19. Groll, M. and Clausen, T., Molecular shredders: how proteasomes fulfill their role, *Curr. Opin. Struct. Biol.*, 13, 665, 2003.

20. Maupin-Furlow, J.A. et al., Proteasomes: perspectives from the Archaea, *Front. Biosci.*, 9, 1743, 2004.

21. Ward, D.E. et al., Proteolysis in hyperthermophilic microorganisms, *Archaea*, 1, 63, 2002.

22. Zwickl, P., Kleinz, J. and Baumeister, W., Critical elements in proteasome assembly, *Nat. Struct. Biol.*, 1, 765, 1994.

23. Baumeister, W. et al., The proteasome: paradigm of a self-compartmentalizing protease, *Cell*, 92, 367, 1998.

24. Zuhl, F. et al., Dissecting the assembly pathway of the 20S proteasome, *FEBS Lett.*, 418, 189, 1997.

25. Maupin-Furlow, J.A., Aldrich, H.C. and Ferry, J.G., Biochemical characterization of the 20S proteasome from the methanoarchaeon *Methanosarcina thermophila*, *J. Bacteriol.*, 180, 1480, 1998.

26. Groll, M. et al., Investigations on the maturation and regulation of archaebacterial proteasomes, *J. Mol. Biol.*, 327, 75, 2003.

27. Maupin-Furlow, J.A. et al., Archaeal proteasomes: proteolytic nanocompartments of the cell, *Adv. Appl. Microbiol.*, 50, 279, 2001.

28. Madding, L.S. et al., Role of β1 subunit in function and stability of the 20S proteasome from the hyperthermophilic archaeon *Pyrococcus furiosus*, *J. Bacteriol.*, 189, 583, 2007.

29. Frankenberg, R.J., Andersson, M. and Clark, D.S., Effect of temperature and pressure on the proteolytic specificity of the recombinant 20S proteasome from *Methanococcus jannaschii*, *Extremophiles*, 7, 353, 2003.

30. Chen, P. and Hochstrasser, M., Autocatalytic subunit processing couples active site formation in the 20S proteasome to completion of assembly, *Cell*, 86, 961, 1996.

31. Seemuller, E., Lupas, A. and Baumeister, W., Autocatalytic processing of the 20S proteasome, *Nature*, 382, 468, 1996.

32. Jager, S. et al., Proteasome beta-type subunits: Unequal roles of propeptides in core particle maturation and a hierarchy of active site function, *J. Mol. Biol.*, 291, 997, 1999.

33. Nandi, D. et al., Intermediates in the formation of mouse 20S proteasomes: Implications for the assembly of precursor beta subunits, *EMBO J.*, 16, 5363, 1997.

34. Humbard, M.A., Stevens, S.M. and Maupin-Furlow, J.A., Posttranslational modification of the 20S proteasomal proteins of the archaeon *Haloferax volcanii*, *J. Bacteriol.*, 188, 7521, 2006.

35. Wilson, H.L., Aldrich, H.C. and Maupin-Furlow, J., Halophilic 20S proteasomes of the archaeon *Haloferax volcanii*: purification, characterization, and gene sequence analysis, *J. Bacteriol.*, 181, 5814, 1999.

36. Whitby, F.G. et al., Structural basis for the activation of 20S proteasomes by 11S regulators, *Nature*, 408, 115, 2000.

37. Smith, D.M., Benaroudj, N. and Goldberg, A., Proteasomes and their associated ATPases: A destructive combination, *J. Struct. Biol.*, 156, 72, 2006.

38. Dennis, A.P. and O'malley, B.W., Rush hour at the promoter: How the ubiquitin-proteasome pathway polices the traffic flow of nuclear receptor-dependent transcription, *J. Steroid Biochem. Mol. Biol.*, 93, 139, 2005.

39. Groll, M. and Huber, R., Substrate access and processing by the 20S proteasome core particle, *International Journal Of Biochemistry & Cell Biology*, 35, 606, 2003.

40. Glickman, M.H. and Adir, N., The proteasome and the delicate balance between destruction and rescue, *Plos Biology*, 2, 25, 2004.

41. Glickman, M.H. and Ciechanover, A., The ubiquitin-proteasome proteolytic pathway: Destruction for the sake of construction, *Physiol. Rev.*, 82, 373, 2002.

42. Pickart, C.M. and Fushman, D., Polyubiquitin chains: polymeric protein signals, *Curr. Opin. Chem. Biol.*, 8, 610, 2004.

43. Wolf, D.H. and Hilt, W., The proteasome: a proteolytic nanomachine of cell regulation and waste disposal, *Biochimica Et Biophysica Acta-Molecular Cell Research*, 1695, 19, 2004.

44. Medalia, N. et al., Functional and structural characterization of the *Methanosarcina mazei* proteasome and PAN complexes, *J. Struct. Biol.*, 156, 84, 2006.

45. Forster, A. et al., The 1.9 A structure of a proteasome-11S activator complex and implications for proteasome-PAN/PA700 interactions, *Mol. Cell*, 18, 589, 2005.

46. Gille, C. et al., A comprehensive view on proteasomal sequences: implications for the evolution of the proteasome, *J. Mol. Biol.*, 326, 1448, 2003.

47. Maupin-Furlow, J.A. and Ferry, J.G., A proteasome from the methanogenic Archaeon *Methanosarcina thermophila*, *J. Biol. Chem.*, 270, 28617, 1995.

48. Kaczowka, S.J. and Maupin-Furlow, J.A., Subunit topology of two 20S proteasomes from *Haloferax volcanii*, *J. Bacteriol.*, 185, 165, 2003.

49. Reuter, C.J., Kaczowka, S.J. and Maupin-Furlow, J.A., Differential regulation of the PanA and PanB proteasome-activating nucleotidase and 20S proteasomal proteins of the haloarchaeon *Haloferax volcanii*, *J. Bacteriol.*, 186, 7763, 2004.

50. Mattar, S. et al., The primary structure of Halocyanin, an archaeal blue copper protein, predicts a lipid anchor for membrane fixation, *J. Biol. Chem.*, 269, 14939, 1994.

51. Klussmann, S. et al., N-terminal modification and amino acid sequence of the ribosomal protein Hmas7 From *Haloarcula marismortui* and homology studies to other ribosomal proteins, *Biol. Chem. Hoppe. Seyler*, 374, 305, 1993.

52. Maras, B. et al., The protein sequence of glutamate dehydrogenase From *Sulfolobus solfataricus*, A thermoacidophilic Archaebacterium - Is the presence Of N-epsilon-methyllysine related to thermostability, *Eur. J. Biochem.*, 203, 81, 1992.

53. Reits, E.A.J. et al., Dynamics of proteasome distribution in living cells, *EMBO J.*, 16, 6087, 1997.

54. Kruger, E., Kloetzel, P.M. and Enenkel, C., 20S proteasome biogenesis, *Biochimie*, 83, 289, 2001.

55. Ogiso, Y., Tomida, A. and Tsuruo, T., Nuclear localization of proteasomes participates in stress-inducible resistance of solid tumor cells to topoisomerase II-directed drugs, *Cancer Res.*, 62, 5008, 2002.

56. Nederlof, P.M., Wang, H.R. and Baumeister, W., Nuclear localization signals of human and Thermoplasma proteasomal alpha subunits are functional in vitro, *Proc. Natl. Acad. Sci. U. S. A.*, 92, 12060, 1995.

57. Wang, H.R. et al., Import of human and *Thermoplasma* 20S proteasomes into nuclei of HeLa cells requires functional NLS sequences, *Eur. J. Cell Biol.*, 73, 105, 1997.

58. Mayr, J. et al., The import pathway of human and Thermoplasma 20S proteasomes into HeLa cell nuclei is different from that of classical NLS-bearing proteins, *Biol. Chem.*, 380, 1183, 1999.

59. Heinemeyer, W. et al., The active sites of the eukaryotic 20 S proteasome and their involvement in subunit precursor processing, *J. Biol. Chem.*, 272, 25200, 1997.

60. Heinemeyer, W., Ramos, P.C. and Dohmen, R.J., Ubiquitin-proteasome system - The ultimate nanoscale mincer: assembly, structure and active sites of the 20S proteasome core, *Cell. Mol. Life Sci.*, 61, 1562, 2004.

61. Finley, D., Ozkaynak, E. and Varshavsky, A., The Yeast polyubiquitin gene is essential for resistance to high temperatures, starvation, and other stresses, *Cell*, 48, 1035, 1987.

62. Ciechanover, A., Finley, D. and Varshavsky, A., Ubiquitin dependence of selective protein-degradation demonstrated in the mammalian-cell cycle mutant Ts85, *Cell*, 37, 57, 1984.

63. Van Den Eynde, B.J. and Morel, S., Differential processing of class-I-restricted epitopes by the standard proteasome and the immunoproteasome, *Curr. Opin. Immunol.*, 13, 147, 2001.

64. Ma, J., Katz, E. and Belote, J.M., Expression of proteasome subunit isoforms during spermatogenesis in *Drosophila melanogaster*, *Insect Mol. Biol.*, 11, 627, 2002.

65. Knipfer, N. et al., Species variation in ATP-dependent protein degradation: protease profiles differ between mycobacteria and protease functions differ between *Mycobacterium smegmatis* and Escherichia coli, *Gene*, 231, 95, 1999.

66. Bauer, M.W., Halio, S.B. and Kelly, R.M., Purification and characterization of a proteasome from the hyperthermophilic archaeon, *Pyrococcus furiosus*, *Appl. Environ. Microbiol.*, 63, 116, 1997.

67. Michels, P.C. and Clark, D.S., Pressure-enhanced activity and stability of a hyperthermophilic protease from a deep-sea methanogen, *Appl. Environ. Microbiol.*, 63, 3985, 1997.

68. Franzetti, B. et al., Characterization of the proteasome from the extremely halophilic archaeon *Haloarcula marismortui*, *Archaea*, 1, 53, 2002.

69. Ruepp, A. et al., Proteasome function is dispensable under normal but not under heat shock conditions in *Thermoplasma acidophilum*, *FEBS Lett.*, 425, 87, 1998.

70. Reuter, C.J. and Maupin-Furlow, J.A., Analysis of proteasome-dependent proteolysis in *Haloferax volcanii* cells, using short-lived green fluorescent proteins, *Appl. Environ. Microbiol.*, 70, 7530, 2004.

71. Rawlings, N.D., Morton, F.R. and Barrett, A.J., MEROPS: the peptidase database, *Nucleic Acids Res.*, 34, D270, 2006.

72. Rohlin, L. et al., Heat shock response of *Archaeoglobus fulgidus*, *J. Bacteriol.*, 187, 6046, 2005.

73. Boonyaratanakornkit, B.B. et al., Transcriptional profiling of the hyperthermophilic methanarchaeon *Methanococcus jannaschii* in response to lethal heat and non-lethal cold shock, *Environ. Microbiol.*, 7, 789, 2005.

74. Frankenberg, R.J. et al., Chemical denaturation and elevated folding temperatures are required for wild-type activity and stability of recombinant *Methanococcus jannaschii* 20S proteasome, *Protein Sci.*, 10, 1887, 2001.

75. Fu, H. et al., Molecular organization of the 20S proteasome gene family from *Arabidopsis thaliana*, *Genetics*, 149, 677, 1998.

76. Michel, J.K. and Kelly, R.M., Unpublished Data.

77. Tachdjian, S. and Kelly, R.M., Dynamic metabolic adjustments and genome plasticity are implicated in the heat shock response of the extremely thermoacidophilic Archaeon *Sulfolobus solfataricus*, *J. Bacteriol.*, 188, 4553, 2006.

78. Yamada, S.I. et al., Archaeal proteasomes effectively degrade aggregation-prone proteins and reduce cellular toxicities in mammalian cells, *J. Biol. Chem.*, 2006.

79. Brannigan, J.A. et al., A protein catalytic framework with An N-terminal nucleophile Is capable of self-activation, *Nature*, 378, 416, 1995.

80. Seemuller, E. et al., Proteasome from *Thermoplasma acidophilum* - A Threonine protease, *Science*, 268, 579, 1995.

81. Kisselev, A.F., Songyang, Z. and Goldberg, A.L., Why does threonine, and not serine, function as the active site nucleophile in proteasomes? *J. Biol. Chem.*, 275, 14831, 2000.

82. Zwickl, P. et al. in *Protein Folding In The Cell* 187-222 (2002).

83. Arendt, C.S. and Hochstrasser, M., Identification of the yeast 20S proteasome catalytic centers and subunit interactions required for active-site formation, *Proc. Natl. Acad. Sci. U. S. A.*, 94, 7156, 1997.

84. Hochstrasser, M., Ubiquitin-dependent protein degradation, *Annu. Rev. Genet.*, 30, 405, 1996.

85. Dick, T.P. et al., Contribution of proteasomal beta-subunits to the cleavage of peptide substrates analyzed with yeast mutants, *J. Biol. Chem.*, 273, 25637, 1998.

86. Nussbaum, A.K. et al., Cleavage motifs of the yeast 20S proteasome beta subunits deduced from digests of enolase 1, *Proc. Natl. Acad. Sci. U. S. A.*, 95, 12504, 1998.

87. Kisselev, A.F., Callard, A. and Goldberg, A.L., Importance of the different proteolytic sites of the proteasome and the efficacy of inhibitors varies with the protein substrate, *J. Biol. Chem.*, 281, 8582, 2006.

88. Rother, M. and Metcalf, W.W., Genetic technologies for Archaea, *Curr. Opin. Microbiol.*, 8, 745, 2005.

89. Allers, T. and Ngo, H.P., Genetic analysis of homologous recombination in Archaea: *Haloferax volcanii* as a model organism, *Biochem. Soc. Trans.*, 31, 706, 2003.

90. Bitan-Banin, G., Ortenberg, R. and Mevarech, M., Development of a gene knockout system for the halophilic archaeon *Haloferax volcanii* by use of the pyrE gene, *J. Bacteriol.*, 185, 772, 2003.

Table 1. Proteasomes from thermophilic and hyperthermophilic archaea.

	(ºC)	α protein	β protein	PAN
Aeropyrum pernix	95	APE1449	APE0521 APE0507	APE2012
Archaeoglobus fulgidus	83	AF0490	AF0481	AF1976
Halobacterium sp. NRC-1	50	VNG0166G	VNG0880G	VNG2000G VNG0510G
Haloarcula marismortui 43049	50-53	AAV46668 AAV46124	AAV45476 AAV46667	AAV47895 AAV48212
Haloferax volcanii	45	T48679	T48677	AAV38127 AAV38126
Methanocaldococcus jannaschii	85	MJ0591	MJ1237	MJ1176
Methanopyrus kandleri AV19	98	MK0385	MK1228	MK0878
Methanosarcina thermophila	50	MTU30483	MTU22157	ND
Methanotherm. thermautotrophicus	65-70	MTH686	MTH1202	MTH728
Natronomonas pharaonis 2160	45	NP3738A	NP3472A	NP1524A NP5038A
Nanoarchaeum equitans Kin4-M	90	AAR39362	AAR39057	AAR39040
Picrophilus torridus DSM 9790	60	PTO0804	PTO0686	PTO0456*
Pyrobaculum aerophilum	100	PAE2215	PAE3595 PAE0807	PAE0696*
Pyrococcus abyssi	96	PAB0417	PAB1867 PAB2199	PAB2233
Pyrococcus furiosus	100	PF1571	PF1404 PF0159	PF0115
Pyrococcus horikoshii	98	PH1553	PH1402 PH0245	PH0201
Sulfolobus acidocaldarius	75	AAY80005	AAY80046 AAY80272	AAO73475
Sulfolobus solfataricus	87	SSO0738	SSO0766 SSO0278	SSO0271
Sulfolobus tokodaii	80	ST0446	ST0477 ST0324	ST0330
Thermoplasma acidophilum	59	TA1288	TA0612	TA0840*
Thermoplasma volcanium	60	TVN0304	TVN0663	TVN0947*
Thermococcus kodakarensis	95	TK1637	TK1429 TK2207	TK2252

ND - No PAN homolog detected

*No ORF annotated as PAN, but possible homolog detected.

(Adapted from Madding, L.S. et al., J. Bacteriol., 189, 583, 2007)

Table 2. Kinetic and physical properties of selected native proteasomes from high temperature microorganisms.

Organism	***Methanococcus jannaschii***	***Methanosarcina thermophila***	***Haloferax volcanii***	***Thermoplasma acidophilum***	***Pyrococcus furiosus***
Preferred Substrate	Cbz-AAL-βNa	Cbz-LLE-βNa	Suc-AAF-Amc	Suc-LLVY-Amc	Suc-VKM-Amc
Sp.Activity (nmol/min mg)	116000 (95ºC)*	115.0 (65ºC)*	340.0 (60ºC)*	0.79	V_m = 2200 (pmol/min μg) k_{cat}/K_m = 3.64 (s^{-1} mM^{-1})
$pH_{optimal}$	7.5-7.8	NR	7.0-9.3	NR	6.5
$T_{optimal}$ (ºC)	119	NR	75	NR	95
References	67	25,47	35	17	66

NR- Not Reported

*Represents assay temperature for reported specific activity.

βNa- β-naphthylamine

Amc- 7-amino-4-methylcoumarin

Table 3. Kinetic and physical properties of selected recombinant proteasomes from high temperature microorganisms.

Organisms	***Methanococcus jannaschii***	***Methanosarcina thermophila***	***Haloferax volcanii***	***Thermoplasma acidophilum***	***Pyrococcus furiosus* (90°C Assembly)**	***Pyrococcus furiosus* (105°C Assembly)**
K_m (μM)	NR	NR	NR	30.0	45.2	36.4
V_m (pmol/min μg)	NR	NR	NR	250	1159	2194
k_{cat} (s^{-1})	NR	NR	NR	0.03	1.0	1.9
k_{cat}/K_m (s^{-1} mM^{-1})	NR	NR	NR	7.0	22.1	51.5
k_i (115°C)	0.018	NR	NR	NR	0.15	0.025
$T_{optimal}$ (°C)	119	75	NR	60	>100.0	>100.0
Substrate Preference[#]	LLE-βNa LLVY-Amc AAF-Amc	LLE-βNa LLVY-Amc AAF-Amc	LLVY-Amc	GGL-Amc LLVY-Amc AAF-Amc	VKM-Amc AAF-Amc LLVY-Amc	VKM-Amc LLVY-Amc AAF-Amc
Reference	29,74	25	35	80,81	28	

NR- Not Reported

βNa- β-naphthylamine

Amc- 7-amino-4-methylcoumarin

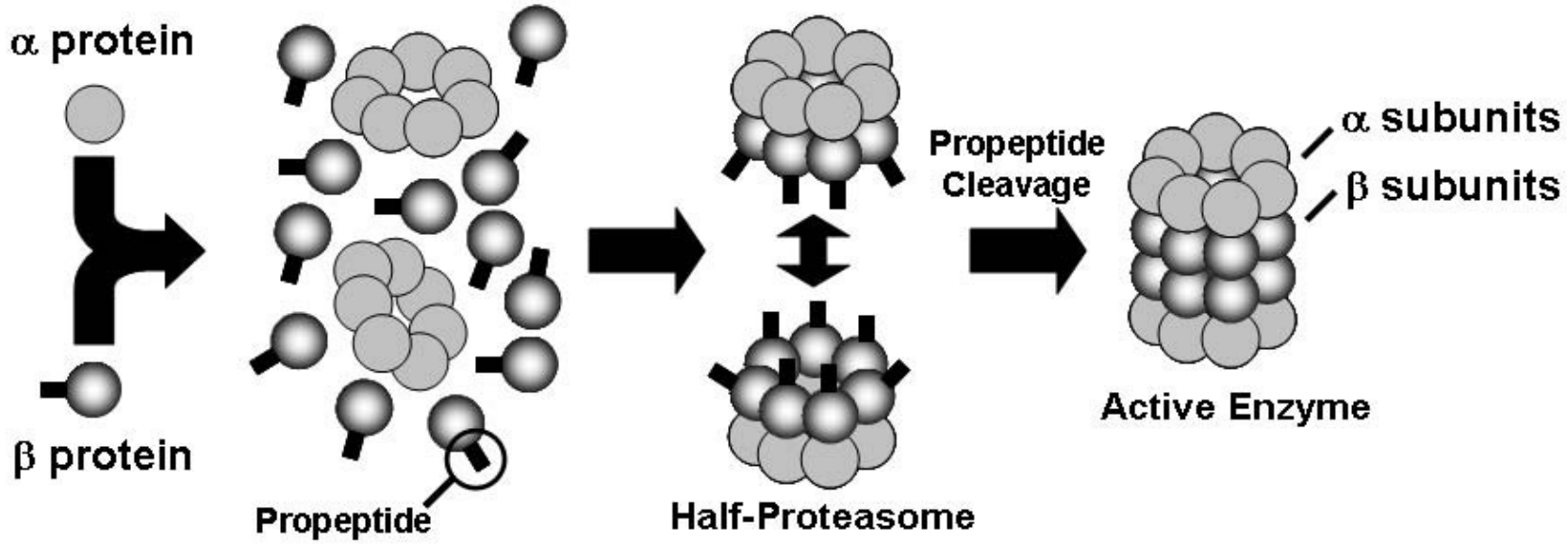

Figure 1. Assembly of the proteasome involves formation of ~300 kDa half-proteasome complexes (which are inactive and contain α and β pro-subunits) prior to cleavage of the β protein pro-peptide region. Combination of two half-proteasomes results in an active 600-700 kDa enzyme capable of degrading peptides and unfolded proteins.

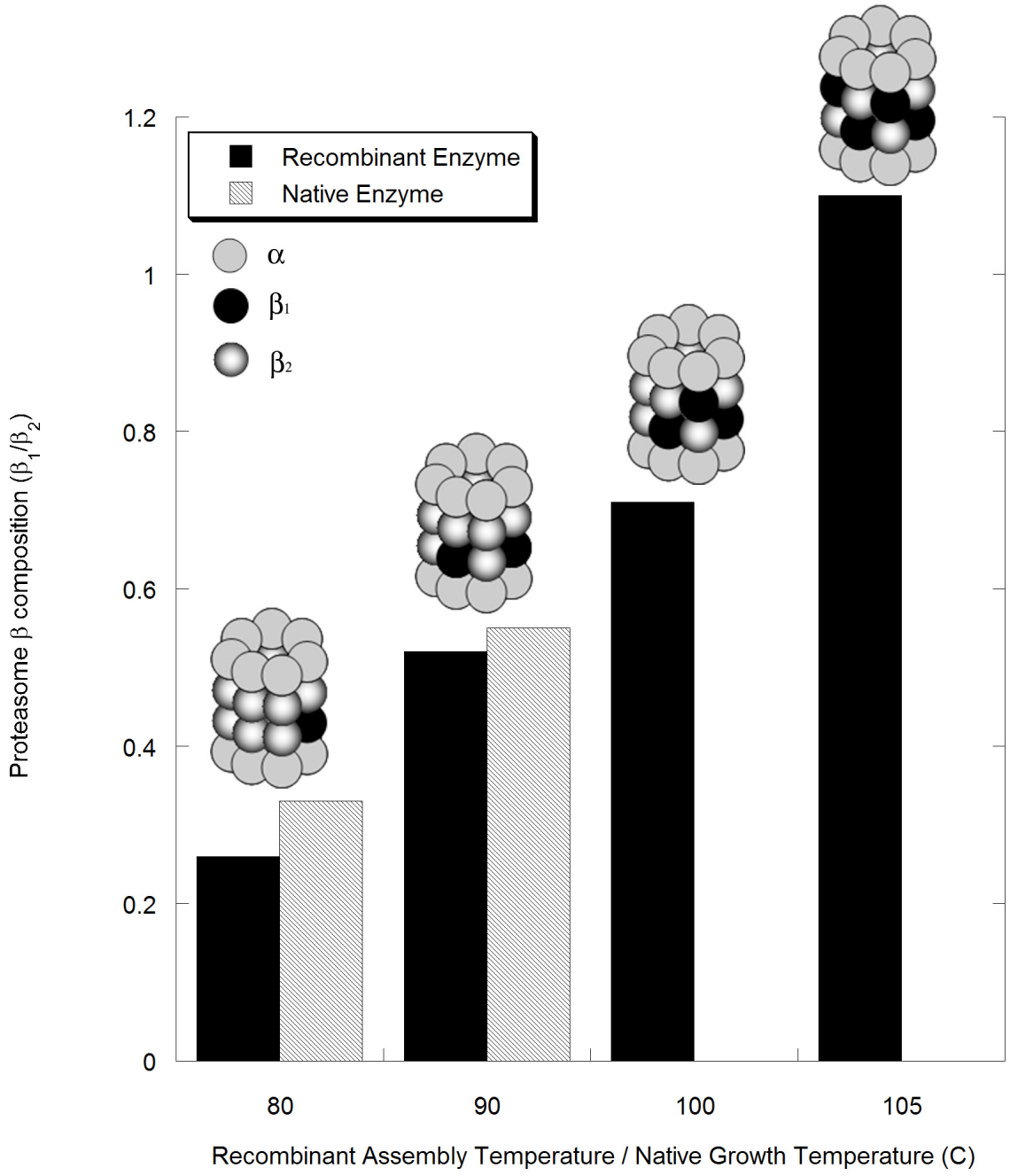

Figure 2. The β_1/β_2 ratio for the recombinant *P. furiosus* proteasomes assembled at temperatures between 80ºC and 105ºC, as well as for the native proteasomes isolated from *P. furiosus* grown at 80ºC and 90ºC. Above each temperature bar, schematic representations of the 20S proteasome assembly are shown accounting for the altered β_1 content.

Chapter 3

Role of β_1 subunit in the function and stability of the 20S proteasome in Hyperthermophilic archaeon *Pyrococcus furiosus*

Lara S. Madding*, Joshua K. Michel*, Keith R. Shockley, Shannon B. Conners,Kevin L. Epting, Matthew R. Johnson and Robert M. Kelly

Published: **Journal of Bacteriology Volume 189 Issue 2 pp. 583-590**
* Lara S. Madding and Joshua K. Michel were cited as co-authors

ABSTRACT

The hyperthermophilic archaeon *Pyrococcus furiosus* genome encodes three proteasome component proteins: one α (PF1571) and two β proteins (β1-PF1404; β2-PF0159), as well as an ATPase (PF0115), referred to as Proteasome-Activating Nucleosidase (PAN). Transcriptional analysis of *P. furiosus* dynamic heat shock response (shift from 90 to 105°C) showed that the β_1 gene was up-regulated over 2-fold within five minutes, suggesting a specific role during thermal stress. Consistent with transcriptional data, two-dimensional SDS PAGE revealed that incorporation of the β_1 protein relative to β_2 into the 20S proteasome (core particle, CP) increased with increasing temperature for both native and recombinant versions. For the recombinant enzyme, the β_2/β_1 ratio varied linearly with temperature from 3.8, when assembled at 80°C, to 0.9 at 105°C. The recombinant $\alpha+\beta_1+\beta_2$ CP assembed at 105°C was more thermostable than either the $\alpha+\beta_1+\beta_2$ version assembled at 90°C or the $\alpha+\beta_2$ version assembled at either 90°C or 105°C, based on melting temperature and biocatalytic inactivation rate at 115°C. The recombinant CP assembled at 105°C was also found to have different catalytic rates and specificity for peptide hydrolysis, compared to the 90°C assembly (measured at 95°C). Combination of the α and β1 proteins yielded neither a large proteasome complex nor demonstrated any significant activity. These results indicate that the β_1 subunit in the *P. furiosus* 20S proteasome plays a thermostabilizing role and influences biocatalytic properties, suggesting that β subunit composition is a factor in archaeal proteasome function during thermal stress when polypeptide turnover is essential to cell survival.

INTRODUCTION

Proteasomes are heteromultimeric proteases found in all domains of life that play a key role in intracellular protein degradation (14-17, 26, 29-31, 33, 38, 42). In eukaryotes, the composition of the proteasome core particle (CP or 20S proteasome) is based on many versions of small α~ and β~type proteins (21-31 kDa) that assemble into heptameric stacked rings ($\alpha_7\beta_7\beta_7\alpha_7$); the set of 14 α and 14 β subunits that comprise the CP assembly in eukaryotes can depend upon cellular status (16). The *Saccharomyces cerevisiae* CP can have up to seven different β proteins in its assembly, which contribute to multiple proteolytic activities (1). The genomes of higher eukaryotes, such as *Arabidopsis thaliana*, encode for as many as 13 α-type and 10 β-type proteins, creating the possibility for numerous versions of the CP (12). Many α and β proteins in a particular eukaryote are more than 90% identical at the amino acid sequence level, possibly representing some degree of redundancy (13). CP composition may, in some cases, also be variable in prokaryotes, although the possibilities are much more limited. In bacteria, 20S proteasomes have been identified in *Rhodococcus erythropolis* (8) as well as in *Mycobacterium tuberculosis* (25), both of which appear to be based on single α and β proteins. In *Haloferax volcanii*, the proteasome CP is found in at least two different isoforms, based on combinations of one β protein and two α proteins (7, 21). The genome of *Haloarcula marismortui* encodes two versions of both the α and β proteins, although it is not known specifically how these contribute to the CP assembly (11). In the hyperthermophilic archaea, available genome sequence data indicate that the CP is based on either one α and one β protein, or two β proteins and one α protein. The role of an additional α or β protein in archaeal proteasome regulation may provide some biochemical and/or biophysical versatility along the lines seen in the eukaryotic proteasome. For example,

in *H. volcanii*, which has two α proteins, it has been proposed that the CP assembly, and association with the proteasome-activating nucleotidases (PanA and PanB), may be growth phase-associated (32). Environmental factors may also contribute to the β protein composition in hyperthermophiles with one α and two β proteins encoded in their genomes. N-terminal sequence analysis of the native CP purified from *Pyrococcus furiosus* grown at 88°C showed that it was based primarily on one α (PF1571) and one β (PF0159, referred to here as β_2) protein (2). However, when *P. furiosus* was exposed to supraoptimal temperatures, transcription of ORF encoding the putative β1 protein (PF1404) was up-regulated after 60 min (37). The extent to which β_1 is incorporated into the *P. furiosus* CP and resulting functional implications has not been examined. Given the relative simplicity of the archaeal proteasome compared to eukaryotic versions, many interesting questions concerning the relationship between CP α and β protein content can be addressed. For example, do hyperthermophilic archaea with genomes encoding a second β protein (e.g., *P. furiosus* (34) and *Sulfolobus solfataricus* (36)) have any physiological or ecological advantages over those with only one β protein (e.g., *Methanococcus jannaschii* (27, 28) and *Archaeoglobus fulgidus* (15))? To begin to answer this question, we examined the influence of temperature on *in vivo* and *in vitro* CP assembly for *P. furiosus*.

MATERIALS AND METHODS

Enzyme assays. CP peptidase activity was determined by endpoint assay in 50 mM sodium phosphate buffer (SPB), pH 7.2 and 95°C (unless otherwise noted), with a microtiter plate reader (Model HTS 7000 Plus Bio Assay Reader, Perkin-Elmer, Wellesley, MA) by detection of 7-amino-4-methylcoumarin (MCA) released from the carboxyl terminus of N-terminally blocked peptides (Sigma-Aldrich, St. Louis, MO) (2). Negative controls (no enzyme) were run in triplicate to account for thermal degradation of substrates. Kinetic constants were determined using a least squares fit of the appropriate model to the initial velocity (U/μg) as a function of substrate concentration (0.01 mM-0.50 mM) data at 95ºC. One unit of protease activity was defined as the amount of enzyme required to release 1 pmol of MCA per min. Total protein concentrations were determined using the Coomassie blue dye-binding method (4) (Bio-Rad, Hercules, CA) in microtiter plates with bovine serum albumin (Sigma-Aldrich, St. Louis, MO) as the standard.

Purification of 20S proteasome from *P. furiosus* grown at 80ºC and 90ºC. *P. furiosus* (DSM 3638) was grown on sea salts media (40 g/L sea salts (Sigma-Aldrich, St. Louis, MO), 3.3 g/L PIPES buffer, 1 ml/L trace elements (VSM), 5 g/L tryptone, 1 g/L yeast extract, 120 g total sulfur). The culture (12 L working volume) was grown in a 14-L fermentor (New Brunswick, Edison, NJ) at an agitation rate of 600 rpm, pressure of 0.5 bar, and sparge rate (N_2) of 0.5 L/min. The cells grew at 80ºC (pH 6.2) for 16.0 h, then shifted to 90.0 ºC and held at this temperature for 1 h. Culture samples of 2.4 L were taken at 16 h and 17 h; the resulting cell pellet was stored at -80ºC.

Purification of the proteasome from cells grown at 80ºC and 90ºC was done using the same purification scheme. The cell pellets were re-suspended in 20 ml of 20 mM Tris, pH 8.0, passed (4x) through a French-pressure cell at 16,000 psi, and centrifuged (10,000 x g, 4ºC) for 20 min. The soluble protein fraction was applied to a 40-ml Q-Sepharose XK 26/20 column (GE Life Sciences, Piscataway, NJ) and eluted between 0.5-0.7 M NaCl. Many of the smaller contaminating proteins were cleared from the resulting VKM-MCA active pool using a Microcon centrifugal concentrator of 100,000 MWCO. This pool was then applied to a hydroxyapatite (Calbiochem, San Diego, CA) XK 16/30 column. Elution occurred between 220-265 mM SPB during a linear gradient of 0.05-0.5 M SPB, pH 8.0. After concentration, this active pool was applied to a HiPrep Sephacryl S-300 High Resolution XK 16/40 column calibrated with a High Molecular Weight Calibration Kit (GE Life Sciences, Piscataway, NJ). All CP VKM-MCA activity was eluted in the first peak which corresponded to a protein of approximately 660 kDa; these fractions were then concentrated using a 30,000 MWCO Centriplus® Centrifugal Filter Device (Millipore, Billerica, MD).

Cloning and expression of the *P. furiosus* CP genes in *Escherichia coli*. The genes for the three proteins associated with the proteasome, *psmA* (α, PF1571, "proteasome, subunit alpha"), *psmB-1* (β1, PF1404, "proteasome, subunit beta"), and *psmB-2* (β2, PF0159, "proteasome, subunit beta"), were separately cloned into the pET-24d(+) vector (Novagen, Madison, WI). The α gene was amplified using the primers: forward: (5'-TGAACGCCATGGCATTTGTTCCACCTCA-3') and reverse: (5'-ATAAAAATTGGATCCAAGTCAGTAGTTGCTATCCA-3'). The β2 gene was amplified with: forward (5'-TTAGGTGGTGCTCATGAAGAAAAAGACTGGAA-3') and the reverse

primer (5'-TAAGGAAGCCTGGATCCTTCATACTACAAACTCTT-3'). The β1 gene was cloned using an ORF that started with the fourth amino acid from the reported amino-terminus (based on locations of start codon and likely ribosomal binding site). N-terminal sequencing confirmed that the unprocessed ß1 subunit was expressed correctly. The primers used for β1 gene amplification were: forward (5'-TGTTGCCCATGGAAGAGAAACTTAAGGGAA-3') and reverse (5'-AAATTGTCGGATCCTTGGACTACTTTAACATTTT-3').

The α gene was expressed in *E. coli* BL21(DE3), while the β1 and β2 genes were separately expressed in *E. coli* BL21-CodonPlus®(DE3)-RIL (Stratagene, La Jolla, CA). Expression was induced with 0.4 mM IPTG (OD_{595} = 0.60); cells were harvested 3-5 hr after induction (37ºC). The resuspended cell pellets were treated with lysozyme, sonicated (Misonix, Inc., Farmingdale, NY), and centrifuged (18,000 x g, 4ºC) for 30 min. Two 20-min heat treatments of the soluble protein fractions for α and β1 were performed, the first at 85ºC and the second at 90ºC, to remove residual *E. coli* protein. Each treatment was followed by cooling on ice for 30 min, centrifugation (18,000 x g, 4ºC) for 30 min to remove insoluble protein. The β2 protein preparation required only one 20-min heat treatment at 85ºC.

Assembly of the recombinant CP. To assemble the CP, the α and β proteins were combined in equimolar ratios to a final total protein concentration of 0.5-0.7 mg/ml. This mixture was then incubated at the indicated temperature for 1 hr, cooled on ice for 1 hr, and precipitated material was removed through centrifugation (16,000 x g, 4ºC) for 30 min. The CP soluble protein was then purified by a gel filtration step to remove unincorporated α and

β proteins, using the approach described above for the native CP. Fractions were concentrated using a 30,000 MWCO membrane filter, as described above for the native CP.

Cloning, expression, and purification of the *P. furiosus* PAN gene in E. coli. The PAN gene (PF0115) was cloned into pET-21b(+) vector (Novagen, WI.) using the primers: forward (5'-GGTGATACATATGAGTGAGGACGAAGCTCAATTT3') and reverse (5'-TAAAAATTAGGATCCTCAGCCGTAAATGACTTCA 3'). PAN was expressed using BL21-CodonPlus®(DE3)-RIL (Stratagene, CA.) with induction by 0.4 mM IPTG (OD_{600} = 0.60); cells were harvested 3-5 hr after induction (37ºC). Cells were resuspended in 20mM Tris pH 8.0 + 0.5% CHAPS + 1mM DTT + 1 mg/ml lysozyme and sonicated (Misonix, Inc., Farmingdale, NY). The samples were centrifuged for 30 min (18,000 x g, 4ºC) and the supernatand removed. The pellet was then resuspended in 20mM Tris pH 8.0 + 0.5% CHAPS + 1mM DTT and heat-treated at 85ºC for 20 min. The sampe was then cooled and centrifuged, and the pellet was then re-suspended in the same manner as before and heat-treated at 90ºC for 20 min. The resulting suspension was centrifuged to remove precipitated debris, with the supernatant containing pure PAN.

Two-dimensional gel electrophoresis of purified CP. Purified samples of the proteasome (45 µg) were precipitated in a 10% trichloroacidic acid (TCA) solution on ice for 1 hr. The resulting pellet was washed 3 times with 150 µL of ice-cold acetone (-20ºC) and then dried for 5 minutes at 60ºC. The protein was resuspended in 125 µL of rehydration buffer (8 M urea, 2% CHAPS, 50 mM dithiothreitol (DTT), 0.2% Bio-Lyte ampholytes (Bio-Rad, Hercules, CA) and applied to a 7.0 cm pH 4-7 isoelectric focusing (IEF) strip (Bio-

Rad). The strip was subjected to active rehydration (50V) for 16 hrs. The conditions used for focusing were: 250 V, linear ramp, 20 min; 4000 V, linear ramp, 2 hr; 4000 V, rapid ramp, 10,000 V-hr. After IEF, the strips were incubated in equilibration buffer I (6 M urea, 0.375 M Tris-HCl, pH 8.8, 2% SDS, 20% glycerol, 2% DTT) for 10 min at room temperature, followed by another 10 min incubation in equilibration buffer II (6 M urea, 0.375 M Tris-HCl, pH 8.8, 2% SDS, 20% glycerol, 2.5% iodoacetamide). For the second dimension, the IEF strip was then placed on top of a 12% SDS PAGE gel and covered with a 2-D agarose overlay gel (0.5 % Low Melting Point Agarose, Tris base 2.9 g/L, glycine 14.4 g/L, SDS 1.0 g/L) . The gels were stained with GelCode® Blue Staining Reagent (Pierce, Rockford, IL) and analyzed on a GS-710 Calibrated Imaging Densitometer (Bio-Rad).

Differential scanning calorimetry of recombinant *P. furiosus* proteasome and PAN. The melting temperatures of all expressed proteins were determined using a CSC nano differential scanning calorimeter (DSC; Calorimetry Sciences Corp., American Fork, UT). All samples were dialyzed against 50 mM SPB, pH 7.2, which was the buffer used to generate the baseline scan. Samples (0.21 mg/ml) were de-gassed and scanned from 25-125ºC using a scan rate of 0.5ºC/min for two heating and cooling cycles. Heat capacity versus temperature curves were generated using the software program accompanying the DSC instrument to determine melting temperatures. After each sample was analyzed on the DSC, activity assays and native gels were used to determine if complete or irreversible denaturation had occurred. Samples were centrifuged (16,000 x g, 4ºC) to remove aggregates, total protein concentrations were determined, and activity assays were run simultaneously against the corresponding initial samples to obtain relative loss of activity.

Thermal inactivation of CP assemblies. High-temperature incubation of the active recombinant proteasome forms ($\alpha+\beta_2$ and $\alpha+\beta_1+\beta_2$ assembled at 90ºC and 105ºC) was used to compare their stabilities. Each assembly was adjusted to a baseline concentration of 0.15 mg/ml and incubated at 115ºC in an oil bath for up to 12 hr. Aliquots were taken at time points from 0-12 hr and stored on ice until the end of the incubation period. The standard VKM-MCA microtiter plate assay was then used to compare the activities of the mixtures (300 ng enzyme, based on pre-incubation concentration, was mixed with 5 μM VKM-MCA and heated to 95ºC for 15 min). The resulting fluorescence scores, with average background values subtracted were determined, and used to determine first-order decay constants.

Transcriptional analysis of dynamic heat shock response. A whole genome cDNA microarray including 2065 open reading frames (ORFs) was printed, following protocols described previously (5). The array was used to determine transient transcriptional response after a temperature shift from 90ºC to 105°C. *P. furiosus* (DSM 3638) was cultured anaerobically at 90°C on Sea Salts Medium (SSM), as described previously (37). Tryptone (Sigma, St. Louis, MO) was added to SSM (final concentration 3.28 g/L) as a carbon source prior to inoculation, along with elemental sulfur (10 g/L). A 60 ml batch culture was used to inoculate 500 ml of SSM medium supplemented with 3.28 g/L tryptone and 10 g/L sulfur in a 1-L pyrex bottle. Two hundred fifty ml of this culture was added to 12 L of media in a 14-L fermentor (New Brunswick Scientific, Edison, NJ). The fermentor contained an internal temperature controller, and the pH was maintained by a Chemcadet controller (Cole Parmer, Vernon Hills, IL). High purity N_2 was used to reduce the medium and to sparge during

inoculation. The culture was grown to mid-log phase at 90°C, after which a sample was collected. The temperature set point was then shifted to 105°C, with the culture taking approximately 2 min to reach the set point temperature. Once the culture reached 105°C, samples were taken at 0, 5, 10, 60 and 90 min. Approximately 20 ml of culture were collected prior to sampling at each time point to eliminate pre-existing fluid in the sampling lines. At each time point, 500 ml of culture were withdrawn and immediately put on ice until processed for RNA extraction. One ml of sample was removed for cell density enumeration by epifluorescent microscopy with acridine orange stain (20).

RNA was extracted from each 500-ml sample culture as described previously (37). The 500-ml samples from the fermentor were centrifuged for 20 min (10,000 x g, 4°C). After treatment with RNA lysis buffer, the samples were stored at –70°C. Extractions proceeded with ethanol precipitation and purification using Ambion RNAqueous kits. Concentrations and degree of purity were determined by optical density at 260 nm and 280 nm, as well as with gel electrophoresis (1% agarose gel, 60 V). Procedures for reverse transcription reactions, aminoallyl-labeling with Cy3 and Cy5, and hybridization reactions are reported elsewhere (5).

A loop experimental design incorporated reciprocal labeling of time point samples with both Cy3 and Cy5. Mixed model analysis was used to evaluate differential expression data using approaches presented elsewhere (5). Briefly, least squares estimates of gene-specific treatment effects, corrected for global and gene-specific sources of error, were used to construct pair-wise contrasts analogous to fold changes for each gene between all pairs of conditions. The statistical significance of these fold changes was determined and a Bonferroni correction was used to establish an experiment-wide false positive rate of

$\alpha = 0.05$ by dividing α by 2,821, the number of comparisons performed for all genes over all possible treatment pairs. The corrected false positive rate was 1.77×10^{-5} (corresponding to a $-\log_{10}$(p-value) > 4.8). Least squares estimates of gene-specific treatment effects were also used to perform hierarchical clustering in JMP 5.0 (SAS Institute, Cary, NC).

RESULTS

Transcriptional analysis of chaperones and proteosome components during *P. furiosus* heat shock response. We previously reported using a targeted cDNA microarray to examine the transcriptional response of *P. furiosus* grown quiescently in serum bottles, comparing before and 60 min after a temperature shift from 90 to 105°C (37). Table 1 shows more recent efforts focused on tracking transcriptional transients for *P. furiosus* grown in a 14-liter agitated fermenter for the same thermal shift. The larger culture volume allowed for multiple time point RNA samples for microarray interrogation. Also, agitation effected rapid equilibration of the entire culture volume to the higher temperature. At the earliest sampling time (0^+), which was 2 min or less following temperature shift, the thermosome (PF1974) and small heat shock protein (PF1883) were up-regulated 8.6-fold and 34.3-fold, respectively, indicative of a heat shock response. The β2 protein and PAN (PF0115) were not responsive at the 0^+ sampling time, while the α protein was down-regulated 2-fold. The β1 protein was up-regulated 2-fold at the earliest sampling time (0^+). In fact, transcript levels for this gene were maintained at normal or above normal levels throughout the 90 min tracking period, in contrast to the β2 and α proteins which both dropped off considerably by 90 min. The gene encoding PAN rose 2-fold at 30 min, but ultimately dropping off more than 3-fold by 60 minutes.

Some differences in transcript levels were noted at the 60 min point between the quiescent (37) and agitated cultures for certain ORFs (data included in Table 1). Agitation seemed to accelerate the dynamics of heat shock response; note that transcript levels at 30 min for the agitated culture were comparable to the 60 min levels for the quiescent cultures. Inspection of cells using epifluoresence microscopy with acridine orange stain showed that significantly more cell lysis was occurring at the 60 min point in the agitated culture compared to the quiescent culture, perhaps reflecting the adverse impact of increased shear sensitivity on cellular function at supraoptimal temperatures.

β subunit composition of the *P. furiosus* proteasome. Since transcriptional analysis indicated that β1 protein transcripts were up-regulated upon heat shock, an effort was made to determine whether growth temperature impacted the β_2/β_1 protein ratio in the CP. Native versions of the proteasome were purified from *P. furiosus* cells grown in the agitated 14-liter fermenter at 80 and 90°C. Significant cell lysis at 105°C, the temperature used to elicit a heat shock response reported in Table 1, made purification of the native proteasome at this temperature problematic. Densitometry on CP proteasome proteins, separated by two-dimensional gel electrophoresis, from the two growth temperatures showed that the ratio of β_2/β_1 dropped from 3.0 at 80°C to 1.8 at 90°C (see Figure 1).

At 90°C, combinations of recombinant versions of α and β1 proteins led to nothing more than α and β1 proteins by themselves as viewed by native PAGE (data not shown). However, the $\alpha+\beta_2$ and $\alpha+\beta_1+\beta_2$ combinations at 90 and 105°C led to active and fully assembled (~660 kDa) proteasomes. Furthermore, recombinant versions of the *P. furiosus* CP reflected the β_2/β_1 observed for the native CP; at 80°C the β_2/β_1 was 3.8 which dropped to

1.9 at 90°C. The effect of assembly temperature on recombinant CP β protein composition at 100°C ($\beta_2/\beta_1 = 1.4$) and 105°C ($\beta_2/\beta_1 = 0.9$) reinforced the trend of increasing β_1 protein content with increasing temperature (see Figure 1).

Biochemical properties *P. furiosus* CP. Recombinant CP assemblies were screened for activity against a number of peptide substrates. For those peptides for which hydrolysis was noted, relative activities of the 105ºC assembled proteasome were as follows: VKM>>LLL>LLE>LLVY>AAF. These results were consistent with previous characterization of the native CP from *P. furiosus* (2). VKM was used as the comparative basis to track the activities of various assemblies of the recombinant 20S complexes. Each individual protein (α, β_1, β_2) was inactive against VKM-MCA when initially expressed and stored at 4ºC or when heated at 90ºC, 98ºC, or 105ºC under the assembly conditions used here. When β_1 and β_2 proteins were combined in a 1:1 molar ratio, they were not active against VKM-MCA after incubation at temperatures of 4ºC, 85ºC, 90ºC, or 105ºC. Compared to the native proteasome, the combinations $\alpha+\beta2$ (assembled from a 1:1 molar ratio) and $\alpha+\beta_1+\beta_2$ (assembled from a 1:1:1 molar ratio) were active after incubation at 90, 98 and 105ºC. The $\alpha+\beta_1$ (1:1 molar ratio) combination was essentially inactive at any assembly temperature. When higher levels of β_1 were added to the assembly mixture so that $\alpha:\beta_1$ molar ratios were 1:5 and 1:10, activity increased slightly with increased β_1, but was still extremely low in comparison to the native form and the other recombinant forms of the CP.

The effect of assembly temperature (and, hence β protein composition) was examined for recombinant versions of the CP. Table 2 shows kinetic parameters determined at 95°C for

recombinant versions of the *P. furiosus* CP assembled at 90°C and 105°C on three different peptide substrates; note that a standard Michaelis-Menten model was used for LLVY and AAF, while substrate inhibition was included in the model for VKM (39). K_m values measured were all between 20-70 μM, which are similar to CPs from *Rhodococcus* and *Mycobacterium* species (25). V_{max} values obtained were also consistent with previously reported values for other prokaryotic CPs (25, 42) and consistent with the native *P. furiosus* CP (2). Based on the information in Figure 1, the CP assembly at 105°C had twice the β_1 protein content than that at 90°C and comprised approximately half of the CP compared to one-third of the CP at 90°C. Thus, β_1 protein content impacted the kinetic parameters for the three substrates tested in Table 2. In all cases, the catalytic efficiency (k_{cat}/K_m), measured at 95°C, was higher for the 105°C assembly than for the 90°C assembly. The k_{cat}/K_m was 2.4, 3.6, and 15-fold higher for the 105°C CP assembly than the 90°C version on VKM, LLVY, and AAF, respectively.

Thermostability of recombinant *P. furiosus* CP proteins and assemblies. The thermostability of the individual recombinant CP proteins was assessed by differential scanning microcalorimetry. The α protein was found to be very thermostable, even relative to other *P. furiosus* proteins; no thermal transitions were noted for scans up to 120-125°C (data not shown), the upper limit that could be tested by the instrument used here. Melting temperatures for the β_1 and β_2 subunits were 104.4ºC and 93.1ºC, respectively (see Figure 2a). In the absence of the α subunit, the pro-peptide region of 6-7 N-terminal residues upstream of the putative active-site Thr within the "TTT" tripeptide in each of the expressed β subunits was retained, as determined by N-terminal sequencing. It is not known whether

the presence or absence of the N-terminal region impacts the thermostability of the β proteins. The *P. furiosus* version of PAN melted at 94.2°C (Figure 2b).

Figure 3 shows the melting curves for the $\alpha+\beta_2$ and $\alpha+\beta_1+\beta_2$ assembly mixtures forms at 90ºC and 105ºC. The $\alpha+\beta_1$ combination was not tested because significant amounts of assembled CP were never obtained. A thermal transition was noted for all cases within 110.5-112ºC. For the $\alpha+\beta_1+\beta_2$ form assembled at 90°C (Curve C), a transition at 104.5°C was noted, likely corresponding to unincorporated β_1 subunit, which melts at that temperature (see Figure 2a). No transition at this temperature was observed for the $\alpha+\beta_1+\beta_2$ form assembled at 105°C (Curve D). Furthermore, analysis of samples twice scanned to 125°C and cooled back to ambient temperatures showed that at least 25% of initial activity on VKM-MCA remained. The fully assembled CP, without evidence of denatured subunits, could also be viewed on SDS-PAGE (Coomassie stain) following thermal scans to 125°C (data not shown). This was consistent with what appeared to be a thermal transition (Curve D) which was beginning at 120°C.

The thermal inactivation of the $\alpha+\beta_2$ and $\alpha+\beta_1+\beta_2$ assemblies is shown in Figure 4. The calculated k_{obs} for $\alpha+\beta_2$ (90ºC assembly temperature), $\alpha+\beta_2$ (105ºC assembly temperature), and $\alpha+\beta_1+\beta_2$ (90ºC assembly temperature) were all relatively close, ranging from 0.15-0.19 hr^{-1}. In contrast, the calculated k_{obs} for $\alpha+\beta_1+\beta_2$ assembled at 105ºC was significantly lower (k_{obs} = 0.025 hr^{-1}). When samples remaining after the 12- hour incubation period were viewed on a 10% native gel, only the $\alpha+\beta_1+\beta_2$ form assembled at 105ºC was visible by Coomassie staining.

DISCUSSION

The *P. furiosus* 20S proteasome β-protein complement differs from several other archaeal proteasomes that have been characterized to date (*A. fulgidus* (15), *T. acidophilum* (26), *M. thermophila* (28), *M. jannaschii* (9, 10, 42), *Haloferax volcanii* (21)), in that it encodes two distinct β protein homologs (see Table 3). Original isolation of the proteasome from *H. marismortui* showed a single α and ß composition(11), however later genome sequencing has revealed the coding possbility for 2 α and 2 ß proteins. Unlike the case in eukaryotes, in which some multiple versions of α and β proteins have been observed to share 90% identitical protein sequences (13), the *P. furiosus* β proteins are only 48% identical at the amino acid level. This suggests that the β subunits can play distinct roles in *P. furiosus* CP structure and function. Recombinant versions of the biocatalytically active *P. furiosus* CP could not be generated based solely on α and β1 proteins but could be obtained using combinations of α and β_2, or all three proteins. Although the combinations of α and β_2, lacking β_1, were fully active, combinations that included β1 had enhanced catalytic efficiency at 95°C. Versions containing α, β_1 and β_2 proteins that had been assembled at 105°C were also significantly more thermostable. Thus, this leads to the conclusion that the β_1 subunit, while not essential for catalytic activity, plays a role in stabilizing and activating the *P. furiosus* CP assembly, particularly at supraoptimal temperatures such as those encountered during thermal stress events. Assembly of the recombinant CP from *M. jannaschii* was found to require the unfolding and re-folding of the α and β proteins to obtain activity levels comparable to the native version (9, 10). In comparison, the *in vitro* CP assembly for *Thermoplasma acidophilum*, *Haloferax volcanii*, and *Methanosacrcina thermophila* did not require unfolding and re-folding to produce a recombinant protein with

biochemical characteristics analogous to those of the respective native enzymes (27, 41, 43). This indicates that the assembly protocol needed for a fully functioning proteasome may vary depending on the individual proteasome being investigated. Here, the native and active recombinant versions ($\alpha+\beta_2$ and $\alpha+\beta_1+\beta_2$) of the *P. furiosus* CP were comparable with respect to relative activity of peptide substrates, such that the functional properties of the recombinant CP did not seem to be impacted significantly by assembly protocol. Certainly, the relationship between temperature and β-subunit composition was similar for native and recombinant assemblies (see Figure 1). This may be the result of the fact that each recombinant protein underwent heat treatment at 85-90°C for at least 20 min to facilitate purification prior to assembly. The melting temperatures determined for the recombinant CP proteins (Figure 2) also appear to be consistent with previous reports on the thermostability of a range of *P. furiosus* proteins. However, hints of thermal transitions beginning at temperatures of 115°C and higher (see Figure 3) raises the prospect that multiple versions of a functional CP can exist when two β subunits are involved.

Even though archaeal 20S proteasomes are based on a limited number of α and β proteins, the results here support the prospect that distinct specialized roles for specific proteins can exist even in prokaryotes. The roles of the two α proteins in *H. volcanii* appear to be different, with separate proteasome structures being assembled based on varying stoichiometric ratios of subunits per structure (21, 42). In fact, *H. volcanii* synthesizes at least two native versions of the CP, $\alpha_1+\beta$ and $\alpha_1+\alpha_2+\beta$, which may recognize and degrade different types of substrates (21). Certainly, in many eukaryotic forms of the proteasome (3, 6, 12), α and β subunits can play specific and distinctive roles. Yeast CPs are comprised of up to seven different β subunits, with certain β subunits responsible for separate proteolytic

specificities (19). In fact, yeast proteasome β proteins interact to form active sites for proteolysis that nonetheless resemble archaeal CP active sites which are based on a single β protein (1).

Proteasome function was found to be essential for cell survival during heat shock but not under normal conditions for *T. acidophilum* (35), which has single α and β subunit types. The relationship between heat shock and CP α/β protein content has not been examained yet to any extent in eukaryotes or prokaryotes with multiple subunit forms. Certainly, temperature was found to be a factor in the composition of other complex multimeric archaeal proteins in thermophilic archaea; e.g., the hetero-oligomeric rosettasome in *Sulfolobus shibatae* has different α/β/γ subunit composition depending upon growth temperature (22, 23). In mammalian murine RM cells, even though heat shock led to decreased proteasome RNA levels and inhibited formation of the protease complex, no drastic alteration of CP α/β protein content was noted (24). In yeast, a heat shock transcription factor was found to coordinate expression of proteasome proteins to control proteasome synthesis under thermal stress, although the impact on this on CP constitution was not determined (18). Recent results from our lab showed that when *S. solfataricus* was shifted from optimal (80°C) to supraoptimal (90°C) temperatures, the transcription of ORFs encoding CP proteins (α, β1, β2) were unaffected throughout the 60 min period following the temperature shift (40). It was also noted that the transcriptional level of CP proteins in *S. solfataricus* were much higher than in *P. furiosus* under normal or stressed conditions, although the ORF encoding *S. solfataricus* PAN decreased significantly following temperature shift. For the hyperthermophilic archaea, it is yet to be determined whether CPs with two β subunits confer any special advantages upon specific microorganisms with

respect to thermal stress response. Perhaps those hyperthermophiles whose genomes encode two β proteins experience frequent temperature excursions in their natural habitats. In any case, the results here suggest that the impact of CP β subunit content on function at suboptimal, optimal and supraoptimal temperatures merits further examination, with an eye towards insights that relate to eukaryotic CPs. Such efforts are currently underway.

ACKNOWLEDGMENTS

This work was supported in part by grants from the NSF Biotechnology Program and the DOE Energy Biosciences Program. JKM acknowledges support from an NIH Biotechnology Traineeship. LSM acknowledges support from a GAANN Biotechnology Fellowship.

REFERENCES

1. **Arendt, C. S., and M. Hochstrasser.** 1997. Identification of the yeast 20S proteasome catalytic centers and subunit interactions required for active-site formation. Proc Natl Acad Sci U S A **94:**7156-61.

2. **Bauer, M. W., S.B. Halio, and R.M. Kelly.** 1997. Purification and characterization of a proteasome from the hyperthermophilic archaeon, *Pyrococcus furiosus*. Appl. Environ. Microbiol. **63:**116-1164.

3. **Baumeister, W., Z. Cejka, M. Kania, and E. Seemuller.** 1997. The proteasome: a macromolecular assembly designed to confine proteolysis to a nanocompartment. Biol Chem **378:**121-130.

4. **Bradford, M. M.** 1976. A rapid and sensitive method for the quantitation of microgram quantities of protein utilizing the principle of protein-dye binding. Anal Biochem **72:**248-254.

5. **Chhabra, S. R., K. R. Shockley, S. B. Conners, K. L. Scott, R. D. Wolfinger, and R. M. Kelly.** 2003. Carbohydrate-induced differential gene expression patterns in the hyperthermophilic bacterium *Thermotoga maritima*. J Biol Chem **278:**7540-7552.

6. **Coux, O., K. Tanaka, and A. L. Goldberg.** 1996. Structure and functions of the 20S and 26S proteasomes. Annu Rev Biochem **65:**801-847.

7. **De Castro, R. E., J. A. Maupin-Furlow, M. I. Gimenez, M. K. Herrera Seitz, and J. J. Sanchez.** 2006. Haloarchaeal proteases and proteolytic systems. FEMS Microbiol Rev **30:**17-35.

8. **De Mot, R., I. Nagy, and W. Baumeister.** 1998. A self-compartmentalizing protease in *Rhodococcus*: the 20S proteasome. Antonie Van Leeuwenhoek **74:**83-7.

9. **Frankenberg, R. J., M. Andersson, and D. S. Clark.** 2003. Effect of temperature and pressure on the proteolytic specificity of the recombinant 20S proteasome from *Methanococcus jannaschii*. Extremophiles **7:**353-60.

10. **Frankenberg, R. J., T. S. Hsu, H. Yakota, R. Kim, and D. S. Clark.** 2001. Chemical denaturation and elevated folding temperatures are required for wild-type activity and stability of recombinant *Methanococcus jannaschii* 20S proteasome. Protein Sci **10:**1887-96.

11. **Franzetti, B., G. Schoehn, D. Garcia, R. W. Ruigrok, and G. Zaccai.** 2002. Characterization of the proteasome from the extremely halophilic archaeon *Haloarcula marismortui*. Archaea **1:**53-61.

12. **Fu, H., J. H. Doelling, C. S. Arendt, M. Hochstrasser, and R. D. Vierstra.** 1998. Molecular organization of the 20S proteasome gene family from *Arabidopsis thaliana*. Genetics **149:**677-692.

13. **Fu, H., P. A. Girod, J. H. Doelling, S. van Nocker, M. Hochstrasser, D. Finley, and R. D. Vierstra.** 1999. Structure and functional analysis of the 26S proteasome subunits from plants. Mol Biol Rep **26:**137-146.

14. **Groll, M., M. Bochtler, H. Brandstetter, T. Clausen, and R. Huber.** 2005. Molecular machines for protein degradation. Chembiochem **6:**222-56.

15. **Groll, M., H. Brandstetter, H. Bartunik, G. Bourenkow, and R. Huber.** 2003. Investigations on the maturation and regulation of archaebacterial proteasomes. J Mol Biol **327:**75-83.

16. **Groll, M., and T. Clausen.** 2003. Molecular shredders: how proteasomes fulfill their role. Curr Opin Struct Biol **13:**665-73.

17. **Groll, M., and R. Huber.** 2004. Inhibitors of the eukaryotic 20S proteasome core particle: a structural approach. Biochim Biophys Acta **1695:**33-44.

18. **Hahn, J. S., D. W. Neef, and D. J. Thiele.** 2006. A stress regulatory network for co-ordinated activation of proteasome expression mediated by yeast heat shock transcription factor. Mol Microbiol **60:**240-51.

19. **Heinemeyer, W., M. Fischer, T. Krimmer, U. Stachon, and D. H. Wolf.** 1997. The active sites of the eukaryotic 20 S proteasome and their involvement in subunit precursor processing. J Biol Chem **272:**25200-9.

20. **Hobbie, J. E., R. J. Daley, and S. Jasper.** 1977. Use of nuclepore filters for counting bacteria by fluorescence microscopy. Appl Environ Microbiol **33:**1225-1228.

21. **Kaczowka, S. J., and J. A. Maupin-Furlow.** 2003. Subunit topology of two 20S proteasomes from *Haloferax volcanii*. J Bacteriol **185:**165-74.

22. **Kagawa, H. K., J. Osipiuk, N. Maltsev, R. Overbeek, E. Quaite-Randall, A. Joachimiak, and J. D. Trent.** 1995. The 60 kDa heat shock proteins in the hyperthermophilic archaeon *Sulfolobus shibatae*. J Mol Biol **253:**712-25.

23. **Kagawa, H. K., T. Yaoi, L. Brocchieri, R. A. McMillan, T. Alton, and J. D. Trent.** 2003. The composition, structure and stability of a group II chaperonin are temperature regulated in a hyperthermophilic archaeon. Mol Microbiol **48:**143-56.

24. **Kuckelkorn, U., C. Knuehl, B. Boes-Fabian, I. Drung, and P. M. Kloetzel.** 2000. The effect of heat shock on 20S/26S proteasomes. Biol Chem **381:**1017-23.

25. **Lin, G., G. Hu, C. Tsu, Y. Z. Kunes, H. Li, L. Dick, T. Parsons, P. Li, Z. Chen, P. Zwickl, N. Weich, and C. Nathan.** 2006. *Mycobacterium tuberculosis* prcBA genes

encode a gated proteasome with broad oligopeptide specificity. Mol Microbiol **59:**1405-16.

26. **Lowe, J., D. Stock, B. Jap, P. Zwickl, W. Baumeister, and R. Huber.** 1995. Crystal structure of the 20S proteasome from the archaeon *Thermoplasma acidophilum* at 3.4 A resolution. Science **268:**533-9.

27. **Maupin-Furlow, J. A., H. C. Aldrich, and J. G. Ferry.** 1998. Biochemical characterization of the 20S proteasome from the methanoarchaeon Methanosarcina thermophila. J Bacteriol **180:**1480-7.

28. **Maupin-Furlow, J. A., and J. G. Ferry.** 1995. A proteasome from the methanogenic archaeon *Methanosarcina thermophila*. J Biol Chem **270:**28617-22.

29. **Maupin-Furlow, J. A., M. A. Gil, I. M. Karadzic, P. A. Kirkland, and C. J. Reuter.** 2004. Proteasomes: perspectives from the Archaea. Front Biosci **9:**1743-58.

30. **Maupin-Furlow, J. A., S. J. Kaczowka, C. J. Reuter, K. Zuobi-Hasona, and M. A. Gil.** 2003. Archaeal proteasomes: potential in metabolic engineering. Metab Eng **5:**151-63.

31. **Maupin-Furlow, J. A., H. L. Wilson, S. J. Kaczowka, and M. S. Ou.** 2000. Proteasomes in the archaea: from structure to function. Front Biosci **5:**D837-65.

32. **Reuter, C. J., S. J. Kaczowka, and J. A. Maupin-Furlow.** 2004. Differential regulation of the PanA and PanB proteasome-activating nucleotidase and 20S proteasomal proteins of the haloarchaeon *Haloferax volcanii*. J Bacteriol **186:**7763-72.

33. **Reuter, C. J., and J. A. Maupin-Furlow.** 2004. Analysis of proteasome-dependent proteolysis in *Haloferax volcanii* cells, using short-lived green fluorescent proteins. Appl Environ Microbiol **70:**7530-8.

34. **Robb, F. T., D. L. Maeder, J. R. Brown, J. DiRuggiero, M. D. Stump, R. K. Yeh, R. B. Weiss, and D. M. Dunn.** 2001. Genomic sequence of hyperthermophile, *Pyrococcus furiosus*: implications for physiology and enzymology. Methods Enzymol **330:**134-57.

35. **Ruepp, A., C. Eckerskorn, M. Bogyo, and W. Baumeister.** 1998. Proteasome function is dispensable under normal but not under heat shock conditions in *Thermoplasma acidophilum*. FEBS Lett **425:**87-90.

36. **She, Q., R. K. Singh, F. Confalonieri, Y. Zivanovic, G. Allard, M. J. Awayez, C. C. Chan-Weiher, I. G. Clausen, B. A. Curtis, A. De Moors, G. Erauso, C. Fletcher, P. M. Gordon, I. Heikamp-de Jong, A. C. Jeffries, C. J. Kozera, N. Medina, X. Peng, H. P. Thi-Ngoc, P. Redder, M. E. Schenk, C. Theriault, N. Tolstrup, R. L. Charlebois, W. F. Doolittle, M. Duguet, T. Gaasterland, R. A. Garrett, M. A. Ragan, C. W. Sensen, and J. Van der Oost.** 2001. The complete genome of the crenarchaeon *Sulfolobus solfataricus* P2. Proc Natl Acad Sci U S A **98:**7835-40.

37. **Shockley, K. R., D. E. Ward, S. R. Chhabra, S. B. Conners, C. I. Montero, and R. M. Kelly.** 2003. Heat shock response by the hyperthermophilic archaeon *Pyrococcus furiosus*. Appl Environ Microbiol **69:**2365-71.

38. **Song, H. K., M. Bochtler, M. K. Azim, C. Hartmann, R. Huber, and R. Ramachandran.** 2003. Isolation and characterization of the prokaryotic proteasome

homolog HslVU (ClpQY) from *Thermotoga maritima* and the crystal structure of HslV. Biophys Chem **100:**437-52.

39. **Stein, R. L., F. Melandri, and L. Dick.** 1996. Kinetic characterization of the chymotryptic activity of the 20S proteasome. Biochemistry **35:**3899-908.

40. **Tachdjian, S., and R. M. Kelly.** 2006. Dynamic metabolic adjustments and genome plasticity are implicated in the heat shock response of the extremely thermoacidophilic archaeon *Sulfolobus solfataricus*. J Bacteriol **188:**4553-9.

41. **Wilson, H. L., H. C. Aldrich, and J. Maupin-Furlow.** 1999. Halophilic 20S proteasomes of the archaeon *Haloferax volcanii*: purification, characterization, and gene sequence analysis. J Bacteriol **181:**5814-24.

42. **Wilson, H. L., M. S. Ou, H. C. Aldrich, and J. Maupin-Furlow.** 2000. Biochemical and physical properties of the *Methanococcus jannaschii* 20S proteasome and PAN, a homolog of the ATPase (Rpt) subunits of the eucaryal 26S proteasome. J Bacteriol **182:**1680-92.

43. **Zwickl, P., F. Lottspeich, and W. Baumeister.** 1992. Expression of functional *Thermoplasma acidophilum* proteasomes in *E. coli*. FEBS Lett **312:**157-60.

Table 1: Changes in expression levels of *P. furiosus* proteasome protein, PAN and heat shock proteins upon shift from 90ºC to 105ºC. Data represent log_2-transformed fold-changes for four time points after culture temperature was increased relative to the 90ºC baseline. Column '0 min - Baseline' represents fold-change upon temperature increase (zero time point), column '5 min - Baseline' is 5 min after temperature change, and columns '30 min - Baseline,' '60 min - Baseline,' and '90 min – Baseline' are 30, 60, and 90 min after temperature change, respectively. Also reported are 60 min HS data (two replicates) from (37), shown in italics.

PF ID[a]	Function[a]	0+ min - Baseline		5 min - Baseline		30 min - Baseline		60 min - Baseline		90 min - Baseline	
		log_2(Fold)	Fold	log_2(Fold)	Fold	log_2(Fold)	Fold	log_2(Fold)	Fold	log_2(Fold)	Fold
PF1974	**Thermosome**	3.1 ± 0.2	**8.6**	2.0 ± 0.2	**4.0**	2.0 ± 0.3	**4.0**	-0.4 ± 0.4	**-1.3**	-1.0 ± 0.2	**-2.0**
								2.00 ±0.25	***4.0***		
								2.07 ±0.16	***4.2***		
PF1883	**SmHSP**	5.1 ± 0.2	**34.3**	3.7 ± 0.2	**13.0**	4.9 ± 0.2	**29.9**	2.9 ± 0.3	**7.5**	1.5 ± 0.2	**2.8**
								>2.95 ±0.34	***> 7.7***		
								>2.80 ±0.12	***> 6.9***		
PF1404	**β1 protein**	1.0 ± 0.2	**2.0**	1.2 ± 0.3	**2.3**	0.4 ± 0.5	**1.3**	0.5 ± 0.5	**1.4**	0.2 ± 0.3	**1.1**
								1.03 ±0.33	***2.0***		
								0.98 ±0.05	***2.0***		
PF0159	**β2 protein**	0.2 ± 0.1	**1.1**	-0.1 ± 0.2	**-1.1**	0.4 ± 0.5	**1.3**	-2.1 ± 0.6	**-4.3**	-2.2 ±0.3	**-4.6**
								0.89 ±0.21	***1.9***		
								0.47 ±0.05	***1.4***		
PF0115	**PAN**	-0.1 ± 0.3	**1.1**	-0.4 ± 0.4	**-1.3**	1.0 ± 0.4	**2.0**	-1.6 ± 0.6	**-3.0**	-1.7 ± 0.6	**-3.2**
								0.25 ±0.16	***1.2***		
								-0.12 ±0.05	***-1.1***		
PF1571	**α protein**	-1.0 ± 0.3	**-2.0**	-0.7 ± 0.5	**-1.6**	-2.1 ± 0.6	**-4.3**	-2.3 ± 0.9	**-4.9**	-1.6 ± 0.8	**-3.0**
								-1.96 ±0.28	***-3.9***		
								-1.16 ±0.03	***-2.2***		

[a] SmHSP=small heat shock protein; PAN = proteasome-activating nucleotidase

Table 2. Effect of Assembly Temperature (β Protein Content) on *P. furiosus* 20S Proteasome Kinetics at 95°C

	V_{max} (U/μg)	K'_m (μM)	K_{s1} (μM)	k_{cat} (s^{-1})	k_{cat}/K'_m	R^2
VKM-MCA*						
90ºC Assembly	1159	45.2	346	1.0	21.9	0.96
105ºC Assembly	2194	36.4	581	1.9	51.5	0.87
Native (2)	2200	460				
LLVY-MCA**						
90ºC Assembly	41	204	NA	0.03	1.8	0.83
105ºC Assembly	150	214	NA	0.12	6.4	0.89
Native (2)	114	360				
AAF-MCA**						
90ºC Assembly	135	695	NA	0.12	0.2	0.99
105ºC Assembly	70	282	NA	0.05	3.0	0.91
Native (2)	162	1780				

*VKM data were fit here using substrate inhibition model. Note that previous data for native 20S Pfu proteasome was fit with standard Michaelis-Menten model (2)

**LLVY, AAF data were fit using standard Michaelis-Menten model

Table 3. Proteasome proteins encoded in prokaryotic genomes

	T (ºC)	α protein		β protein		PAN	
Archaea							
Aeropyrum pernix	95	APE1449		APE0521	APE0507	APE2012	
Archaeoglobus fulgidus	83	AF0490		AF0481		AF1976	
Ferroplasma acidarmanus	37	EAM94259		EAM93969		EAM94439*	
Halobacterium sp. NRC-1	50	VNG0166G		VNG0880G		VNG2000G	VNG0510G
Haloarcula marismortui 43049	50-53	AAV46668	AAV46124	AAV45476	AAV46667	AAV47895	AAV48212
Haloferax volcanii	45	T48679		T48677		AAV38127	AAV38126
Haloquadratum walsbyi	37	HQ1516A	HQ2454A	HQ2661A		HQ3115A	HQ1544A
Methanocaldococcus jannaschii	85	MJ0591		MJ1237		MJ1176	
Methanococcoides burtonii 6242	30-35	ABE51206		ABE51369		ABE53157	ABE52987
Methanopyrus kandleri AV19	98	MK0385		MK1228		MK0878	
Methanosarcina acetivorans	35-40	MA1779		MA3873		MA4268	MA4123
Methanosarcina barkeri	37	AAZ71416		AAZ69178		AAZ69383	AAZ69600
Methanosarcina mazei Goel	30-40	MM2620		MM0694		MM1006	MM0798
Methanosarcina thermophila	50	MTU30483		MTU22157		ND	
Methanospirillum hungatei JF	30-37	ABD41987		ABD40598		ABD40790	ABD40788
Methanotherm. thermautotrophicus	65-70	MTH686		MTH1202		MTH728	
Methanococcus maripaludis S2	35-40	MMP0251		MMP0695		MMP1647	
Natronomonas pharaonis 2160	45	NP3738A		NP3472A		NP1524A	NP5038A
Nanoarchaeum equitans Kin4-M	90	AAR39362		AAR39057		AAR39040	
Picrophilus torridus DSM 9790	60	PTO0804		PTO0686		PTO0456*	
Pyrobaculum aerophilum	100	PAE2215		PAE3595	PAE0807	PAE0696*	
Pyrococcus abyssi	96	PAB0417		PAB1867	PAB2199	PAB2233	
Pyrococcus furiosus	100	PF1571		PF1404	PF0159	PF0115	
Pyrococcus horikoshii	98	PH1553		PH1402	PH0245	PH0201	
Sulfolobus acidocaldarius	75	AAY80005		AAY80046	AAY80272	AAO73475	
Sulfolobus solfataricus	87	SSO0738		SSO0766	SSO0278	SSO0271	
Sulfolobus tokodaii	80	ST0446		ST0477	ST0324	ST0330	
Thermoplasma acidophilum	59	TA1288		TA0612		TA0840*	
Thermoplasma volcanium	60	TVN0304		TVN0663		TVN0947*	
Thermococcus kodakarensis	95	TK1637		TK1429	TK2207	TK2252	
Bacteria							
Mycobacterium tuberculosis	37	MT2169		MT2170		ND	
Rhodococcus erythropolis	10-40	AAC45741	AAC45737	AAC45740	AAC45736	ND	
Streptomyces coelicolor	10-37	SCO1643		SCO1644		ND	

ND - No PAN homolog detected
*No ORF annotated as PAN, but possible homolog detected.

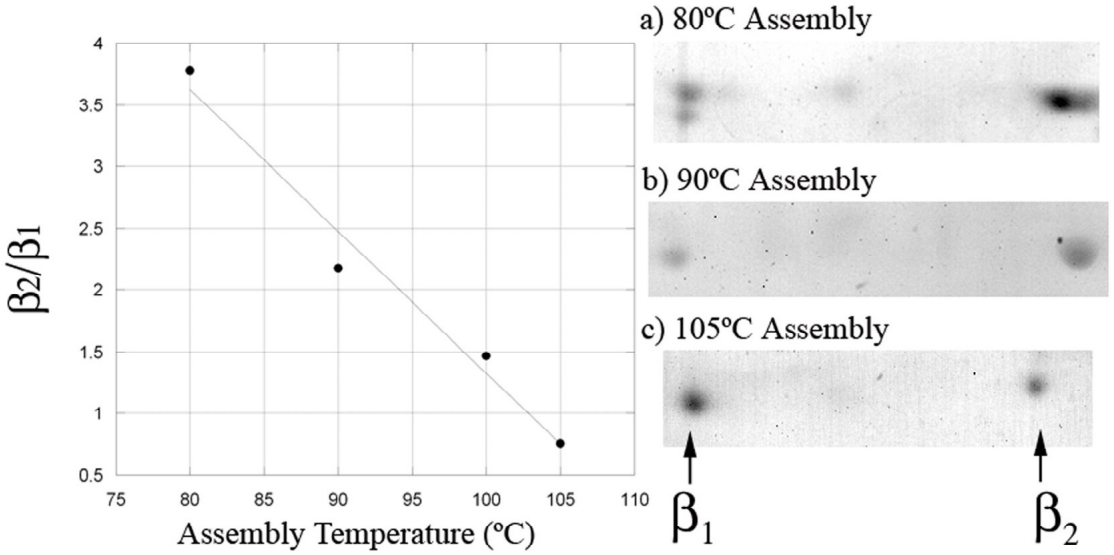

Recombinant Enzyme		Native Enzyme	
Assembly Temperature (°C)	**β_2/β_1**	**Growth Temperature (°C)**	**β_2/β_1**
80	3.8	80	3.0
90	1.9	90	1.8
100	1.4	Not determined	
105	0.9		

Figure 1. The graph shows the ratio of β_2 to β_1 proteins in recombinant *P. furiosus* 20S proteasome as a function of assembly temperature as determined by densitometry of proteins separated by 2D gel electrophoresis. Enlargements of 2D gels for various recombinant proteasome assemblies are shown a-c, in which the ß1 subunit is located on the left and the ß2 is on the right. The ß2 to ß1 ratios for the native enzyme purified from cells grown at either 80ºC or 90ºC are shown in the table and are compared to the ratio for the recombinant assembly.

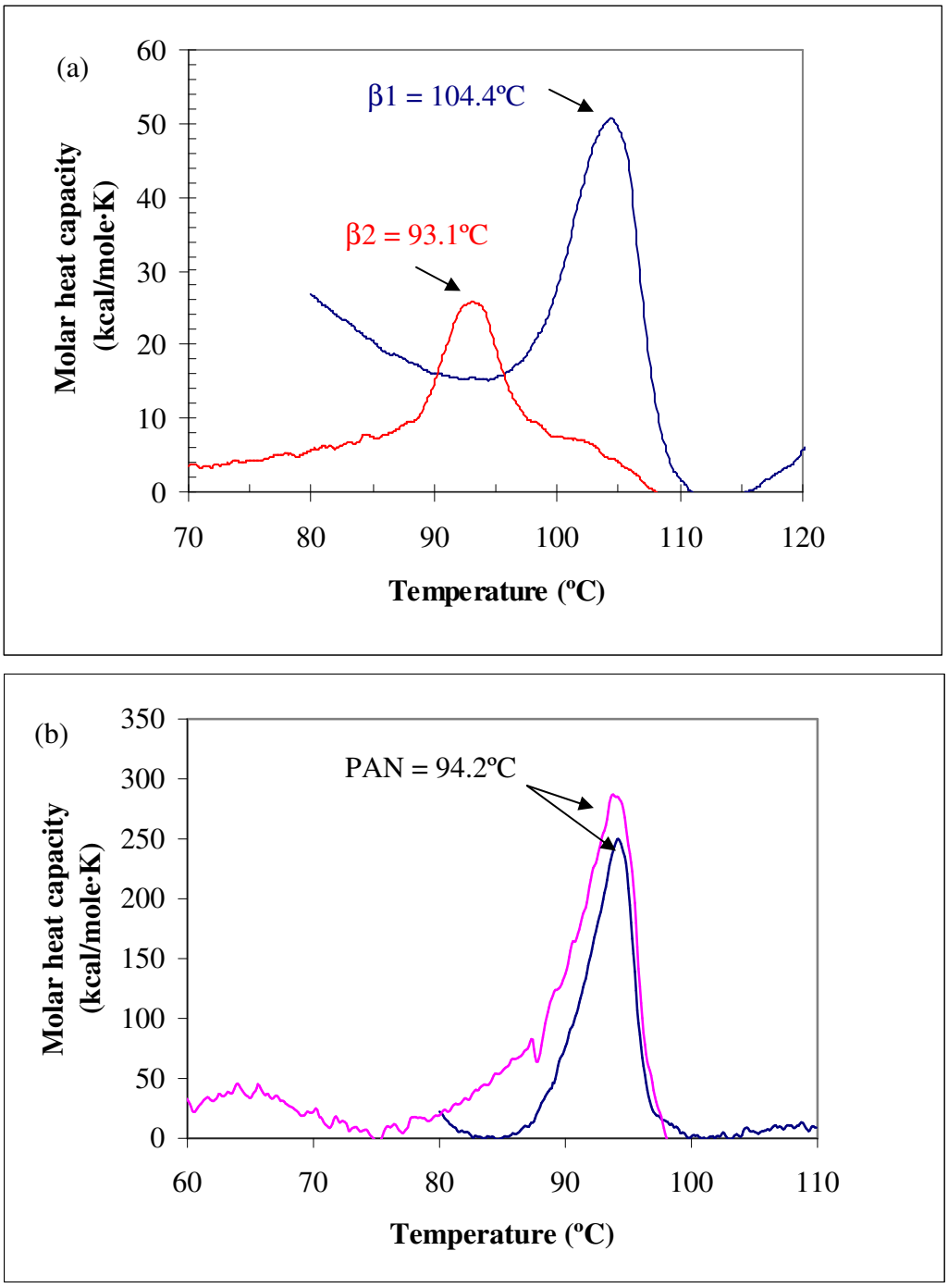

Figure 2. Differential scanning calorimetry showing melting points of *P. furiosus* (a) recombinant proteasome β proteins, and (b) recombinant PAN. No thermal transition was noted for α protein up to 125°C. Recombinant PAN (b) was analyzed in two separate scans, with both melting peaks occurring at the same temperature of 94.2ºC.

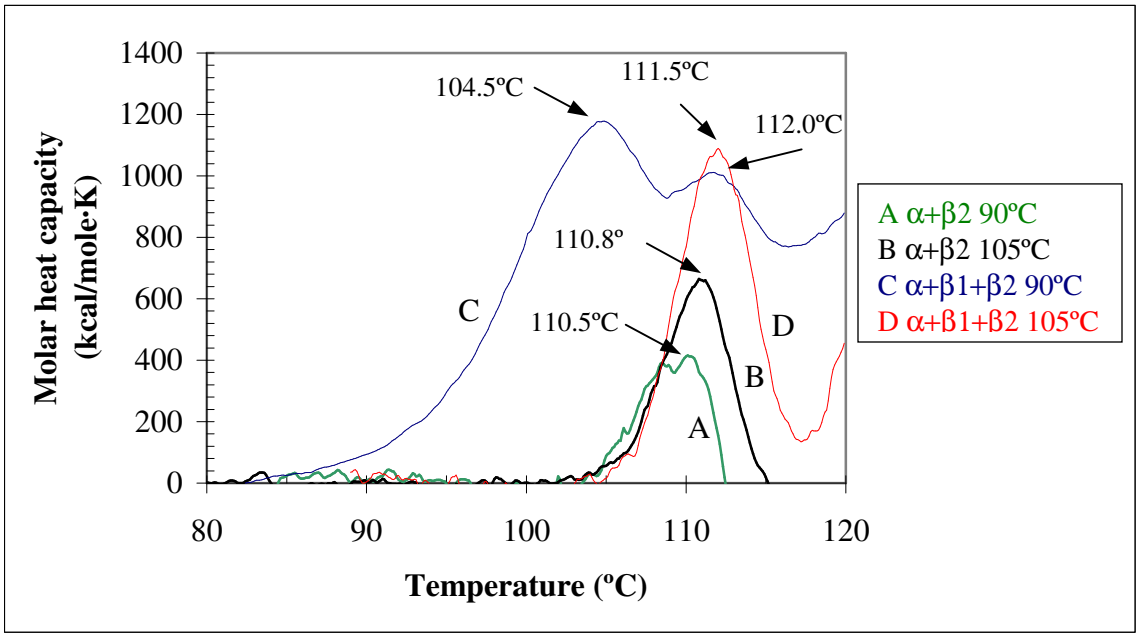

Figure 3. Differential scanning calorimetry showing thermal transitions for *P. furiosus* recombinant 20S proteasome assemblies. A = α+β2 assembled at 90°C, B = α+β2 assembled at 105°C, C = α+β1+β2 assembled at 90°C, and D = α+β1+β2 assembled at 105°C.

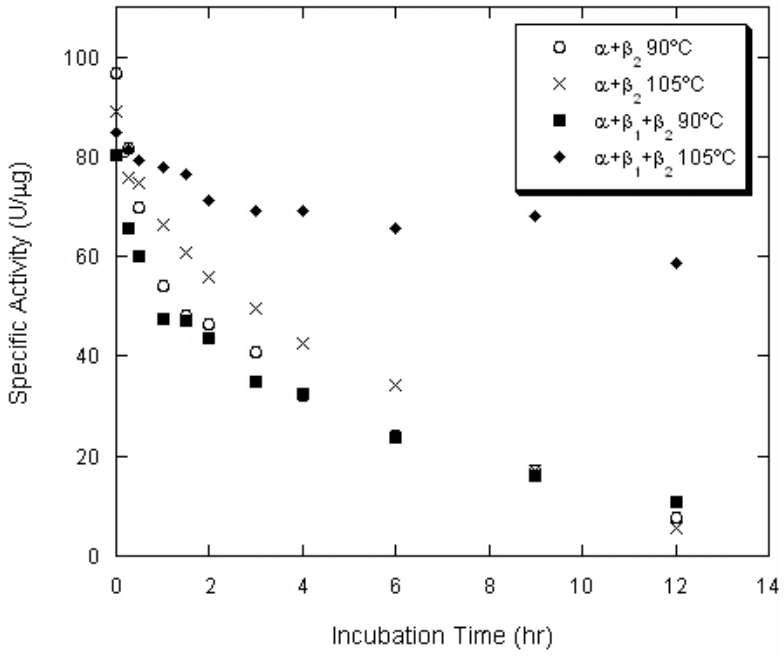

Proteasome form	Decay constant (k_{obs})
α+β2 90°C	0.18 ± 0.01
α+β2 105°C	0.19 ± 0.01
α+β1+β2 90°C	0.15 ± 0.01
α+β1+β2 105°C	0.025 ± 0.004

Figure 4. Specific Activity of VKM-MCA by *P. furiosus* proteasomes versus incubation time at 115°C. Error bars are shown on plots. VKM-MCA endpoint activities for all points were determined using a fixed volume of each aliquot in triplicate in microtiter plates and at an assay incubation temperature of 95°C with 5 µM substrate.

Chapter 4

Inter-genus compatibility of 20S proteasome alpha and beta subunits in hyperthermophilic archaea*

Joshua K. Michel and Robert M. Kelly

* Submission anticipated to Applied and Environmental Microbiology

ABSTRACT

The hyperthermophilic archaeon *Archaeoglobus fulgidus* produces a 20S proteasome (or core particle, CP) comprised of two distinct subunits α (AF0490) and β (AF0481). In contrast, the *Pyrococcus furiosus* genome encodes three proteasome components, one α (PF1571) and two β proteins (β1-PF1404; β2-PF0159); *in vitro* the functional 20S proteasome assembly in *P. furiosus* requires α and β2 but not β1. The ratio of the two different β subunits incorporated in *P. furiosus* proteasome was previously shown to vary in accordance with growth temperature and *in vitro* assembly temperatures, which led to altered biochemical and biophysical characteristics (27). In this work, we demonstrate the ability to form hybrid proteasome CPs comprised of *A. fulgidus* α and *P. furiosus* β_1 and/or β_2 that display characteristics different then the wild-type enzymes. Of particular significance was the finding that *P. furiosus* β_1 preferentially assembles with *A. fulgidus* α in the presence of AFβ. The *A. fulgidus* recombinant proteasome exhibited comparable biochemical properties to the *P. furiosus* enzyme (α+β2 or α+β1+β2), albeit with a reduced temperature optimum. However, the *A. fulgidus* and hybrid CPs were not substrate-inhibited as was the case for the *P. furiosus* CP. Consistent with the 20°C difference in optimal growth temperatures for these two organisms, thermostability of the two wild-type proteasomes were markedly different; the 1st order inactivation constant (k_d) for *A. fulgidus* proteasome was 0.35 at 90°C compared to a k_d of 0.15 at 115.0°C for the *P. furiosus* CP (PFα+PFβ_1+PFβ_2) assembled at 90°C. A melting temperature of 104°C was determined by DSC for AFα+AFβ, compared to >115°C for PFα+PFβ_1+PFβ_2. The melting temperature for *P. furiosus* α was estimated to be 135°C,

which likely contributes significantly to the extreme thermostability of the native *P. furiosus* proteasome. Combination of AFα with PFβ_1, PFβ_2, or both PFβ_1+PFβ_2 resulted in active proteases of approximately 700 kDa. PFα and AFβ did not form a CP. The chimeric, or hybrid, proteasomes exhibited inactivation constants, k_d, in the range of 0.3-0.4 when measured at 80°C. The hybrid CP based on AFα and both PFβ1 and PFβ2 demonstrated an optimal temperature comparable to that of PFα+PFβ_1+PFβ_2 The substrate specificity of the hybrid proteasomes differed biochemically from the wild-type proteasome; AFα+PFβ_1 and AFα+PFβ_2 both degraded VKM-, AAF-, and LLVY-MCA. However, AFα+PFβ_1+PFβ_2 hydrolyzed FVA- and QRR-MCA in addition to VKM-, AAF-, and LLVY-MCA. Taken together, these results demonstrate that hybrid proteasomes can be constructed from different hyperthermophiles and that subunit composition influences biochemical and biophysical properties. They also suggest that CPs in particular archaea may have arisen from common sources, given the fact that hybrid inter-generic versions can be created *in vitro*.

INTRODUCTION

Proteasomes are heteromultimeric proteases found in all domains of life that play a key role in intracellular protein degradation (15-17, 20, 26, 31, 33, 34, 38, 41, 44). In eukaryotes, the composition of the proteasome core particle (CP or 20S proteasome) is based on many versions of small α- and β-type proteins (21-31 kDa) that assemble into heptameric stacked rings ($\alpha_7\beta_7\beta_7\alpha_7$); the set of 14 α and 14 β subunits that comprise the CP assembly can vary depending upon cellular status (17). For example, the *Saccharomyces cerevisiae* CP can have up to seven different β proteins in its assembly, which contributes to multiple proteolytic specificities (1). The genomes of higher eukaryotes, such as *Arabidopsis thaliana*, encode for as many as 13 α-type and 10 β-type proteins, creating the possibility of numerous CP versions (13). Three γ-interferon-inducible mammalian β subunits are linked to the generation of major histocompatibility complex class 1 peptides (2, 9, 14, 35). All archaeal and some bacterial genomes that have been sequenced to date encode α and β proteins that comprise the 20S proteasome (30). In some cases, 20S proteasome composition may also be variable in archaea, although the possibilities appear much more limited since typically only one or two α/β proteins are found in their genomes (15, 27, 30, 31).

In bacteria, 20S proteasomes have been identified in *Streptomyces coelicolor* as well as in *Mycobacterium tuberculosis*, both of which appear to be based on single α and β proteins (25, 36). In the hyperthermophilic archaea, available genome sequence data indicate that the CP is most commonly based on either one α and one β protein, or two β proteins and one α protein. In *Haloferax volcanii*, the proteasome CP is found in at least two different isoforms, based on combinations of one β protein and two α proteins (6, 22). The additional

α or β protein in archaeal proteasomes may provide some biochemical and/or biophysical versatility, along the lines seen in the eukaryotic proteasome (17, 18). It has been proposed that the *H. volcanii* CP assembly, and association with the proteasome-activating nucleotidases (PanA and PanB), may be growth phase-associated (37). Environmental factors may contribute to the β protein composition in hyperthermophiles, as demonstrated by the *P. furiosus* proteasome which alters β composition as a function of growth temperature (27). The purpose of the additional β subunit in archaeal proteasomes is not known, although in *P. furiosus* the alternate β subunit has been linked to increased thermostabililty and altered biochemical properties (27). The less expansive inventory of 20S proteasome subunits in bacteria and archaea could facilitate efforts to pinpoint the specific roles of these individual components in proteasome function both *in vivo* and *in vitro*.

For many thermophilic archaea*, in vitro* combination of the α and β proteins leads to spontaneous, self-directing assembly of the 20S proteasome, without need for chaperones or other accessory proteins (31, 32). However, this process can be extremely inefficient, such as is the case for the *Methanosarcina thermophila* 20S proteasome in which only 50% of the β proteins were processed and incorporated into a fully active 20S CP (28). Likewise, the assembly of the *P. furiosus* 20S proteasome at physiologically relevant temperatures yielded a substantial amount of unincorporated β proteins (Michel and Kelly, unpublished data). In vitro assembly of the 20S proteasome can be problematic. Indeed, the recombinant 20S proteasome from *Methanococcus jannaschii* required denaturation of α and β subunits with urea, followed by their combination at high temperature and subsequent refolding by removal of the denaturant using dialysis (12). Without unfolding-refolding of the *M. jannaschii* proteasome, an active enzyme was produced, but with a markedly decreased optimal

temperature (95ºC) compared to the native version (119ºC) (11). Conversely, the recombinant proteasome from *P. furiosus* and *M. thermophila* demonstrated similar biochemical and physical characteristics to their native counterparts (27, 28). It was noted that the recombinant *P. furiosus* proteasome contained more β_1 subunits when assembled at higher temperatures (27). Yet, no proteasome formation was noted when *P. furiosus* α and β_1 were combined in the absence of β_2 at any assembly temperature tested (80-105°C) (27).

Large heteromultimeric proteases are vital and ubiquitous components of cellular proteolytic systems (15). In addition to the architectural similarity among the ATP-dependent proteases Clp and the proteasome, other degrading enzymes display similar self-compartmentalizing structures. The proteasome genes have also been found in close proximity to those associated with RNA/DNA processing, leading to the region being termed the exosome (24). Proposed as a functional homolog in organisms lacking the proteasome, the caseinolytic protease (Clp) demonstrates the ability to selectively degrade proteins based on target residue sequences or with the aid of adaptor proteins (4, 5). The alteration of Clp subunit composition has been linked to changes in protein targeting, possibly in response environmental changes (7, 8). Within the ubiquitin-proteasome system, chimeric proteins have been used to regulate degradation rates for specific cellular targets (46). However, generally little is known about the properties of hetero- and homo-multimeric enzymes formed from the replacement of component subunits with heterologous counterparts. Additionally, the use of genetic variability of individual subunits within multimeric proteins has yet to be fully exploited for tailoring enzyme function.

Within a single organism's genome, archaeal proteasome subunits exhibit a high level of conservation to each other, although not to the degree (90% similarity) found in

euckaryotic genomes. However, the archaeal subunits in distinct organisms also display a level of similarity comparable to those found within a single species (27). The possibility to form *in vitro* hybrid, or chimeric, proteasomes consisting of subunits from different organisms was first noted for *Aeropyrum pernix* and *A. fulgidus* (16). This assembly of *A. pernix* α with *A. fulgidus* β suggested that a common assembly pathway for the CP of these two organisms existed (16). Formation of such hybrids might be of biotechnological relevance in light of reports demonstrating the *in vivo* degradation of aggregation-prone proteins by a mesophilic archaeal proteasome expressed in mammalian cells (45); this system may provide an opportunity for the *in vivo* combination of heterologous proteasome proteins. Here, we present the first detailed description of biochemical and biophysical properties for the hybrid proteasomes formed from *P. furiosus* and *A. fulgidus* CP components.

MATERIALS AND METHODS

Note on Nomenclature: Typically the terms 20 proteasome and core particle(CP) are used interchangeably when referring to the central catalytic barrel of the proteasome. However, in this work we will use CP, which we believe is more general and thus better suited for describing enzymes comprised of heterlogous subunits. The term 20S proteasome will be reserved for descriptions of enzymes formed by combination of subunits from a single organism.

Enzyme assays. Core particle peptidase activity was determined by endpoint assay in 50 mM sodium phosphate buffer (SPB), pH 7.2 and 95°C (unless otherwise noted), with a microtiter plate reader (Model HTS 7000 Plus Bio Assay Reader, Perkin-Elmer, Wellesley,

MA) by detection of 7-amino-4-methylcoumarin (MCA) released from the carboxyl terminus of N-terminally blocked peptides (Sigma-Aldrich, St. Louis, MO) (3). Negative controls (no enzyme) were run in triplicate to account for thermal degradation of substrates. Kinetic constants were determined using a least squares fit of an appropriate model (Michaelis-Menten with or without inhibition) to the initial velocity (U/µg) as a function of substrate concentration (0.01 mM-0.50 mM) data at 95ºC. The optimal catalytic temperature of each assembly was determined using 200 ng of enzyme in 0.05 mM VKM-MCA, incubated at temperatures ranging from 50ºC to 100ºC. One unit of protease activity was defined as the amount of enzyme required to release 1.0 pmol of MCA per min. Total protein concentrations were determined using the Coomassie blue dye-binding method (Bio-Rad, Hercules, CA) in microtiter plates with bovine serum albumin (Sigma-Aldrich, St. Louis, MO) as the standard. The optimal catalytic temperature of each assembly was determined using 200 ng of enzyme in 0.05 mM VKM-MCA, incubated at temperatures ranging from 50ºC to 100ºC.

Cloning and expression of the *P. furiosus* and *A. fulgidus* 20S proteasome genes in *Escherichia coli*. The genes for the three proteins associated with the *P. furiosus* proteasome, *psmA* (PFα, PF1571, "proteasome, subunit alpha"), *psmB-1* (PFβ_1, PF1404, "proteasome, subunit beta"), and *psmB-2* (PFβ_2, PF0159, "proteasome, subunit beta"), were separately cloned into the pET-24d(+) vector (Novagen, Madison, WI). The PF α gene was amplified using the primers: forward: (5'-TGAACGCCATGGCATTTGTTCCACCTCA-3') and reverse: (5'-ATAAAAATTGGATCCAAGTCAGTAGTTGCTATCCA-3'). The PF β2 gene was amplified with: forward (5'-

TTAGGTGGTGCTCATGAAGAAAAAGACTGGAA-3') and the reverse primer (5'-TAAGGAAGCCTGGATCCTTCATACTACAAACTCTT-3'). The PF β_1 gene was cloned using an ORF that started with the fourth amino acid from the reported amino-terminus (based on locations of start codon and likely ribosomal binding site). N-terminal sequencing confirmed that the unprocessed β_1 subunit was expressed correctly. The primers used for β1 gene amplification were: forward (5'-TGTTGCCCATGGAAGAGAAACTTAAGGGAA-3') and reverse (5'- AAATTGTCGGATCCTTGGACTACTTTAACATTTT-3').

The gene for the *A. fulgidus* alpha proteasome protein (AF0490) was cloned into pET-24d(+) vector, while the corresponding beta protein (AF0481) was cloned into pET15b vector (Novagen, Madison, WI), which codes for a removable N-terminal $(Histidine)_6$-tag. The AF α gene was amplified using the primers: forward: (5'-GCGCCATATGATGCATTTACCGCAAATGGGATA-3') and reverse: (5'-GCGCGTCGACTCACTTCTTCAGCAGCTCCCTA -3'). The primers used for AF β gene amplification were: forward (5'-GCGCCATATGATGAGCATGATAGAGGAGAAGAT-3') and reverse (5'-GCGCCTCGAGTTATTTCCTGAACTTGGCCAGTA-3').

The *P. furiosus* α gene was expressed in *E. coli* BL21(DE3), while the PF β1 and PF β_2 genes were separately expressed in *E. coli* BL21-CodonPlus®(DE3)-RIL (Stratagene, La Jolla, CA). Expression was induced with 0.4 mM IPTG (OD_{595} = 0.60); cells were harvested 3-5 hr after induction (37ºC). The re-suspended cell pellets were treated with lysozyme, sonicated (Misonix, Inc., Farmingdale, NY), and centrifuged (18,000 x g, 4ºC) for 30 min. Two 20-min heat treatments of the soluble protein fractions for α and β_1 were performed: the first at 85ºC and the second at 90ºC, to remove residual *E. coli* protein. Each treatment was followed by cooling on ice for 30 min, centrifugation (18,000 x g, 4ºC) for 30 min to

remove insoluble protein. The β_2 protein preparation required only one 20-min heat treatment at 85ºC.

The *A. fulgidus* α and β genes were also expressed separately in *E. coli* BL21(DE3). Cultures were grown at 37ºC, expression was induced with 1.0 mM (final concentration) IPTG (OD_{595} = 0.70-1.0) and shifted to 30ºC; cell harvest occurred 5 hr after induction. The re-suspended cell pellets were treated with lysozyme, sonicated (Misonix, Inc., Farmingdale, NY), and centrifuged (18,000 x g, 4ºC) for 30 min. A single 20-min heat treatment of the soluble protein fraction for *A. fulgidus* α was performed at 60ºC to remove residual *E. coli* protein. The *A. fulgidus* β protein was purified using a HiTrap Chelating HP column (GE Life Sciences, Piscataway, NJ) followed by a 20-min heat treatment at 60C. The N-terminal His-tag was cleaved by overnight digestion with Thrombin (Novagen, Madison, WI) at 37ºC, followed by a second 20 min teat treatment at 60°C.

Expression of the *A. fulgidus* β protein (AF0481). The *A. fulgidus* β protein was expressed with an N-terminal $(His)_6$-tag that aided in expression and purification. However, the N-terminal His residues blocked the formation of an active proteasome when combined with the AFα protein. This is most likely due to a hindrance effect from the $(His)_6$ region which prevented ring formation, as well as N-terminal hydrolysis. For this reason, the N-terminal region (approximately 3 kDa in size) was cleaved using the mesophilic protease Thrombin. Figure 1 shows the SDS PAGE gel of the expressed AFβ uncleaved (lane 2), AFβ thrombin cleaved (lane 3), and AFβ thrombin cleaved & heat-treated (lane 4). Following thrombin cleavage and heat treatment the AFβ recombinant protein exhibited a similar molecular weight (~28 kDa) to that calculated from sequence data (27.6 kDa). The

heat treatment step following Thrombin cleavage removed both residual *E. coli* proteins, as well as the Thrombin present, resulting in a pure β protein sample.

Assembly of the recombinant CP. To assemble the CP, the α and β proteins were combined in equimolar ratios to a final total protein concentration of 0.5-0.7 mg/ml. This mixture was then incubated at the indicated temperature for 1 hr, cooled on ice for 1 hr, and precipitated material was removed through centrifugation (16,000 x g, 4ºC) for 30 min. In order to remove unincorporated α and β proteins, the sample was applied to a S-300 High Resolution XK 16/40 column, calibrated with a High Molecular Weight Calibration Kit (GE Life Sciences, Piscataway, NJ). All CP VKM-MCA activity was eluted in the first peak which corresponded to a protein of approximately 660 kDa; these fractions were then concentrated using a 30,000 MWCO Centriplus® Centrifugal Filter Device (Millipore, Billerica, MD).

Two-dimensional gel electrophoresis of purified CP. Purified samples of the CP (45 µg) were precipitated in a 10% trichloroacidic acid (TCA) solution on ice for 1 hr. The resulting pellet was washed 3 times with 150 µL of ice-cold acetone (-20ºC) and then dried for 5 minutes at 60ºC. The protein was re-suspended in 125 µL of re-hydration buffer (8 M urea, 2% CHAPS, 50 mM dithiothreitol (DTT), 0.2% Bio-Lyte ampholytes (Bio-Rad, Hercules, CA) and applied to a 7.0 cm pH 3-10 isoelectric focusing (IEF) strip (Bio-Rad). The strip was subjected to active re-hydration (50V) for 16 hrs. The conditions used for focusing were: 250 V, linear ramp, 20 min; 4000 V, linear ramp, 2 hr; 4000 V, rapid ramp, 10,000 V-hr. After IEF, the strips were incubated in equilibration buffer I (6 M urea, 0.375

M Tris-HCl, pH 8.8, 2% SDS, 20% glycerol, 2% DTT) for 10 min at room temperature, followed by another 10 min incubation in equilibration buffer II (6 M urea, 0.375 M Tris-HCl, pH 8.8, 2% SDS, 20% glycerol, 2.5% iodoacetamide). For the second dimension, the IEF strip was then placed on top of a 12% SDS PAGE gel and covered with a 2-D agarose overlay gel (0.5 % Low Melting Point Agarose, Tris base 2.9 g/L, glycine 14.4 g/L, SDS 1.0 g/L) . The gels were stained with GelCode® Blue Staining Reagent (Pierce, Rockford, IL) and analyzed on a GS-710 Calibrated Imaging Densitometer (Bio-Rad).

Differential scanning calorimetry of recombinant CP's and proteasome subunit proteins. The melting temperatures of all expressed proteins were determined using a CSC nanodifferential scanning calorimeter (DSC; Calorimetry Sciences Corp., American Fork, UT). All samples were dialyzed against 50 mM SPB, pH 7.2, which was the buffer used to generate the baseline scan. Samples (0.21 mg/ml) were de-gassed and scanned from 25-125ºC using a scan rate of 0.5ºC/min for two heating and cooling cycles. Heat capacity as a function of temperature was determined using the software program accompanying the DSC instrument to estimate melting temperatures. After each sample was analyzed on the DSC, activity assays and native gels were used to determine if complete or irreversible denaturation had occurred. Samples were centrifuged (16,000 x g, 4ºC) to remove aggregates, total protein concentrations were determined, and activity assays were run simultaneously against the corresponding initial samples to obtain relative loss of activity.

Thermal inactivation of CP assemblies. High-temperature incubation of the active recombinant proteasome forms (AFα+AFβ, AFα+PFβ$_1$, AFα+PFβ$_2$, and AFα+PFβ$_1$+PFβ$_2$

assembled at 90ºC) was done to examine thermal inactivation rates. Each assembly was adjusted to a baseline concentration of 0.01 mg/ml and incubated at 80ºC, 90ºC, or 100ºC in a Polymerase Chain Reaction machine (Perkin Elmer, Waltham, MA) for up to 12 hr. Aliquots were taken at time points from 0-12 hr and stored on ice until the end of the incubation period. The standard VKM-MCA microtiter plate assay was then used to compare the activities of the mixtures; 100 ng enzyme, based on pre-incubation concentration, was mixed with 50 μM VKM-MCA and heated to 95ºC for 1-10 min depending on the sample. The resulting fluorescence scores, with average background values subtracted, were determined, and used to calculate first-order decay constants.

RESULTS

Composition of the *A. fulgidus* and *A. fulgidus-P. furiosus* hybrid CP. The purified, functional CP constructs were subjected to analysis by 2D gel electrophoresis to determine subunit composition. Separation of the proteasome subunits was facilitated by the difference in molecular weight and isoelectric points, as noted in Table 1. As shown in Figure 2, the 2D gel image for AFα+AFβ exhibited 2 spots corresponding to the α and β proteins, while the AFα+PFβ$_1$+PFβ$_2$ gel image showed three spots corresponding to α, β$_1$, and β$_2$. Densitometry analysis of the *A. fulgidus* recombinant proteasome showed a 1:1 ratio between AFα and AFβ that is consistent with the $\alpha_7\beta_7\beta_7\alpha_7$ proteasome architecture. The hybrid enzyme, AFα+PFβ$_1$+PFβ$_2$, yielded a β$_1$:β$_2$ ratio of 1.0, which is similar to that found for the recombinant *P furiosus* proteasome assembled at 105ºC (27). In contrast, the 2D gel of the AFα+AFβ+PFβ$_1$ hybrid shows only 2 spots, corresponding to the AFα and PFβ$_1$

proteins. Thus, the *A. fulgidus* α protein appears to preferentially incorporate the *P furiosus* β_1 in place of the *A. fulgidus* β.

Biochemical properties of *A. fulgidus* and hybrid *A. fulgidus-P. furiosus* CP assemblies. The recombinant *A. fulgidus* CP assembly was screened for activity against a number of peptide substrates, shown in Table 3. For substrates that were hydrolyzed, relative activities were as follows: VKM >> AAF >LLVY > AAA > QRR > GPLPG > RR > FVR. The preferential cleavage of VKM-MCA by the recombinant *A. fulgidus* proteasome was similar to that reported for the *P. furiosus* native and recombinant enzymes (3, 27). Each individual protein (AFα, AFβ, PFα, $PF\beta_1$, $PF\beta_2$) was inactive against VKM-MCA and all other substrates tested, when initially expressed and stored at 4ºC or when heated to 80ºC, 90ºC or 95ºC. The hybrid proteasome formed from $AF\alpha+PF\beta_1+PF\beta_2$ showed a substrate preference of VKM > LLVY > AAF > FVR > AAA > QRR, which is similar to the native *P. furiosus* proteasome and recombinant 20S proteasome $PF\alpha+PF\beta_1+PF\beta_2$ (3). The hybrid CP $AF\alpha+PF\beta_1$ showed a substrate preference of VKM >> AAA > LLVY > AAF, while $AF\alpha+PF\beta_2$ demonstrated the preference VKM >> AAF > LLVY. Thus, the incorporation of either $PF\beta_1$ or $PF\beta_2$ has a significant impact on CP substrate preference, which is consistent with previous work on the recombinant *P. furiosus* proteasome (27). Due to the preferential degradation, VKM-MCA was used as a comparative basis to track the activities of various assemblies of the recombinant CP complexes.

The effect of subunit composition on kinetic properties was examined for the various recombinant versions of the CP. Table 2 summarizes the kinetic parameters for the 6 different 20S proteasome versions ($AF\alpha+AF\beta$, $AF\alpha+PF\beta_1$, $AF\alpha+PF\beta_2$, $AF\alpha+PF\beta_1+PF\beta_2$,

PFα+PFβ$_1$+PFβ$_2$, & PFα+PFβ$_2$) assembled at 90ºC. Degradation of VKM-MCA by the *P. furiosus* recombinant proteasome (PFα+PFβ$_1$+PFβ$_2$) was fit to a substrate inhibition model, while the other proteasome constructions exhibited standard Michaelis-Menten kinetics. The K_m values of all proteasomes forms on VKM-MCA were in the range of 40-240 μM, which was consistent with results for CPs from *Rhodococcus*, *Mycobacterium,* and *Thermoplasma* species (23, 25, 39, 42). The hybrid proteasome AFα+PFβ$_1$ exhibited the highest K_m (237 μM), while the *P. furiosus* proteasome PFα+PFβ$_1$+PFβ$_2$ was at the low point of the range (45.2 μM). The incorporation of β$_1$ into the active proteasome was accompanied by a decrease in K_m. The catalytic efficiency (k_{cat}/K_m) of all proteasomes tested fell within the range of 12.0-35.0 s^{-1} mM^{-1}, with the highest noted for AFα+PFβ1+PFβ$_2$ at 34.8 s^{-1} mM^{-1}. The catalytic efficiency of AFα+PFβ$_1$+PFβ$_2$, in which β$_1$ and β$_2$ combined in a 1:1 ratio, was consistent with the recombinant *P. furiosus* proteasome, however no substrate inhibition was noted (27). In addition, AFα+PFβ$_1$+PFβ$_2$ exhibited a significantly higher V_{max} at 95°C then the recombinant *P. furiosus* proteasome assembled at 90°C; this may be attributed to the substrate inhibition found for the *P. furiosus* enzyme.

The specific rate of VKM-MCA hydrolysis for temperatures ranging from 50°C to 100°C is shown in Figure 3. The *A. fulgidus* 20S proteasome (AFα+AFβ) and chimeric CPs (AFα+PFβ1 and AFα+PFβ2) exhibited similar temperature optima (~100°C). In contrast, the *P. furiosus* 20S proteasome (PFα+PFβ1+PFβ2) and hybrid CP (AFα+PFβ1+PFβ2) demonstrated optimal temperatures above 100°C.

Thermostability of recombinant *A. fulgidus* CP proteins and hybrid assemblies. Thermostability of the individual recombinant CP proteins was determined by differential

scanning microcalorimetry (DSC). The AFα protein was found to be very thermostable; in phosphate buffer no thermal transitions were noted for scans up to 125°C (data not shown), the upper limit that could be tested by the instrument in use. In the presence of 6M urea, a transition was noted at approximately 120ºC, indicating an extremely high melting point for AFα under standard conditions. The melting temperature for AFβ was 81.0 ºC (see Figure 4a). In the absence of the α subunit, the pro-peptide region of 10 N-terminal residues upstream of the putative active-site Thr within the "TTT" tripeptide in the expressed β protein was retained, as determined by 2D gel electrophoresis (data not shown). The thermostabilizing properties of the N-terminal region, if any, are not known.

The melting curve for AFα+AFβ exhibited a thermal transition at 105°C, as shown in Figure 4b. For the AFα+PFβ1 hybrid form, a transition at 104.5°C was noted, likely corresponding to unincorporated β1 subunit, which also melts at that temperature (27); the transition corresponding to AFα+PFβ_1 was found at 91.0ºC. The *P. furiosus* proteasome (Figure 4C) demonstrated a thermal transition at 112.0ºC, as well as the beginning of another transition at 125ºC, resulting from an additional proteasome sub-type (27). Samples that were twice scanned to 125°C and cooled back to ambient temperatures showed that at least 25% of the initial activity on VKM-MCA remained. To fully denature all forms of the *P. furiosus* proteasome, scans were performed to 125ºC in the presence of 2-6 M Urea. Extrapolating the altered melting points back to the 0 M Urea condition, provided an estimate of 134.0ºC for the high melting form of the *P. furiosus* proteasome.

The thermal inactivation constants for all the proteasome forms tested are shown in Table 2. Due to their relative thermal stabilities, the inactivation constants were necessarily determined at different temperatures. At 90ºC, the k_d for AFα+AFβ (*A. fulgidus* proteasome)

was 0.35 s^{-1}, compared to a k_d of 0.15 s^{-1} for PFα+PFβ_1+PFβ_2 (*P. furiosus* proteasome) at 115º. The hybrid proteasomes AFα+PFβ_1 and AFα+PFβ_2 exhibited inactivation constants, k_d, of 0.26 and 0.37, respectively, at 80ºC. Conversely, AFα+PFβ_1+PFβ_2 yielded a k_d of 1.18 when measured at 100ºC. The recombinant *P. furiosus* proteasome (PF_α+PFβ_1+PFβ_2) was the most stable form, which remained active at a temperature of 115ºC over 12 hours.

DISCUSSION

The catalytic component of the *A. fulgidus* 20S proteasome is formed from a single type of β-protein, as is the case with several other archaeal proteasomes that have been characterized to date (*T. acidophilum* (26)*, M. thermophila* (29)*, M. jannaschii* (11, 12, 44), *Haloferax volcanii* (22)). In comparison, *P. furiosus* encodes two different β proteins, which is less common among the sequenced archaeal genomes but found for *Aeropyrum pernix*, *Haloarcula marimorui*, *Sulfolobus solfataricus*, *Sulfolobus tokodaii*, *Thermococcus kodakarensis*. Unlike the case in eukaryotes, in which some multiple versions of α and β proteins have been observed to have 90% identical protein sequences (13), the *P. furiosus* β proteins are only 48% identity at the amino acid level. As Figure 5 demonstrates, a high level of sequence similarity exists among the hyperthermophilic α proteins. The β protein amino acid sequences are more variable than the α subunits, but universally contain the N-terminal active Thr residue as noted in Figure 6. Furthermore, the identity between the two β proteins in *P. furiosus* is approximately the same as the identity between A. fulgidus β and either of the *P. furiosus* β proteins. As was noted in Table 1, the *A. fulgidus* β protein is 45% and 47% identical to the *P. furiosus* β_1 and β_2 proteins, respectively. In comparison, PFβ_1 is

48% identical to PFβ_2. Thus, we noted that PFβ_1 and PFβ_2 proteins could potentially replace AFβ, at least to some extent, *in vitro*. The differential incorporation of the discrete β proteins in *P. furiosus* have been shown to change the kinetic properties and thermal stability of this archaeon's CP (27).

The *A. fulgidus* α protein formed an active proteasome CP when combined to either *PF*β_1, PFβ_2, or the combination of both PFβ_1 and PFβ_2. Both AFα+PFβ_1 and AFα+PFβ_2 showed overlapping activities against VKM-, AAF-, and LLVY-MCA; however the proteasome with β_1 also degraded the fluorescent peptide AAA-MCA. The two *P. furiosus* β subunits, along with *A. fulgidus* β, contain an active N-terminal Thr residue. By comparison, the yeast proteasome contains three active sites composed of β subunits containing the N-terminal Thr residue (β_1,β_2, and β_3) (18). Five distinct chromogenic substrate preferences have been identified by substitution of the Thr residue and can be attributed to particular active sites within the yeast CP. The β1 site displays peptidy-glutamyl-peptide hydrolysising activity (21). The β2 pocket is associated with tryptic activity; while β5 exhibits chymotryptic degradation in addition to a preference for branched chain and neutral amino acid residues (18, 19, 21). Substitution of the immuno-proteasome subunits results in changes to the β_1 associated substrate pocket, but little alteration is noted in those connected to the β_2 and β_5 sites (10, 15, 40). Our results show that in the *P. furiosus-A. fulgidus* hybrid there is overlapping substrate specificity for CPs composed of either β1 or β2, in addition to a preference for AAA-MCA by AFα+PFβ_1 CP. However, recombinant proteasomes that contain both subunits exhibit a preference for QRR-MCA and FVA-MCA, which cannot be attributed solely to either β_1 or β_2. This indicates that the interaction between PFβ_1 and PFβ_2

is important in substrate selection. Combination of PFα and PFβ_1 did not yield an active enzyme, but extrapolation of the hybrid CP result to the homogenous *P. furiosus* 20S proteasome suggests a modulation proteasome activity occurs by a change in subunit composition. While the yeast proteasome changes cleavage patterns to produce MHC-1-associated peptides, the possible reasons for changes in substrate preference in archaea has yet to be elucidated.

The formation of an active enzyme by AFα+PFβ_1 was significant due to the fact that PFβ_1 does not from an active CP when combined with PFα (27). AFα+PFβ_1 had a similar catalytic efficiency to both recombinant *A. fulgidus* and *P. furiosus* 20S proteasomes (PFα+PFβ_1+PFβ_2 assembled at 90°C), indicating a fully assembled and functioning enzyme. While the recombinant *M. jannaschii* 20S proteasome requires specific protocols for proper assembly (11, 12), correct CP formation *in vitro* for *Thermoplasma acidophilum*, *Haloferax volcanii*, and *Methanosacrcina thermophila* is spontaneous after subunit combination (28, 43, 47). This indicates that the assembly protocol needed for a fully functioning proteasome may vary depending on the individual proteasome being investigated. Furthermore, the ability of PFβ_1 to form an active proteasome with AFα, and not with PFα, suggests that the CP assembly is significantly influenced by the α protein. From this limited sample of simple archaeal proteasomes, the requirement for folding and refolding appears related to the enzymes temperature stability. The *M. jannaschii* proteasome had an optimal temperature of 115°C and needs to be assembled at an elevated temperature to be fully functional (11, 12). In contrast, the *in vitro* assembly of *P. furiosus* CPs results in a fully active enzyme at all temperatures, but displays altered β subunit composition dependent on temperature. Presumably, the hyperthermophilic proteasome subunits are less flexible at lower

temperatures, which may influence their rate of incorporation. This may also be indicative of a tradeoff between thermostability and folding efficiency for large multimeric proteases. In regard to the *P. furiosus* proteasome, the possibility exists that PFα and PFβ$_1$ form an active enzyme when subjected to optimal folding conditions.

When AFα was combined with PFβ$_1$ and AFβ, the result was a preference of AFα to form an active proteasome with PFβ$_1$ (no AFβ appeared in fully assembled enzymes). Formation of AFα + PFβ$_1$ indicates that in some cases the formation of a hybrid proteasome is preferred. Thus, assuming that proteasome proteins from a single organism will preferentially self-assemble is not necessarily the case. Furthermore, the formation of heterologous multi-subunit enzymes may be relevant to other similar enzymes, such as the Clp protease in which subunits demonstrate high conservation.. Formation of chimeric proteasomes may be of particular significance in view of reported efforts showing that archaeal proteasomes expressed in mammalian cells degrade aggregation prone proteins associated with certain neurodegenerative diseases (45). The ability of the archaeal proteasome proteins to form hybrid enzymes with the corresponding eukaryotic version has yet to be investigated. The formation of chimeric proteasome sub-types during the expression of recombinant archaeal proteins in mammalian cells merits further examination. However, the probability of this occurring would be low due to the complex proteasome assembly mechanisms in mammalian cells. Hybrid proteasomes raise the prospect for designing these proteases with preferred characteristics - different substrate preference or thermostability.

ACKNOWLEDGMENTS

This work was supported in part by grants from the NSF Biotechnology Program and the DOE Energy Biosciences Program. JKM acknowledges support from an NIH T32 Biotechnology Traineeship.

REFERENCES

1. **Arendt, C. S., and M. Hochstrasser.** 1997. Identification of the yeast 20S proteasome catalytic centers and subunit interactions required for active-site formation. Proc. Natl. Acad. Sci. U. S. A. **94:**7156-61.

2. **Bai, A. L., and J. Forman.** 1997. The effect of the proteasome inhibitor lactacystin on the presentation of transporter associated with antigen processing (TAP)-dependent and TAP-independent peptide epitopes by class I molecules. J. Immunol. **159:**2139-2146.

3. **Bauer, M. W., S.B. Halio, and R.M. Kelly.** 1997. Purification and characterization of a proteasome from the hyperthermophilic archaeon, *Pyrococcus furiosus*. Appl. Environ. Microbiol. **63:**116-1164.

4. **Bochtler, M., L. Ditzel, M. Groll, C. Hartmann, and R. Huber.** 1999. The proteasome. Annu. Rev. Biophys. Biomol. Struct. **28:**295-317.

5. **Bochtler, M., L. Ditzel, M. Groll, and R. Huber.** 1997. Crystal structure of heat shock locus V (HslV) from *Escherichia coli*. Proc. Natl. Acad. Sci. U. S. A. **94:**6070-4.

6. **De Castro, R. E., J. A. Maupin-Furlow, M. I. Gimenez, M. K. Herrera Seitz, and J. J. Sanchez.** 2006. Haloarchaeal proteases and proteolytic systems. FEMS Microbiol. Rev. **30:**17-35.

7. **Dougan, D. A., A. Mogk, and B. Bukau.** 2002. Protein folding and degradation in bacteria: To degrade or not to degrade? That is the question. Cell. Mol. Life Sci. **59:**1607-1616.

8. **Dougan, D. A., A. Mogk, K. Zeth, K. Turgay, and B. Bukau.** 2002. AAA plus proteins and substrate recognition, it all depends on their partner in crime. FEBS Lett. **529:**6-10.

9. **Driscoll, J., M. G. Brown, D. Finley, and J. J. Monaco.** 1993. MHC-linked LMP gene-products specifically alter peptidase activities of the proteasome. Nature **365:**262-264.

10. **Fehling, H. J., W. Swat, C. Laplace, R. Kuhn, K. Rajewsky, U. Muller, and H. Vonboehmer.** 1994. Mhc Class-I Expression In Mice Lacking The Proteasome Subunit Lmp-7. Science **265:**1234-1237.

11. **Frankenberg, R. J., M. Andersson, and D. S. Clark.** 2003. Effect of temperature and pressure on the proteolytic specificity of the recombinant 20S proteasome from *Methanococcus jannaschii*. Extremophiles **7:**353-60.

12. **Frankenberg, R. J., T. S. Hsu, H. Yakota, R. Kim, and D. S. Clark.** 2001. Chemical denaturation and elevated folding temperatures are required for wild-type activity and stability of recombinant *Methanococcus jannaschii* 20S proteasome. Protein Sci. **10:**1887-96.

13. **Fu, H., J. H. Doelling, C. S. Arendt, M. Hochstrasser, and R. D. Vierstra.** 1998. Molecular organization of the 20S proteasome gene family from *Arabidopsis thaliana*. Genetics **149:**677-92.

14. **Gaczynska, M., K. L. Rock, and A. L. Goldberg.** 1993. Gamma-interferon and expression of MHC genes regulate peptide hydrolysis by proteasomes. Nature **365:**264-267.

15. **Groll, M., M. Bochtler, H. Brandstetter, T. Clausen, and R. Huber.** 2005. Molecular machines for protein degradation. Chembiochem **6:**222-56.

16. **Groll, M., H. Brandstetter, H. Bartunik, G. Bourenkow, and R. Huber.** 2003. Investigations on the maturation and regulation of archaebacterial proteasomes. J. Mol. Biol. **327:**75-83.

17. **Groll, M., and T. Clausen.** 2003. Molecular shredders: how proteasomes fulfill their role. Curr. Opin. Struct. Biol. **13:**665-73.

18. **Groll, M., L. Ditzel, J. Lowe, D. Stock, M. Bochtler, H. D. Bartunik, and R. Huber.** 1997. Structure of 20S proteasome from yeast at 2.4 A resolution. Nature **386:**463-71.

19. **Groll, M., W. Heinemeyer, S. Jager, T. Ullrich, M. Bochtler, D. H. Wolf, and R. Huber.** 1999. The catalytic sites of 20S proteasomes and their role in subunit maturation: A mutational and crystallographic study. Proc. Natl. Acad. Sci. U. S. A. **96:**10976-10983.

20. **Groll, M., and R. Huber.** 2004. Inhibitors of the eukaryotic 20S proteasome core particle: a structural approach. Biochim. Biophys. Acta **1695:**33-44.

21. **Heinemeyer, W., M. Fischer, T. Krimmer, U. Stachon, and D. H. Wolf.** 1997. The active sites of the eukaryotic 20 S proteasome and their involvement in subunit precursor processing. J. Biol. Chem. **272:**25200-9.

22. **Kaczowka, S. J., and J. A. Maupin-Furlow.** 2003. Subunit topology of two 20S proteasomes from *Haloferax volcanii*. J. Bacteriol. **185:**165-74.

23. **Kisselev, A. F., Z. Songyang, and A. L. Goldberg.** 2000. Why does threonine, and not serine, function as the active site nucleophile in proteasomes? J. Biol. Chem. **275:**14831-7.

24. **Koonin, E. V., Y. I. Wolf, and L. Aravind.** 2001. Prediction of the archaeal exosome and its connections with the proteasome and the translation and transcription machineries by a comparative-genomic approach. Genome Res. **11:**240-252.

25. **Lin, G., G. Hu, C. Tsu, Y. Z. Kunes, H. Li, L. Dick, T. Parsons, P. Li, Z. Chen, P. Zwickl, N. Weich, and C. Nathan.** 2006. *Mycobacterium tuberculosis* prcBA genes encode a gated proteasome with broad oligopeptide specificity. Mol. Microbiol. **59:**1405-16.

26. **Lowe, J., D. Stock, B. Jap, P. Zwickl, W. Baumeister, and R. Huber.** 1995. Crystal structure of the 20S proteasome from the archaeon *T. acidophilum* at 3.4 A resolution. Science **268:**533-9.

27. **Madding, L. S., K.R. Shockley, S.B. Conners, K.L. Epting, M.R. Johnson and R.M. Kelly.** 2007. Role of β1 subunit in function and stability of the 20S proteasome from the hyperthermophilic archaeon *Pyrococcus furiosus*. J. Bacteriol. **189:**583-590.

28. **Maupin-Furlow, J. A., H. C. Aldrich, and J. G. Ferry.** 1998. Biochemical characterization of the 20S proteasome from the methanoarchaeon *Methanosarcina thermophila*. J. Bacteriol. **180:**1480-7.

29. **Maupin-Furlow, J. A., and J. G. Ferry.** 1995. A proteasome from the methanogenic archaeon *Methanosarcina thermophila*. J. Biol. Chem. **270:**28617-22.

30. **Maupin-Furlow, J. A., M. A. Gil, M. A. Humbard, P. A. Kirkland, W. Li, C. J. Reuter, and A. J. Wright.** 2005. Archaeal proteasomes and other regulatory proteases. Curr. Opin. Microbiol. **8:**720-8.

31. **Maupin-Furlow, J. A., M. A. Gil, I. M. Karadzic, P. A. Kirkland, and C. J. Reuter.** 2004. Proteasomes: perspectives from the Archaea. Front. Biosci. **9:**1743-58.

32. **Maupin-Furlow, J. A., S. J. Kaczowka, M. S. Ou, and H. L. Wilson.** 2001. Archaeal proteasomes: proteolytic nanocompartments of the cell. Adv. Appl. Microbiol. **50:**279-338.

33. **Maupin-Furlow, J. A., S. J. Kaczowka, C. J. Reuter, K. Zuobi-Hasona, and M. A. Gil.** 2003. Archaeal proteasomes: potential in metabolic engineering. Metab Eng **5:**151-63.

34. **Maupin-Furlow, J. A., H. L. Wilson, S. J. Kaczowka, and M. S. Ou.** 2000. Proteasomes in the archaea: from structure to function. Front. Biosci. **5:**D837-65.

35. **Milligan, S. A., M. W. Owens, and M. B. Grisham.** 1996. Inhibition of I kappa B-alpha and I kappa B-beta proteolysis by calpain inhibitor I blocks nitric oxide synthesis. Arch. Biochem. Biophys. **335:**388-395.

36. **Nagy, I., T. Tamura, J. Vanderleyden, W. Baumeister, and R. De Mot.** 1998. The 20S proteasome of *Streptomyces coelicolor*. J. Bacteriol. **180:**5448-5453.

37. **Reuter, C. J., S. J. Kaczowka, and J. A. Maupin-Furlow.** 2004. Differential regulation of the PanA and PanB proteasome-activating nucleotidase and 20S proteasomal proteins of the haloarchaeon *Haloferax volcanii*. J. Bacteriol. **186:**7763-72.

38. **Reuter, C. J., and J. A. Maupin-Furlow.** 2004. Analysis of proteasome-dependent proteolysis in *Haloferax volcanii* cells, using short-lived green fluorescent proteins. Appl. Environ. Microbiol. **70:**7530-8.

39. **Seemuller, E., A. Lupas, D. Stock, J. Lowe, R. Huber, and W. Baumeister.** 1995. Proteasome from *Thermoplasma acidophilum*: a threonine protease. Science **268:**579-82.

40. **Sibille, C., K. G. Gould, K. Willardgallo, S. Thomson, A. J. Rivett, S. Powis, G. W. Butcher, and P. Debaetselier.** 1995. Lmp2(+) Proteasomes Are Required For The Presentation Of Specific Antigens To Cytotoxic T-Lymphocytes. Curr. Biol. **5:**923-930.

41. **Song, H. K., M. Bochtler, M. K. Azim, C. Hartmann, R. Huber, and R. Ramachandran.** 2003. Isolation and characterization of the prokaryotic proteasome homolog HslVU (ClpQY) from *Thermotoga maritima* and the crystal structure of HslV. Biophys. Chem. **100:**437-52.

42. **Tamura, T., I. Nagy, A. Lupas, F. Lottspeich, Z. Cejka, G. Schoofs, K. Tanaka, R. Demot, and W. Baumeister.** 1995. The first characterization of a eubacterial proteasome - The 20S complex Of *Rhodococcus*. Curr. Biol. **5:**766-774.

43. **Wilson, H. L., H. C. Aldrich, and J. Maupin-Furlow.** 1999. Halophilic 20S proteasomes of the archaeon *Haloferax volcanii*: purification, characterization, and gene sequence analysis. J. Bacteriol. **181:**5814-24.

44. **Wilson, H. L., M. S. Ou, H. C. Aldrich, and J. Maupin-Furlow.** 2000. Biochemical and physical properties of the *Methanococcus jannaschii* 20S

proteasome and PAN, a homolog of the ATPase (Rpt) subunits of the eucaryal 26S proteasome. J. Bacteriol. **182:**1680-92.

45. **Yamada, S. I., J. I. Niwa, S. Ishigaki, M. Takahashi, T. Ito, J. Sone, M. Doyu, and G. Sobue.** 2006. Archaeal proteasomes effectively degrade aggregation-prone proteins and reduce cellular toxicities in mammalian cells. J. Biol. Chem.

46. **Zhou, P. B.** 2005. Targeted protein degradation. Curr. Opin. Chem. Biol. **9:**51-55.

47. **Zwickl, P., F. Lottspeich, and W. Baumeister.** 1992. Expression of functional *Thermoplasma acidophilum* proteasomes in *Escherichia coli*. FEBS Lett. **312:**157-60.

Table I – Comparison of physical characteristics of proteasome component proteins from *P. furiosus* and *A. fulgidus* before and after assembly. Comparison of β sequence identity/similarity was based on amino acid sequence prior to pro-peptide cleavage.

	Pre-Assembly		**Post-Assembly**		**Percent Identity/Similarity**				
	M_r (kDa)	pI	M_r (kDa)	pI	Pfu α	AF α	Pfu ß$_1$	Pfu ß$_2$	AF ß
Pfu α	29.0	4.8	NC	NC		57/78	27/46	26/46	29/53
AF α	27.6	5.2	NC	NC	57/78		29/51	29/48	28/50
Pfu ß$_1$	22.4	7.6	21.2	5.8	27/46	29/51		48/70	45/69
Pfu ß$_2$	21.6	4.9	20.9	4.8	26/46	29/58	48/70		47/67
AF ß	23.4	5.3	22.1	5.3	29/53	28/50	45/69	47/67	

NC ~ No cleavage, the α proteins are not cleaved during assembly of the 20S proteasome.

Table 2 – Biochemical and biophysical properties for *A. fulgidus*, *P. furiosus*, and *A. fulgidus – P. furiosus* hybrid proteasomes.

	AF α+AF β	**AF α+Pfu β_2**	**AF α+Pfu β_1**	**AF α+Pfu β_1+Pfu β_2**	**Pfu α+Pfu β_1+Pfu β_2**	**Pfu α+Pfu β_2**
K_m (μM)	162.0	237.0	74.8	64.9	45.2	88.5
V_m (U/μg)	2324	3632	2125	2766	1159	1383
k_{cat} (s^{-1})	1.95	5.91	1.74	2.26	1.0	1.15
k_{cat}/K_m (s^{-1} mM^{-1})	12.0	24.9	23.3	34.8	22.1	13.0
k_i	0.35	0.27	0.36	1.18	0.15	0.18
$T_{inactivation}$ (ºC)	90.0	80.0	80.0	100.0	115.0	115.0
$T_{optimal}$ (ºC)	~100.0	~100.0	~100.0	>100.0	>100.0	>100.0

Table 3 – Substrate preference (1= highest activity/8=lowest activity) against MCA-linked peptides for the hybrid proteasomes (AFα+PFβ$_1$, AFα+PFβ$_2$, and AFα+PFβ$_1$+PFβ$_2$) as well as recombinantwild-type *P. furiosus* and *A. fulgidus* proteasomes.

	VKM	AAF	LLVY	AAA	QRR	GPLPG	RR	FVA
AFα+PFβ$_1$	1	4	3	2	-	-	-	-
AFα+PFβ$_2$	1	2	3	-	-	-	-	-
AFα+PFβ$_1$+PFβ$_2$	1	3	2	5	6	-	-	4
PFα+PFβ$_1$+PFβ$_2$	1	3	2	ND	ND	-	-	-
AFα+AFβ	1	2	3	4	5	6	7	8

ND-Not Determined

"-" – No Activity Noted

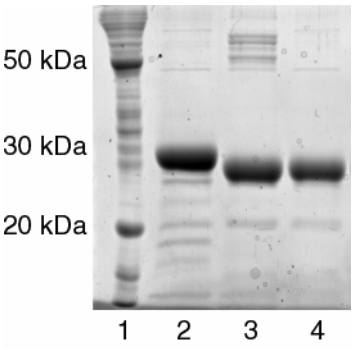

Figure 1 – SDS PAGE (12%) showing the recombinant *A. fulgidus* β protein (AF0481). A Benchmark Ladder is shown in lane 1. The other lanes show AF0481 after HiTrap purification (lane 2), AF0481 after HiTrap purification and Thrombin cleavage (lane 3), and AF0481 after HiTrap purification/Thrombin cleavage/Heat Treatment (lane 4).

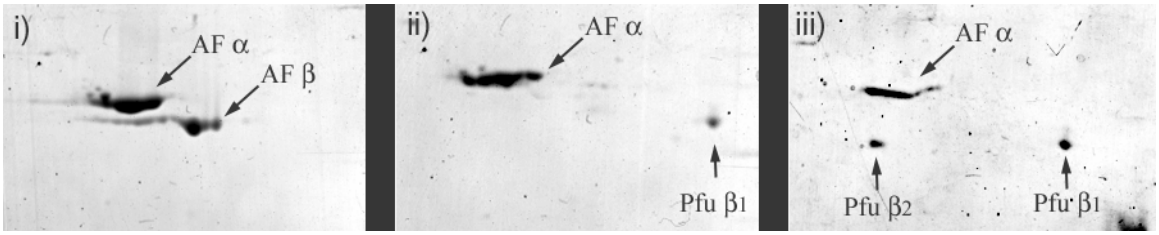

Figure 2 – Composition of recombinant active proteasome assemblies, as determined by 2-dimensional electrophoresis. Shown are (i) the recombinant *A. fulgidus* proteasome AFα + AFβ, and hybrid proteasome (ii) AFα + AFβ + Pfuβ$_1$, and (iii) AFα + Pfuβ$_1$ + Pfuβ$_2$. The ratio of PFβ1 and PFβ2 was 1.0 as determined by the densitometry of the spots, indicating an equal amount of both subunits incorporated into the CP.

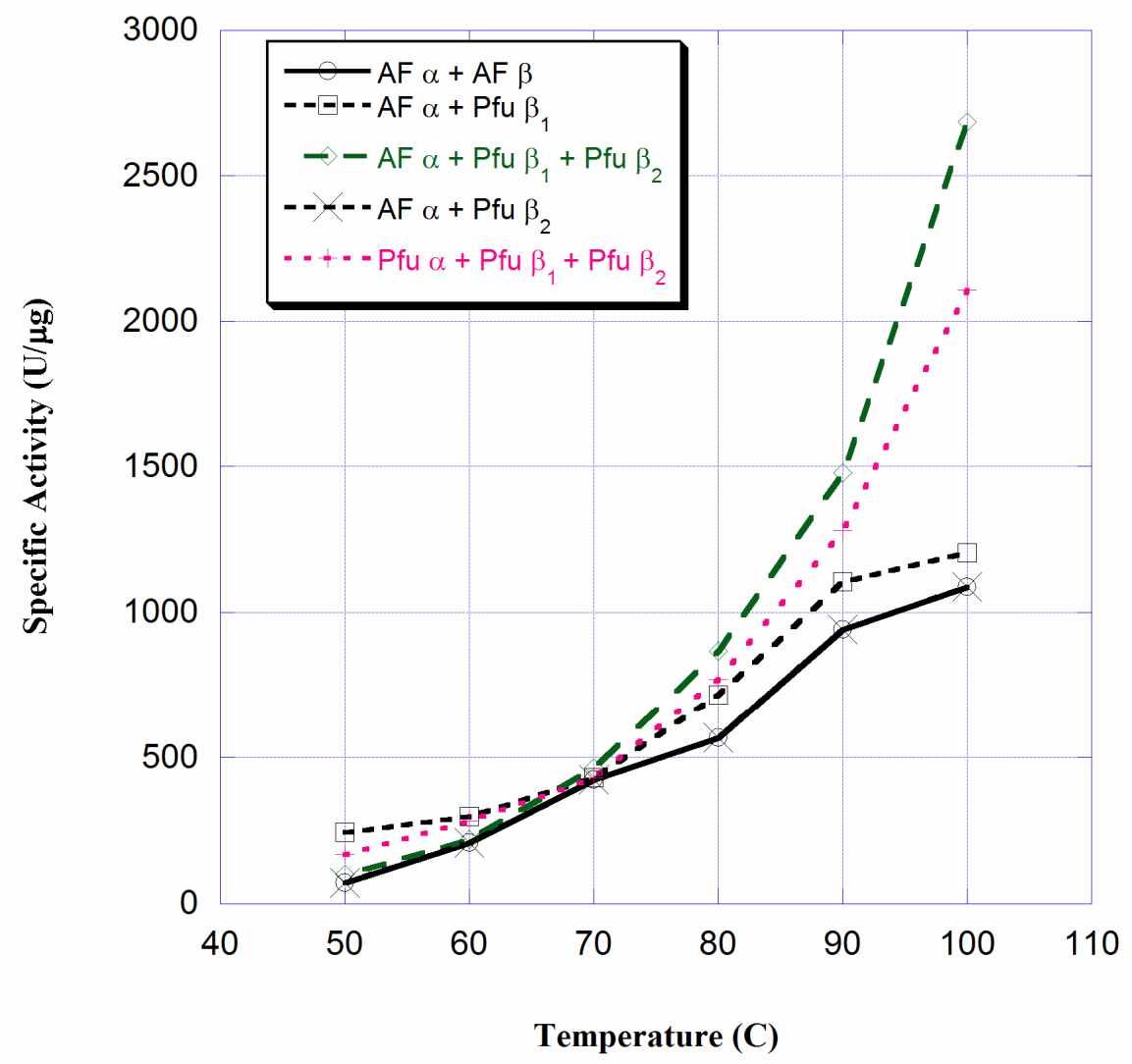

Figure 3 – Thermal activation profiles (50°-100°C), based on hydrolysis of VKM-MCA, for CPs of differing subunit composition. Activity curves for AFα+AFβ (o) and AFα+PFβ$_2$ (x) cross at 70°C; along with AF+PFβ$_1$(□) these hybrid exhibit optimal temperatures of approximately 100°C. CPs based on AFα+PFβ$_1$+PFβ$_2$ and PFα+PFβ$_1$+PFβ$_2$ had optimal temperatures well in excess of 100°C.

Figure 4 – Differential scanning calorimetry (DSC) of *A. fulgidus* 20S CP and individual pro-subunits. **(a)** Melting curve for AFβ protein before cleavage of the pro-peptide region indicates a thermal transition at 82°C. **(b)** AFα + AFβ transition indicated by the arrow at 105°C while the AF α+PF ß$_1$ sample showed two melting transitions of 92°C (b1) and 104°C (b2); the 104°C transition likely is related to unincorporated β1. **(c)** *P. furiosus* proteasome PFα+PFβ$_1$+PFβ$_2$ assembled at 90°C shows two transitions at 104°C (c1) and 112°C (c3), along with the beginning of a third transition (c3) at the limit of the DSC instrument.

a)

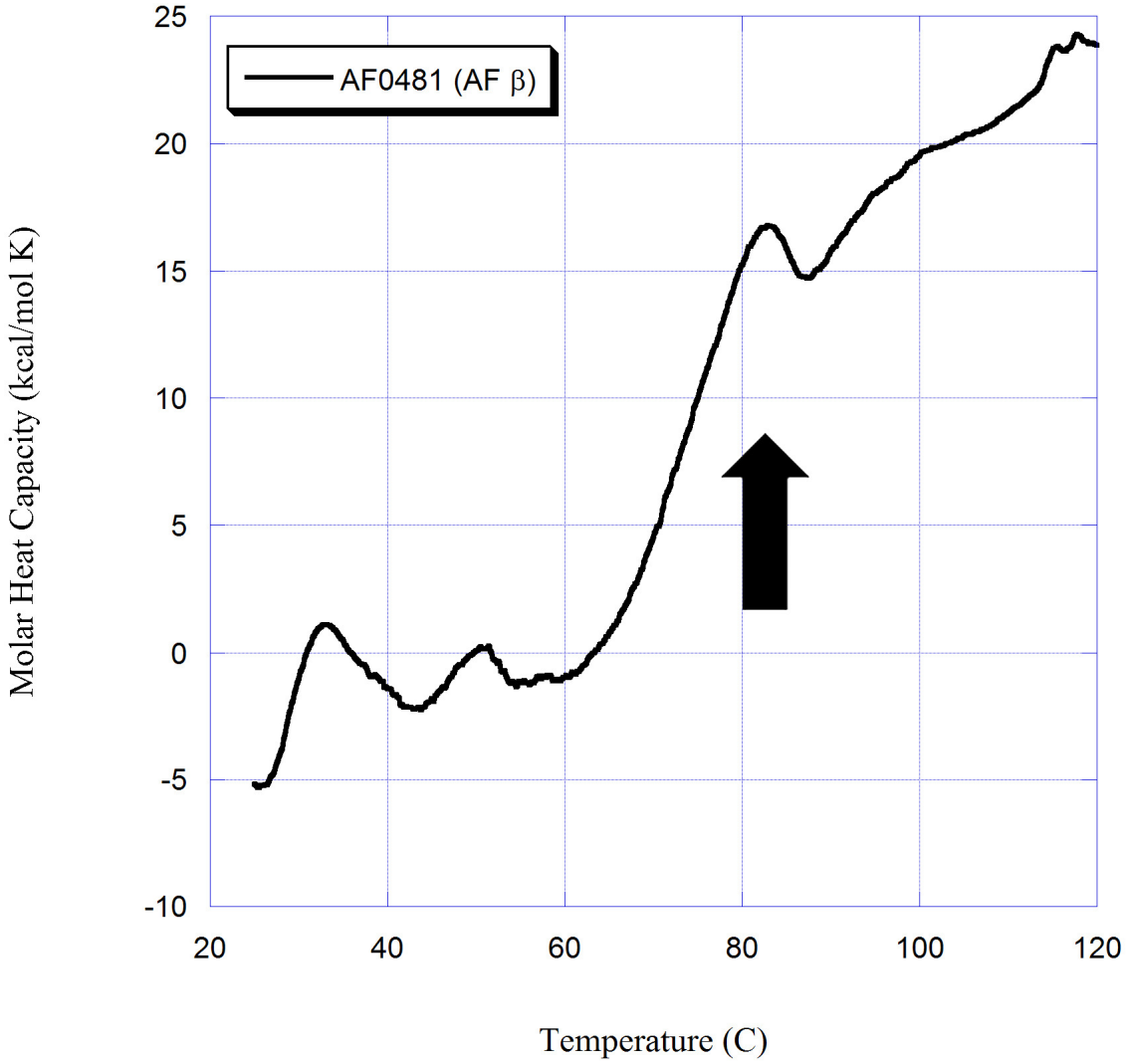
AF0481 (AF β)
Molar Heat Capacity (kcal/mol K)
Temperature (C)
25
20
15
10
5
0
-5
-10
20
40
60
80
100
120

b)

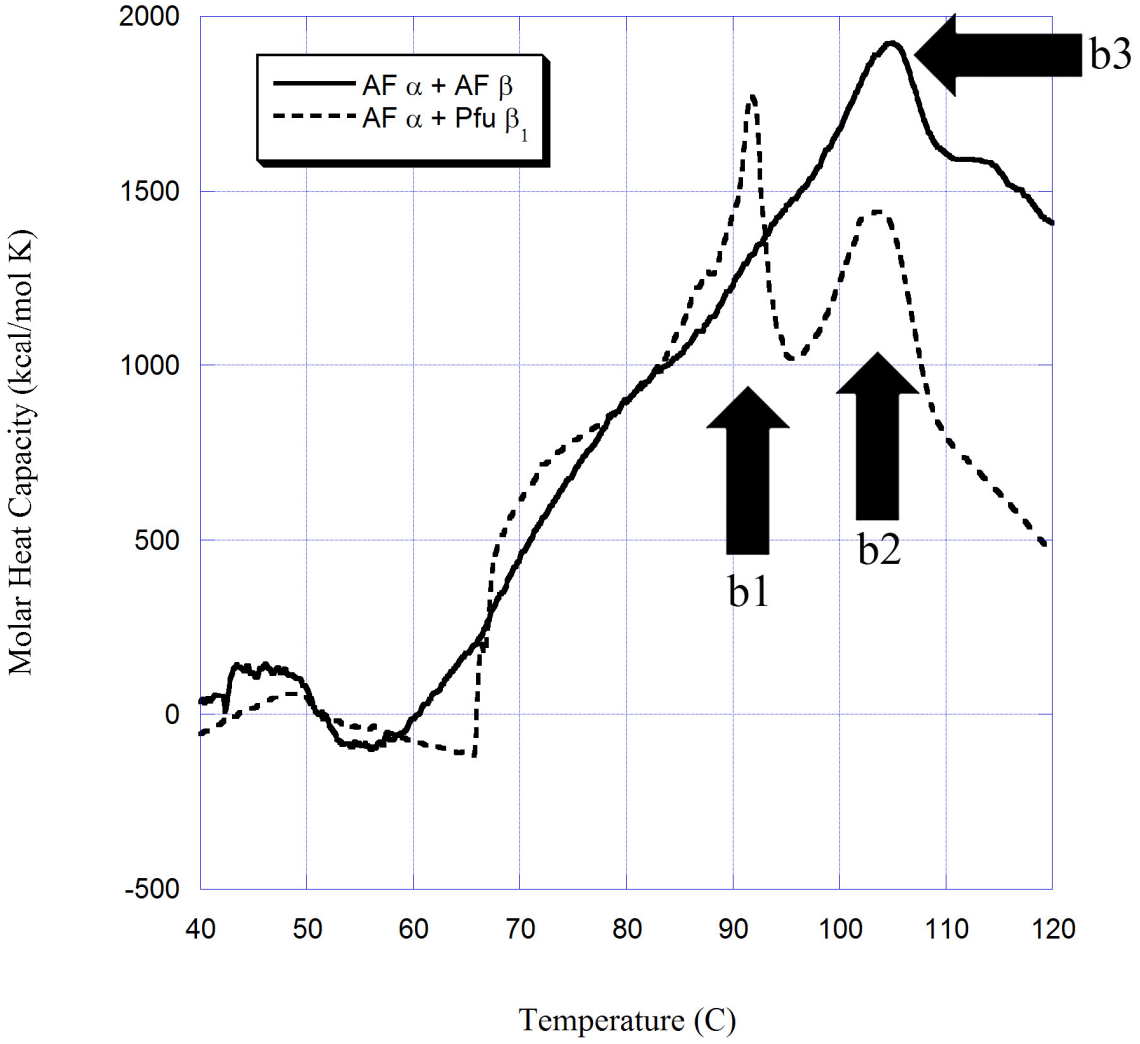
2000
1500
1000
500
0
-500
40
50
60
70
80
90
100
110
120
AF α + AF β
AF α + Pfu β1
b1
b2
b3
Molar Heat Capacity (kcal/mol K)
Temperature (C)

c)

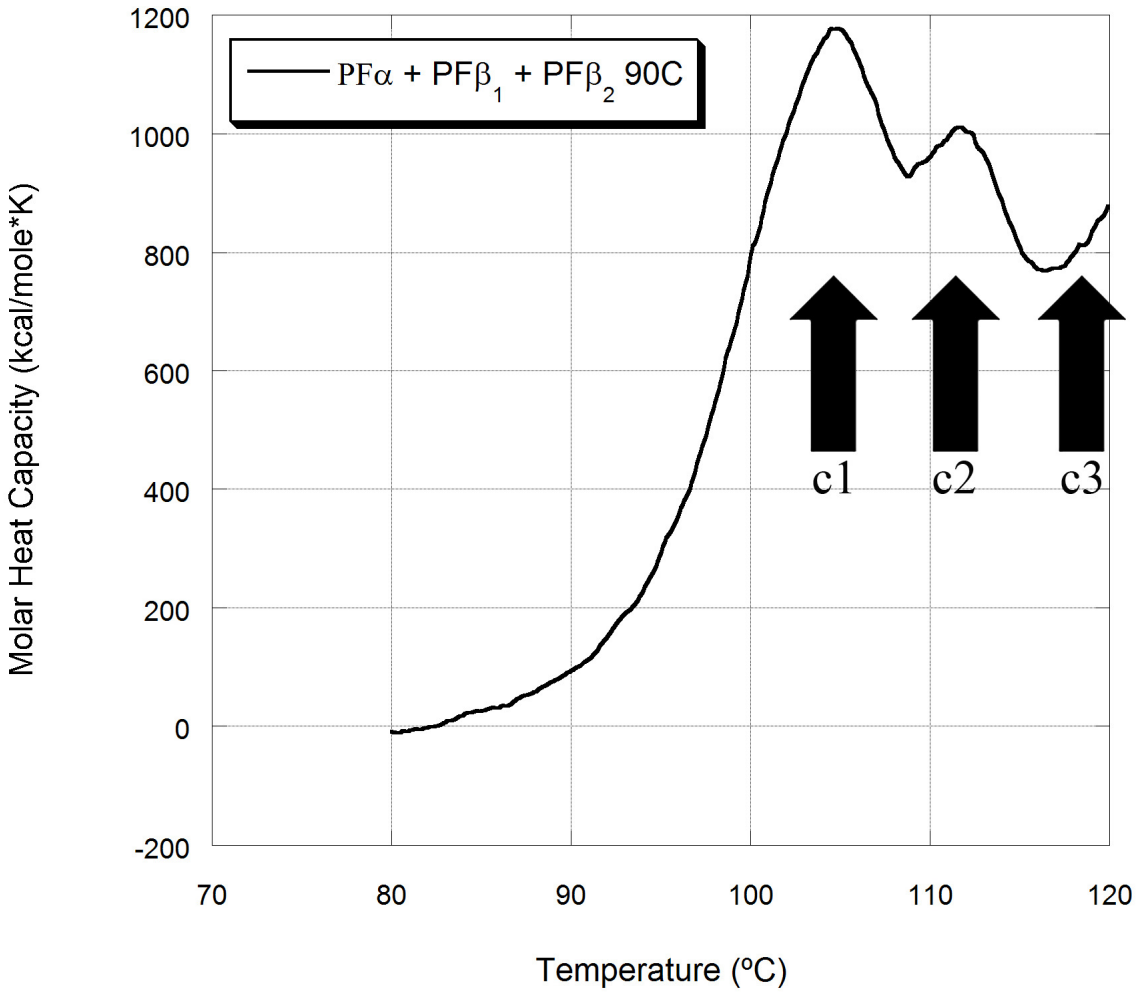
PFα + PFβ1 + PFβ2 90C
Molar Heat Capacity (kcal/mole*K)
1200
1000
800
600
400
200
0
-200
70
80
90
100
110
120
Temperature (ºC)
c1
c2
c3

Figure 5 – Primary sequence alignment (using ClustalW) of proteasome α proteins from *Archaeoglobus fulgidus* (AF0490), *Pyrococcus furiosus* (PF1571), *Methanococcus jannaschii* (MJ0591), *Sulfolobus solfataricus* (SSO0738), and *Thermoplasma acidophilum* (TA1288). Helix 1 and 2 regions are involved in α and β subunit interaction, while helix 3 and 4 are part of α-α association, as determined from the *T. acidophilum* structure.

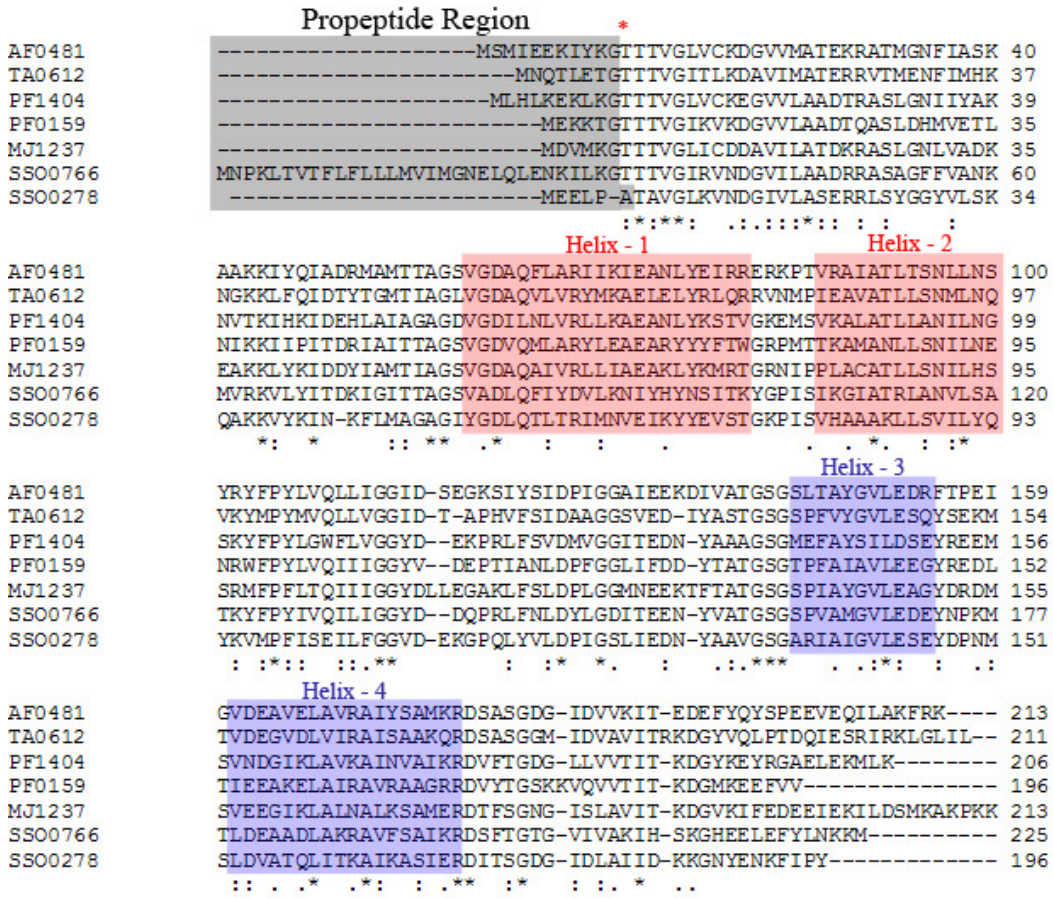

Figure 6 – Primary sequence alignment (ClustalW) of proteasome β proteins from *Archaeoglobus fulgidus* (AF0481), *Pyrococcus furiosus* (PF1404 and PF0159), *Methanococcus jannaschii* (MJ1237), *Sulfolobus solfataricus* (SSO0766 and SSO0278), and *Thermoplasma acidophilum* (TA0612). Helix 1 and 2 regions are involved in α and β subunit interaction, while helix 3 and 4 are part of β-β association, as determined from the *T. acidophilum* structure.

Chapter 5

Transcriptional analysis of the hyperthermophilic bacterium *Thermotoga maritima* in response to extracellular acetate and increased media acidity

Joshua K. Michel, Shannon B. Connors, and Robert M. Kelly

ABSTRACT

The transcriptional response of the hyperthermophilic bacteria *Thermotoga maritima* was analyzed in response to pulse addition and increased extracellular acetate levels as a function of medium pH. During exponential growth, a pulse addition of acetate (final concentration 200 mM) yielded an immediate cessation of growth and down-regulation of a number of metabolic genes. In contrast, growth of *T. maritima* in the presence of an initial acetate concentration of 40 mM at both pH 5.6 and 6.8 resulted in a more diverse transcriptional response. A significant difference in overall transcription levels was noted between the response to acetate at pH 5.6 compared to 6.8, which was expected due to the higher flux of acetate across the cellular membrane under acidic conditions. During growth with acetate at pH 5.6, *T. maritima* showed increased transcription for certain proteolytic genes, including the ClpC ATPase (+1.7-fold) which may be related to the removal of damaged enzymes or degradation of regulatory proteins. However, the molecular chaperone GroEL was down-regulated (-2.0-fold) in the presence of extracellular acetate; GroEL increased (1.7-fold) as a result of decreased pH. The enzymes associated with the fermentative pathway showed a general decrease in transcription, except for phosphate acetyltransferase and phosphoglycerate mutase, which were both slightly up-regulated. This indicated a general strategy of reduced acetate production in response to the presence of extracellular acetate. While the pulse addition of acetate to exponentially growing cells resulted in an immediate transition to stationary-phase, *T. maritima* was able to grow in moderate levels of acetate at both pH 5.6 and 6.8.

INTRODUCTION

Hyperthermophilic organisms have been found to grow in extremely basic and acidic environments, in addition to neutral pH niches (2, 43). Survival within these diverse habitats has required that these organisms develop a myriad of strategies for maintenance of cellular integrity. This feature is not unique to hyperthermophiles. Many microorganisms have the ability to maintain intracellular pH at near neutral levels, even in highly acidic and basic environments (18). For example, some bacteria that grow optimally in media at less then pH 5 exhibit an internal pH between 6.5 and 7.0 (2). The anaerobic thermophilic bacterium *Clostridium thermocellum* has a cytoplasmic pH of 8.5, while the external media was pH 6.8 (3). Additionally, fluctuations in environmental conditions may result in an organisms' exposure to a range of pH levels. In response, cellular organisms modulate ion-transport, carbohydrate utilization, catabolism, and growth rates (4, 6, 24, 34).

Fermentative growth can be based on conversion of carbohydrates to short chain acids (e.g. acetate, formate, lactate), which is coupled with energy production. Under batch conditions the resulting rise in extracellular acid levels causes a decrease in medium pH (42). For example, *C. thermocellum* maintains a membrane pH gradient of 0.6 until the media reaches a pH of 5.0, at which time the ΔpH collapses (26, 41); it has been proposed that gradient maintenance is facilitated by the presence of a Na^+/H^+ anti-porter in this organism (41). In contrast, *Thermoanaerobacter wiegelii* is insensitive to Na^+/H^+ anti-porter inhibitors, suggesting an alternative method for cytoplasmic alkalization, possibly similar to that found in *Clostridium acetobutylicum* (10, 11). In either case, the pH gradiant is kept low in order to avoid the intracellular accumulation of toxic fermentation products.

While a common product of fermentative growth, acetate has been shown to

deleteriously alter cellular function at concentrations as low as 5 g/L (21). The inhibitory effects noted for acetate, and the other weak acids, increase as the environment becomes more acidic (10, 11, 32). The toxicity of acetate is facilitated by the ability of the undissociated acid to diffuse freely across the hydrophobic lipid membrane, where the neutral cytoplasm leads to H^+ release (6). The increase in intracellular ion concentrations leads to a decrease in membrane potential and a reduction of ATP production (31). Additionally, high intracellular concentrations of acetate have been linked to acetyl-CoA accumulation, which is suggested as an indicator of cellular concentration; increased acetyl-CoA concentrations may result in a shift to stationary-phase (44). Furthermore, weak acids have also been linked to alteration of membrane functions as well as inhibitory effects resulting from the charged anions presence (40).

The anaerobic hyperthermophilic bacteria *Thermotoga maritima* utilizes an Embden-Meyerhof ferementative pathway, shown in Figure 1, which converts glucose to hydrogen, CO_2, and acetate (19, 37). Batch growth of *T. maritima* results in an accumulation of extracellular acetate combined with a decreased pH (37). In order to determine the cellular response to increased acetate levels at low pH, we utilized cDNA microarrays to analyze the transcriptional changes resulting from increased initial extracellular acetate levels at pH 5.6 and pH 6.8. Additionally, the transcriptional changes resulting from growth at pH 5.6 and 6.8 were examined in the absence of acetate in the initial growth media. Finally, we analyzed the shock response of *T. maritima* to a pulse addition of sodium acetate during exponential growth.

MATERIALS AND METHODS

Growth of *T. maritima* and pulse addition of acetate. *T. maritima* was cultured anaerobically at 80°C on Sea Salts Medium (SSM), as described previously (30). Maltose (Sigma, St. Louis, MO) was added to SSM (final concentration 5.0 g/L) as a carbon source prior to inoculation and 10 ml of 10% Na_2S was added as a reducing agent. A 30 ml batch culture was used to inoculate 1.5 L of media in a 2.4 L bioreactor (New Brunswick Scientific, Edison, NJ). The glass fermentor was maintained at 80°C by immersion in mixed oil bath and the pH was monitored by an internal pH meter. High purity N_2 was used to reduce the medium and to sparge during inoculation. The culture was grown to mid-log phase (~5.5 hr after inoculation), after which a 400 mL sample was collected to provide a baseline reading. The culture was then brought to an extracellular acetate level of 200 mM by addition of 120 mL of 3 M Sodium Acetate (Sigmas, St. Louis, MO). After 10 minutes another 400 ml sample was collected and immediately put on ice until processed for RNA extraction. During the entire 8 hr run, 1 ml of sample was removed act every hour for cell density determination by epifluorescent microscopy with acridine orange stain (17).

Growth of *T. maritima* in different media with altered pH and/or extracellular acetate concentration. *T. maritima* was cultured anaerobically at 80°C on Sea Salts Medium (SSM), as described above. The pH and extracellular acetate levels were altered as shown in the experimental design in Figure 2. *T. maritima* was grown in SSM Maltose media at pH 5.6 and pH 6.8, both with and without the presence of 40 mM extracellular sodium acetate at the start of growth; a total of 4 batch growth experiments were performed.

A 400 mL sample was harvested during mid-log cell growth during the 4 conditions and RNA extraction proceeded as described below.

Transcriptional analysis of harvested samples by cDNA microarray. A whole genome cDNA microarray including 1928 open reading frames (ORFs) was printed, following protocols described previously (8, 29, 30). RNA was extracted from each 400-ml sample culture, as described previously (8). The 400-ml samples from the fermentor were centrifuged for 20 min (10,000 x g, 4°C). After treatment with RNA lysis buffer, the samples were stored at –70°C. Extractions proceeded with ethanol precipitation and purification using Ambion RNAqueous kits. Concentrations and degree of purity were determined by optical density at 260 nm and 280 nm, as well as by gel electrophoresis (1% agarose gel, 60V). Procedures for reverse transcription reactions, aminoallyl-labeling with Cy3 and Cy5, and hybridization reactions are reported elsewhere (8).

A loop experimental design, shown in Figure 2, incorporated reciprocal labeling of time point samples with both Cy3 and Cy5. Mixed model analysis was used to evaluate differential expression data using approaches presented elsewhere (8). Briefly, least squares estimates of gene-specific treatment effects, corrected for global and gene-specific sources of error, were used to construct pair-wise contrasts analogous to fold changes for each gene between all pairs of conditions. The statistical significance of these fold changes was determined and a Bonferroni correction was used to establish an experiment-wide false positive rate of $\alpha = 0.05$ by dividing α by 2,821, the number of comparisons performed for all genes over all possible treatment pairs. The corrected false positive rate was 1.77×10^{-5} (corresponding to a $-\log_{10}(\text{p-value}) > 4.8$). Least squares estimates of gene-specific

treatment effects were also used to perform hierarchical clustering in JMP 5.0 (SAS Institute, Cary, NC).

RESULTS AND DISCUSSION

Transcriptional response of *T. maritima* to a pulse addition of sodium acetate during the exponential growth phase. Addition of sodium acetate, to a final concentration of 200 mM, resulted in an immediate cessation of growth as shown in Figure 3a. As would be expected, this was accompanied by decreased transcription of a number of genes including those involved in various metabolic functions such as galactokinase and glutamate dehydrogenase. The volcano plot in Figure 3b shows that the highest increases transcription noted was 1.7-fold; this corresponded to an iron-dependent transcriptional repressor (TM0510). Increased transcription of iron-related genes has previously been described during the entry into stationary phase (9). In *Escherichia coli*, the global response to external acetate appears to be the avoidance of internal acetate production as evidenced by the reduced transcription of genes involved in the uptake and degradation of carbohydrates (28). The genes showing a down-regulation of 2-fold or increased transcription above 1.4–fold are listed in Table 1. The increased transcription of the acetate kinase (TM0274) by 1.5-fold appeared to be a specific acetate shock response. The *T. maritima* acetate kinase is a 90 kDa protein comprised of 244 kDa subunits and is responsible for the reversible conversion of acetyl phosphate + ADP to acetate + ATP (5). Mutation studies in *E. coli* have shown that removal of acetate kinase and acetyl phosphotransferase leads to increased levels of acetyl-Co-A, similar to those encountered during growth in the presence of exogenous acetate (22).

It has been suggested that increased acetate conversion to acetyl-CoA may act as an indicator of high cell density, resulting in stationary-phase response (22).

Several genes within the arginine succinyl transferase (Ast) pathway were significantly down-regulated in response to the 200 mM sodium acetate shock. In *E. coli,* the Ast pathway is a five enzyme catabolic system responsible for the primary conversion of arginine into succinate and glutamate, which results in the production of ammonia (36). The AstB/chuR related genes TM1324 and TM1325 were down-regulated 2.5- and 2.0-fold, respectively. Additionally, the associated ABC transporter (TM1327) was down 2.4-fold along with several other genes sequentially located within the same operon (TM1329 and TM1331). The decreased need for arginine breakdown and ammonia production is most likely linked to the rapid decrease in growth rate resulting from acetate stress. In contrast, entry of *E. coli* into stationary phase has been shown to include the up-regulation of *ast* genes (23). These results suggest the exceedingly high acetate concentration of 200 mM moves *T. maritima* into stationary phase, in addition to causing a mild stress response.

Effect of pH and extracellular acetate on the glycolysis and acetate fermentation pathway. The central metabolic by-product of fermentative energy production is acetate, which is typically exported from the cell using active transport mechanisms (37). However, decreased environmental pH coupled with increasing acidic acid levels results in the diffusion of neutral acetate molecules back across the cellular membrane (1). To avoid the deleterious results of this natural process organisms have developed a wide array of strategies to offset or respond to higher intracellular acetate levels. Even during aerobic growth, *E. coli* produces significant amounts of both acetate and formate as the result of fermentation (20).

In response to increased concentrations of short chain acids, *E. coli* induces lactate dehydrogenase A (*ldhA*) which produces lactate in place of acetate and formate, but at a cost of fermentative energy production (22). Alternatively, transcriptional analysis of *E. coli* has shown a trend of reduced transcription of genes involved in the uptake and metabolism of carbohydrates; this may represent a strategy to reduce intraceullar acetate by reducing its production and may be an initial cellular signal to enter stationary phase (28). In response to extracellular acetate at high and low pH, *T. maritima* exhibited a significant transcriptionl response, shown in Figure 4, as opposed during the pulse addition of sodium acetate.

Within the fermentation/glycolysis metabolic pathway only two genes demonstrated a significant transcriptional change when *T. maritima* was grown in media with 40 mM sodium acetate at a pH of 6.8 as shown in Table 2; glyceraldehyde-3-phosphate (TM0688) was down 1.6-fold, while the 4 pyruvate ferredoxin oxidoreductase subunits were up-regulated approximately 1.5-fold. In contrast, when grown at pH 5.6 in the presence of extracellular acetate, fructose-bisphosphate aldolase (TM0273) and glyceraldehyde-3-phosphate (TM0688) showed decreased transcription of 1.6- and 2.0-fold, respectively. Additionally, the acetate kinase (TM0274) was down-regulated 1.9-fold; but phosphate acetyltransferase (TM1130) showed a slight increase in transcription. The differential transcription of these two enzymes might be related to a strategy of reduced acetate production while avoiding acetyl-CoA accumulation. The conversion of acetate to acetyl-CoA has been suggested as a general signal of high cellular-density resulting in stationary-phase response (22). The intermediate formed during conversion of acetate to acetyl-CoA, acetyl-phophate, reduces expression of flagellum and chemotaxis genes in *E. coli* (38). Additionally, a 1.6-fold increased transcription for phosphoglycerate mutase (TM1374) was the same as that reported

for the *Lactobacillus plantarum* homolog during lactic acid stress (27). In contrast to *T. maritima*, the transcriptional analysis of *L. plantarum* suggested a metabolic re-routing during lactic acid stress at lower growth rates (27).

Proteolytic and chaperone response to growth at below optimal pH and increased extracellular acetate. The ATP-dependent protease system Clp demonstrated the highest transcriptional increase in response to an initial sodium acetate concentration of 40 mM. As shown in Figure 5, the proteolytic core (ClpP; TM0695) and ATPase complement (TM0198) also showed the highest transcriptional levels of all *T. maritima* proteases over the conditions tested in this study. In the presence of extracellular acetate at pH 6.8, ClpP showed a 2.0-fold transcriptional increase, but demonstrated no significant response to acetate at pH 5.6. In the presence of 40 mM sodium acetate, the Clp ATPase subunit TM0146 was 1.7-fold and 1.4-fold up-regulated at pH 6.8 and 5.6, respectively. Interestingly, in *Staphylococcus aureus*, the loss of ClpC has been linked to acetate accumulation due to reduced expression/activation of aconitase, which is part of the TCA cycle (7). The Clp ATPase homologs TM0873 and TM1391 showed no response to either altered initial pH or sodium acetate levels. In response to lactic acid stress, *L. plantarum* showed an increased transcription of ClpE by 1.7-fold; ClpE was up-regulated slightly (1.4-fold) during growth at acidic pH (27). Significant transcriptional changes were also noted for the membrane-associated, ATP-dependent protease FtsH (TM0580), which was 1.9-fold up in response to acetate at pH 6.8; when grown at pH 5.6 TM0580 was only 1.5-fold higher in response to the same conditions. This suggests that there may be a membrane specific effect of extracellular acetate due to FtsH involvement in membrane protein degradation. This

work assumed the ion effects from sodium acetate were negligible due to the high salt concentration of the SSM media; but further experimentation would be needed to confirm this hypothesis. A third large multimeric protein (TM0785) was not significantly affected by higher initial acetate conditions at either pH 6.8 nor 5.6. Demonstrating similarity to bacteriocin proteins in both *Brevibacterium linens* and *Mycobacterium tuberculosis*, TM0785 possesses weak proteolytic activity, but the function of this hyperthermophilic bacteriocin homolog has yet to be elucidated (15, 16). The *M. tuberculosis* homolog has been found to accumulate in the membrane where it is gradually released into the extracellular environment, but the activity has yet to be determined (33). The purpose or function of the *T. maritima* protein version during acetate challenge is unclear, but may be related to the slowing of cellular growth.

The serine peptidase, TM0587, showed a 2.8-fold increase for growth at an initial pH of 5.6 compared to the optimal pH, which is 6.8. However, TM0587 responded to initial acetate conditions differently then the ATP-dependent proteases. This serine peptidase was 1.5-fold up on 40 mM acetate at pH 6.8, but showed a -1.8 fold change to acetate at the lower pH condition. Alternatively, the methionine aminopeptidase (TM1478) showed no response to acetate concentration, but was 1.6-fold higher when grown at pH 5.6 compared to pH 6.8. The increased transcription of select proteolytic enzymes during acid and base stress has been well documented (13). Three genes coding for aminopeptidases (TM1048, TM1049, and TM1050) were all up-regulated approximately 1.5 fold in the presence of acetate at both pH 5.6 6.8. These enzymes may play a role in either initial degradation of proteins or the cleavage of smaller products produced by ATP-dependent proteolysis. The increased

occurrence of misfolded and aggregated proteins at acidic pH levels provides the most likely explanation for higher transcription of proteolytic genes.

The chaperone GroEL was up-regulated 1.7-fold at pH 5.6 compared to pH 6.8. However, in the presence of extracellular acetate, GroEL was down-regulated 2.5-fold at pH 5.6. In contrast, there was no significant change of GroEL at pH 6.8 in the presence of higher initial sodium acetate. This is in contrast to previous work showing that in response to acid stress a number of general stress genes are significantly up-regulated (e.g. *groEL, dnaK, dnaJ*) (25, 35, 39); the three *T. maritima* homologs of GroEL, dnaK, and dnaJ were down-regulated in cultures with 40mM initial acetate levels. Furthermore, the up-regulation of GroEL-related genes has been noted as a consistent response to stress inducing conditions (12, 14). This disparity might suggest that *T. maritima* interprets the accumulation of acetate not solely as a stress condition, but as a natural progression into stationary phase.

CONCLUSIONS

T. maritima exhibited the ability to compensate for higher initial sodium acetate concentrations at both the optimal pH, as well as at pH 5.6 (coinciding with late-exponential growth in batch cultures). In contrast, the pulse addition of acetate (200 mM) resulted in an immediate transition to stationary phase and a down-regulation of most genes. However, in response to the lower acetate levels *T. maritima* exhibited decreased transcription of a number of fermentative enzymes in what may be a strategy to reduce acetate production. Most notably, acetate kinase was down-regulated 2-fold in the presence of acetate at low pH. Additionally the Clp ATPase genes are found to play a vital role in the acetate response.

Overall, the response of *T. maritima* to acetate indicates a movement into stationary-phase in conjunction with the down-regulations of a number of carbohydrate utilizing proteins. However, further studies are needed to confirm the acetate specific responses isolated from growth-phase variability arising from the use of batch cultures. Continuous culture would provide a stable platform for growth and thus alleviate many of these inconsistencies.

ACKNOWLEDGMENTS

This work was supported in part by grants from the NSF Biotechnology Program and the DOE Energy Biosciences Program. JKM acknowledges support from an NIH Biotechnology Traineeship.

REFERENCES

1. **Axe, D. D., and J. E. Bailey.** 1995. Transport of Lactate and Acetate through the energized cytoplasmic membrane of *Escherichia coli*. Biotechnol Bioeng **47:**8-19.

2. **Baker-Austin, C., and M. Dopson.** 2007. Life in acid: pH homelostasis in acidophiles. Trends Microbiol **15:**165-171.

3. **Baronofsky, J. J., W. J. A. Schreurs, and E. R. Kashket.** 1984. Uncoupling by acetic acid limits growth of and acetogenesis by *Clostridium thermoaceticum*. Appl Environ Microbiol **48:**1134-1139.

4. **Bearson, S., B. Bearson, and J. W. Foster.** 1997. Acid stress responses in enterobacteria. FEMS Microbiol Lett **147:**173-180.

5. **Bock, A. K., J. Glasemacher, R. Schmidt, and P. Schonheit.** 1999. Purification and characterization of two extremely thermostable enzymes, phosphate acetyltransferase and acetate kinase, from the hyperthermophilic Eubacterium *Thermotoga maritima*. J Bacteriol **181:**1861-1867.

6. **Booth, I. R., P. Cash, and C. O'Byrne.** 2002. Sensing and adapting to acid stress. Antonie Van Leeuwenhoek International Journal Of General And Molecular Microbiology **81:**33-42.

7. **Chatterjee, I., P. Becker, M. Grundmeier, M. Bischoff, G. A. Somerville, G. Peters, B. Sinha, N. Harraghy, R. A. Proctor, and M. Herrmann.** 2005. *Staphylococcus aureus* ClpC Is required for stress resistance, Aconitase activity, growth recovery, and death. J. Bacteriol. **187:**4488-4496.

8. **Chhabra, S. R., K. R. Shockley, S. B. Conners, K. L. Scott, R. D. Wolfinger, and R. M. Kelly.** 2003. Carbohydrate-induced differential gene expression patterns in the hyperthermophilic bacterium *Thermotoga maritima*. J Biol Chem **278:**7540-7552.

9. **Clark, M. E., Q. He, Z. He, K. H. Huang, E. J. Alm, X. F. Wan, T. C. Hazen, A. P. Arkin, J. D. Wall, J. Z. Zhou, and M. W. Fields.** 2006. Temporal Transcriptomic Analysis as *Desulfovibrio vulgaris* Hildenborough Transitions into Stationary Phase during Electron Donor Depletion. Appl. Environ. Microbiol. **72:**5578-5588.

10. **Cook, G. M.** 2000. The intracellular pH of the thermophilic bacterium *Thermoanaerobacter wiegelii* during growth and production of fermentation acids. Extremophiles **4:**279-284.

11. **Cook, G. M., J. B. Russell, A. Reichert, and J. Wiegel.** 1996. The intracellular pH of *Clostridium paradoxum*, an anaerobic, alkaliphilic, and thermophilic bacterium. Appl Environ Microbiol **62:**4576-4579.

12. **Fukuda, D., M. Watanabe, Y. Aso, K. Sonomoto, and A. Ishizaki.** 2002. The groESL operon of the halophilic lactic acid bacterium *Tetragenococcus halophila*. Biosci Biotechnol Biochem **66:**1176-1180.

13. **Groll, M., M. Bochtler, H. Brandstetter, T. Clausen, and R. Huber.** 2005. Molecular machines for protein degradation. Chembiochem **6:**222-256.

14. **Hennequin, C., A. Collignon, and T. Karjalainen.** 2001. Analysis of expression of GroEL (Hsp60) of *Clostridium difficile* in response to stress. Microb Pathog **31:**255-260.

15. **Hicks, P. M., L. S. Chang, and R. M. Kelly.** 2001. Homomultimeric protease and putative bacteriocin homolog from *Thermotoga maritima*, p. 455-460, Hyperthermophilic Enzymes, Pt A, vol. 330.

16. **Hicks, P. M., K. D. Rinker, J. R. Baker, and R. M. Kelly.** 1998. Homomultimeric protease in the hyperthermophilic bacterium *Thermotoga maritima* has structural and amino acid sequence homology to bacteriocins in mesophilic bacteria. FEBS Lett **440:**393-398.

17. **Hobbie, J. E., R. J. Daley, and S. Jasper.** 1977. Use of nuclepore filters for counting bacteria by fluorescence microscopy. Appl Environ Microbiol **33:**1225-1228.

18. **Hornbaek, T., M. Jakobsen, J. Dynesen, and A. K. Nielsen.** 2004. Global transcription profiles and intracellular pH regulation measured in *Bacillus licheniformis* upon external pH upshifts. Arch Microbiol **182:**467-474.

19. **Huber, R., T. A. Langworthy, H. Konig, M. Thomm, C. R. Woese, U. B. Sleytr, and K. O. Stetter.** 1986. *Thermotoga maritima* Sp-Nov represents a new genus of unique extremely thermophilic eubacteria growing up to 90-degrees C. Arch Microbiol **144:**324-333.

20. **Ito, K., and Y. Akiyama.** 2005. Cellular functions, mechanism of action, and regulation of FtsH protease. Annu Rev Microbiol **59:**211.

21. **Jensen, E. B., and S. Carlsen.** 1990. Production of recombinant human growth hormone in *Escherichia coli* - expression of different precursors and physiological effects of glucose, acetate, and salts. Biotechnol Bioeng **36:**1-11.

22. **Kirkpatrick, C., L. M. Maurer, N. E. Oyelakin, Y. N. Yoncheva, R. Maurer, and J. L. Slonczewski.** 2001. Acetate and formate stress: Opposite responses in the proteome of *Escherichia coli*. J Bacteriol **183:**6466-6477.

23. **Kiupakis, A. K., and L. Reitzer.** 2002. ArgR-independent induction and ArgR-dependent superinduction of the ast CADBE operon in *Escherichia coli*. J. Bacteriol. **184:**2940-2950.

24. **Koutsoumanis, K. P., and J. N. Sofos.** 2004. Comparative acid stress response of *Listeria monocytogenes*, *Escherichia coli* O157: H7 and *Salmonella typhimurium* after habituation at different pH conditions. Lett Appl Microbiol **38:**321-326.

25. **Lemos, J. A. C., Y. Y. M. Chen, and R. A. Burne.** 2001. Genetic and physiologic analysis of the groE operon and role of the HrcA repressor in stress gene regulation and acid tolerance in *Streptococcus mutans*. J Bacteriol **183:**6074-6084.

26. **Nochur, S. V., A. L. Demain, and M. F. Roberts.** 1992. Carbohydrate utilization by *Clostridium thermocellum* - Importance of internal pH in regulating growth. Enzyme Microb Technol **14:**338-349.

27. **Pieterse, B., R. J. Leer, F. H. J. Schuren, and M. J. van der Werf.** 2005. Unravelling the multiple effects of lactic acid stress on *Lactobacillus plantarum* by transcription profiling. Microbiol-Sgm **151:**3881-3894.

28. **Polen, T., D. Rittmann, V. F. Wendisch, and H. Sahm.** 2003. DNA Microarray analyses of the long-term adaptive response of *Escherichia coli* to acetate and propionate. Appl Environ Microbiol **69:**1759-1774.

29. **Pysz, M. A., S. B. Conners, C. I. Montero, K. R. Shockley, M. R. Johnson, D. E. Ward, and R. A. Kelly.** 2004. Transcriptional analysis of biofilm formation

processes in the anaerobic, hyperthermophilic bacterium *Thermotoga maritima*. Appl Environ Microbiol **70:**6098-6112.

30. **Pysz, M. A., D. E. Ward, K. R. Shockley, C. I. Montero, S. B. Conners, M. R. Johnson, and R. M. Kelly.** 2004. Transcriptional analysis of dynamic heat-shock response by the hyperthermophilic bacterium *Thermotoga maritima*. Extremophiles **8:**209-17.

31. **Roe, A. J., D. McLaggan, I. Davidson, C. O'Byrne, and I. R. Booth.** 1998. Perturbation of anion balance during inhibition of growth of *Escherichia coli* by weak acids. J Bacteriol **180:**767-772.

32. **Roe, A. J., C. O'Byrne, D. McLaggan, and I. R. Booth.** 2002. Inhibition of *Escherichia coli* growth by acetic acid: a problem with methionine biosynthesis and homocysteine toxicity. Microbiol-Sgm **148:**2215-2222.

33. **Rosenkrands, I., P. B. Rasmussen, M. Carnio, S. Jacobsen, M. Theisen, and P. Andersen.** 1998. Identification and characterization of a 29-kilodalton protein from *Mycobacterium tuberculosis* culture filtrate recognized by mouse memory effector cells. Infect Immun **66:**2728-2735.

34. **Rowbury, R. J.** 2001. Cross-talk involving extracellular sensors and extracellular alarmones gives early warning to unstressed *Escherichia coli* of impending lethal chemical stress and leads to induction of tolerance responses. J Appl Microbiol **90:**677-695.

35. **Salotra, P., D. K. Singh, K. P. Seal, N. Krishna, H. Jaffe, and R. Bhatnagar.** 1995. Expression of DnaK and GroEl homologs in *Leuconostoc esenteroides* in

response to heat-shock, cold shock or chemical stress. FEMS Microbiol Lett **131:**57-62.

36. **Schneider, B. L., A. K. Kiupakis, and L. J. Reitzer.** 1998. Arginine catabolism and the arginine succinyltransferase pathway in *Escherichia coli*. J. Bacteriol. **180:**4278-4286.

37. **Schroder, C., M. Selig, and P. Schonheit.** 1994. Glucose fermentation to acetate, Co_2 and H_2 in the anaerobic hyperthermophilic eubacterium *Thermotoga maritima* - Involvement of the Embden-Meyerhof pathway. Arch Microbiol **161:**460-470.

38. **Shin, S., and C. Park.** 1995. Modulation of flagellar expression in *Escherichia coli* by acetyl phosphate and the osmoregulator OmpR. J Bacteriol **177:**4696-4702.

39. **Spory, A., A. Bosserhoff, C. von Rhein, W. Goebel, and A. Ludwig.** 2002. Differential regulation of multiple proteins of *Escherichia coli* and *Salmonella enterica* serovar typhimurium by the transcriptional regulator SlyA. J Bacteriol **184:**3549-3559.

40. **Stratford, M., and P. A. Anslow.** 1998. Evidence that sorbic acid does not inhibit yeast as a classic 'weak acid preservative'. Lett Appl Microbiol **27:**203-206.

41. **Terracciano, J. S., W. J. A. Schreurs, and E. R. Kashket.** 1987. Membrane H+ conductance of *Clostridium thermoaceticum* and *Clostridium acetobutylicum* - evidence for electrogenic Na+/H+ antiport in *Clostridium thermoaceticum*. Appl Environ Microbiol **53:**782-786.

42. **Wang, F. Q., S. Kashket, and E. R. Kashket.** 2005. Maintenance of Delta pH by a butanol-tolerant mutant of *Clostridium beijerinckii*. Microbiol-Sgm **151:**607-613.

43. **Wiegel, J., and V. V. Kevbrin.** 2004. Alkalithermophiles. Biochem Soc Trans **32:**193-198.

44. **Wolfe, A. J.** 2005. The acetate switch. Microbiol Mol Biol Rev **69:**12-+.

Table 1 – Fold changes for *T. maritima* genes that demonstrated significant up or down regulation in response to the pulse addition of sodium acetate during the mid-log growth phase.

Gene	Predicted Protein Function	Fold-Change
TM0260	Conserved	1.4
TM0846	cytidine deaminase	1.4
TM0019	oxidoreductase	1.4
TM1499	50S ribosomal protein L4	1.4
TM0945	hypothetical protein	1.4
TM1780	argininosuccinate synthase	1.4
TM0332	decarboxylase (putative)	1.4
TM1112	hypothetical protein	1.4
TM0051	iron(II) transport protein B	1.4
TM1425	NADH dehydrogenase I chain F	1.5
TM0254	hypothetical protein	1.5
TM0689	phosphoglycerate kinase	1.5
TM1076	conserved hypothetical protein	1.5
TM0274	acetate kinase	1.5
TM1245	phosphoribosylformylglycinamidine synthase I	1.5
TM1248	phosphoribosylglycinamide formyltransferase	1.6
TM0160	conserved hypothetical protein	1.6
TM0688	glyceraldehyde-3-phosphate dehydrogenase	1.6
TM0510	iron-dependent transcriptional repressor (putative)	1.7
TM0211	Aminomethyltransferase	-2.5
TM0236	MurF (putative)	-2.6
TM0269	homocysteine methyltransferase (putative)	-2.6
TM0319	hypothetical protein	-2.3
TM0426	PHT4-related protein (putative)	-2.6
TM0565	sugar fermentation stimulation protein, putative	-2.2
TM0614	Cell Envelope Protein (putative)	-2.5
TM0621	hypothetical protein	-2.1
TM0972	hypothetical protein	-2.0
TM1015	glutamate dehydrogenase	-2.5
TM1017	conserved hypothetical protein	-2.1
TM1190	galactokinase	-2.3
TM1324	astB/chuR-related protein	-2.5
TM1325	astB/chuR-related protein	-2.0
TM1327	ATP-binding protein	-2.4
TM1329	hypothetical protein	-2.5
TM1331	hypothetical protein	-2.4
TM1341	hypothetical protein	-2.5
TM1359	sensor histidine kinase	-2.1
TM1366	flagellar hook-basal body complex protein	-2.1
TM1402	hypothetical protein	-2.4
TM1683	cold shock protein	-2.2
TM1856	transcriptional regulator, LacI family	-2.1
TM1874	cold shock protein	-2.4

Table 2 –At pH 5.6 and 6.8 the fold changes of metabolic genes resulting from increased extracellular aceatate are shown for *Thermotoga maritima*. Also shown are the resulting fold changes from lower initial media pH.

Gene ID	Enzyme Name	**pH 5.6** 0 vs. 40 mM NaOAc	**pH 6.8** 0 vs. 40 mM NaOAc	**pH 5.6 vs. pH 6.8**
TM1155	Glucose-6-phosphate dehydrogenase	**-1.1**	**-1.3**	**-1.3**
TM1385	Phosphoglucose isomerase	**-1.2**	**1.0**	**1.2**
TM0209	6-phosphofructokinase	**-1.5**	**1.4**	**2.1**
TM0289	6-phosphofructokinase (P-dependent)	**-1.2**	**-1.3**	**1.0**
TM0273	Fructose-bisphosphate aldolase	**-1.6**	**-1.1**	**1.9**
TM0688	Glyceraldehyde-3-phosphate	**-2.0**	**-1.6**	**1.1**
TM0689	Phosphoglycerate kinase	**-1.8**	**-1.4**	**1.1**
TM1374	Phosphoglycerate mutase	**1.6**	**-1.2**	**-1.6**
TM0877	Enolase	**-1.4**	**1.1**	**1.7**
TM0208	Pyruvate kinase	**-1.3**	**1.6**	**1.7**
TM0015	Pyruvate ferredoxin oxidoreductase subunit	**-1.4**	**1.5**	**1.7**
TM0016	Pyruvate ferredoxin oxidoreductase subunit	**-1.3**	**1.6**	**1.7**
TM0017	Pyruvate ferredoxin oxidoreductase subunit	**-1.5**	**1.6**	**1.6**
TM0018	Pyruvate ferredoxin oxidoreductase subunit	**-1.2**	**1.4**	**1.4**
TM1130	Phosphate acetyltransferase	**1.3**	**-1.1**	**-1.3**
TM0274	Acetate kinase	**-1.9**	**-1.3**	**1.7**
TM1867	Lactate dehydrogenase	**-1.2**	**-1.2**	**1.0**

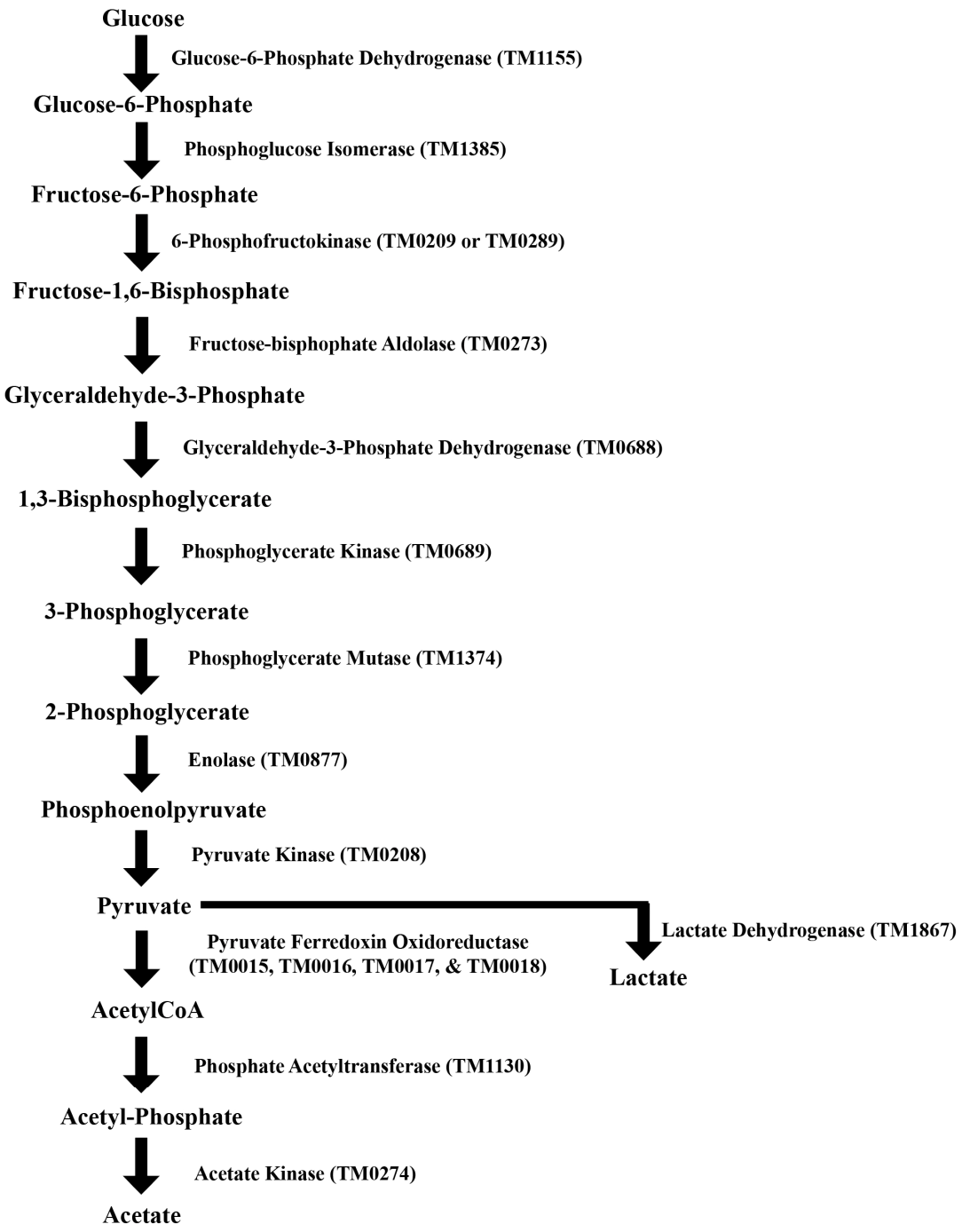

Figure 1 – Pathway for the conversion of glucose to acetate in the hyperthermophilic bacteria *Thermotoga maritima*. The specific enzymes for each reaction are shown along with the corresponding tigr identification numbers.

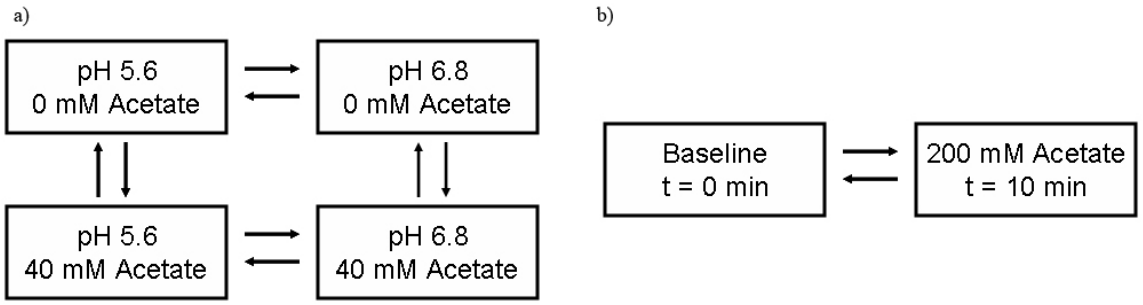

Figure 2 – Loop design for cDNA microarray experiments on *T. maritima* for the conditions: (a) growth in media of pH 6.8 or 5.6 in the presence and absence of a 40 mM sodium acetate initial concentration; (b) effect of pulse addition of sodium acetate (final concentration 200 mM) after 10 minutes during mid-log growth. Each set of arrows represents a single cDNA microarray slide using both Cy-3 and Cy-5 dyes.

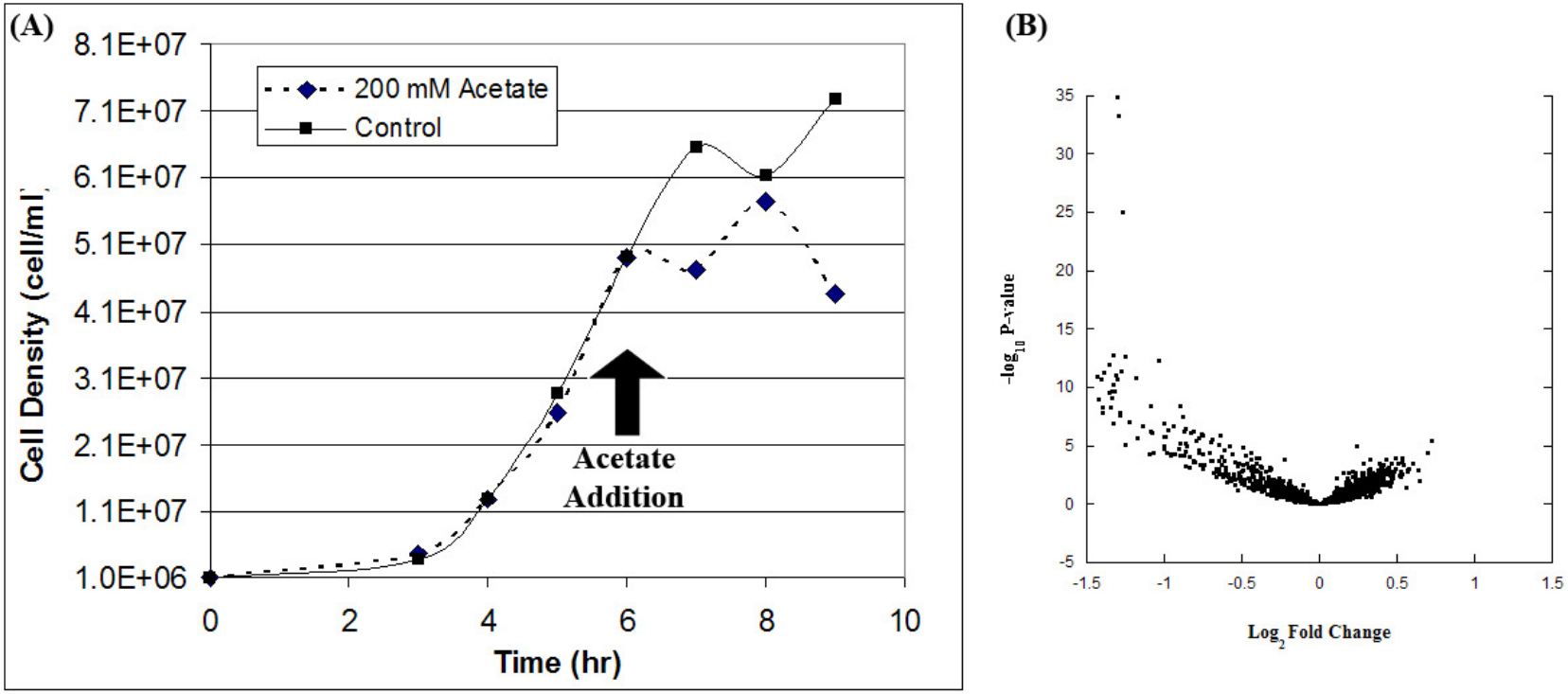

Figure 3 – (a) Growth Curve for *T. maritima* grown on maltose at 80°C and subjected to a pulse addition of acetate to a 200 mM final concentration. (b) Volcano plot of $\log_2$ fold change versus p-value for baseline condition compared to 10 minutes after the pulse addition of sodium acetate.

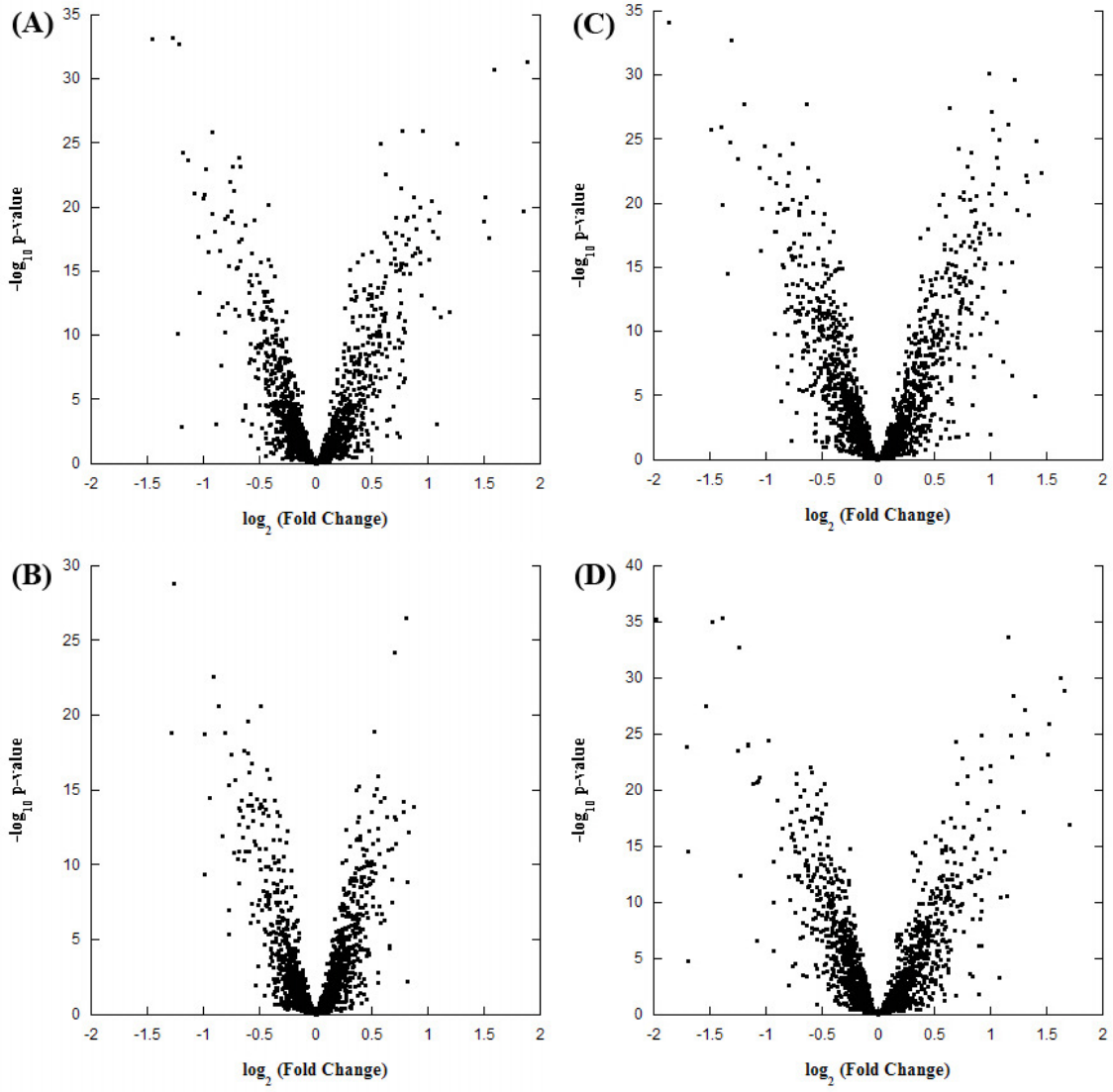

Figure 4 – Volcano plots of fold change versus p-value for (a) pH 5.6/0 mM acetate - pH 6.8/0 mM acetate (b) pH 5.6/40mM acetate – pH 6.8/40mM acetate (c) pH 6.8/0 mM acetate – pH 6.8/40 mM acetate (d) pH 5.6/0 mM acetate – pH 5.6 and 40 mM acetate

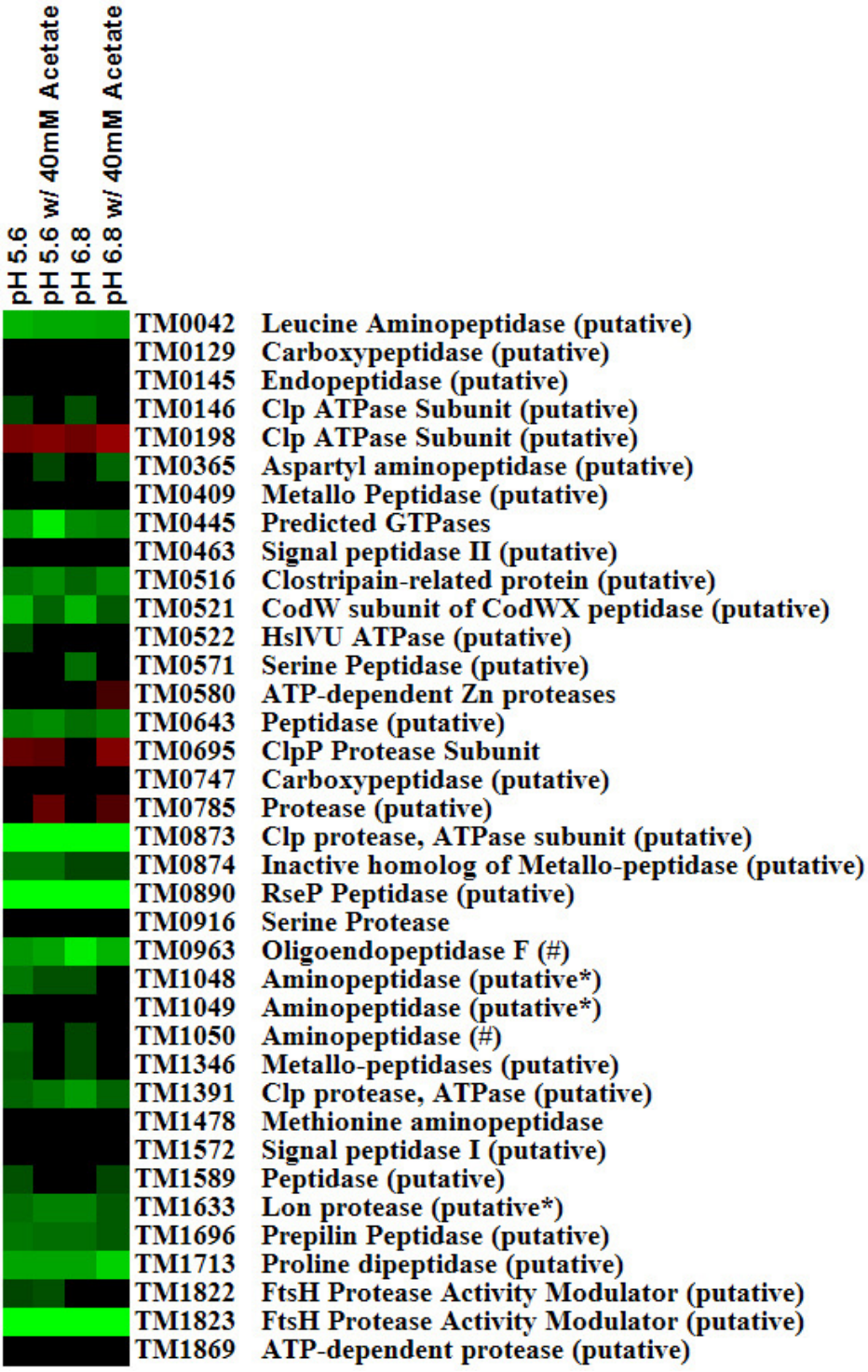

Figure 5 – Heat plot of transcriptional change for proteolytic enzymes in *T. maritima* for growth at pH 5.6 and pH 6.8 in the presence and absence of 40mM extracellular sodium acetate.

Figure 6 – Heat plot of genes showing significant changes during at least one of the four conditions tested. The columns show (1) pH 5.6 / 0 mM acetate (2) pH 5.6 / 40 mM acetate (3) pH 6.8 / 0 mM acetate (4) pH 6.8 / 0 mM acetate

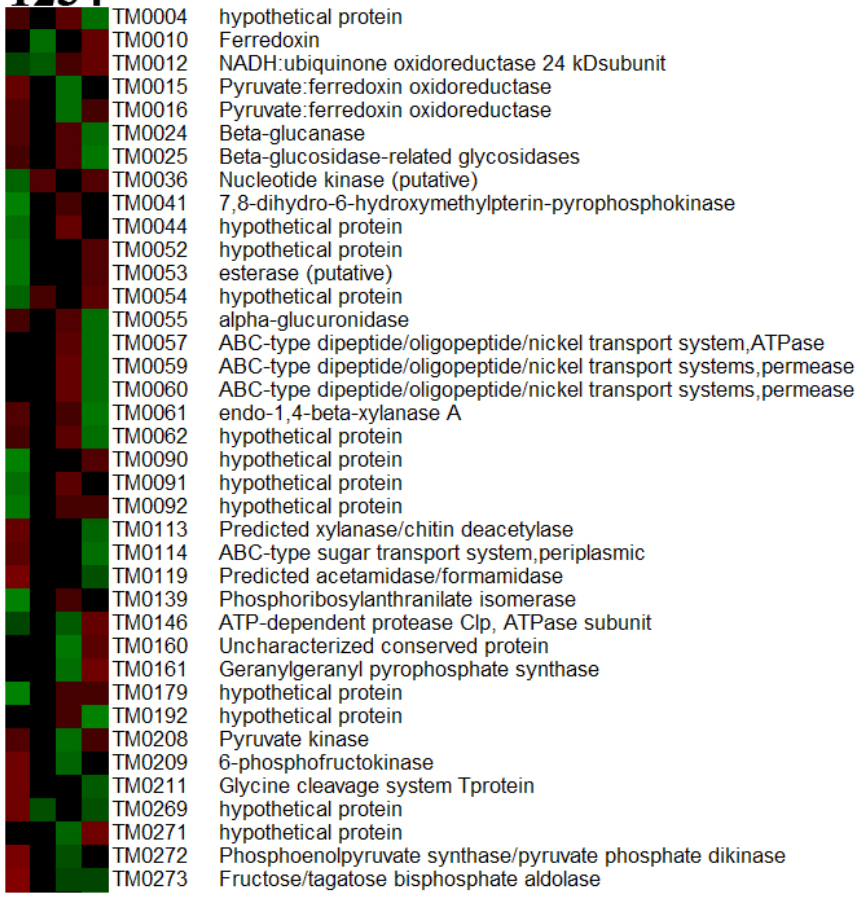
1234
TM0004 hypothetical protein
TM0010 Ferredoxin
TM0012 NADH:ubiquinone oxidoreductase 24 kDsubunit
TM0015 Pyruvate:ferredoxin oxidoreductase
TM0016 Pyruvate:ferredoxin oxidoreductase
TM0024 Beta-glucanase
TM0025 Beta-glucosidase-related glycosidases
TM0036 Nucleotide kinase (putative)
TM0041 7,8-dihydro-6-hydroxymethylpterin-pyrophosphokinase
TM0044 hypothetical protein
TM0052 hypothetical protein
TM0053 esterase (putative)
TM0054 hypothetical protein
TM0055 alpha-glucuronidase
TM0057 ABC-type dipeptide/oligopeptide/nickel transport system,ATPase
TM0059 ABC-type dipeptide/oligopeptide/nickel transport systems,permease
TM0060 ABC-type dipeptide/oligopeptide/nickel transport systems,permease
TM0061 endo-1,4-beta-xylanase A
TM0062 hypothetical protein
TM0090 hypothetical protein
TM0091 hypothetical protein
TM0092 hypothetical protein
TM0113 Predicted xylanase/chitin deacetylase
TM0114 ABC-type sugar transport system,periplasmic
TM0119 Predicted acetamidase/formamidase
TM0139 Phosphoribosylanthranilate isomerase
TM0146 ATP-dependent protease Clp, ATPase subunit
TM0160 Uncharacterized conserved protein
TM0161 Geranylgeranyl pyrophosphate synthase
TM0179 hypothetical protein
TM0192 hypothetical protein
TM0208 Pyruvate kinase
TM0209 6-phosphofructokinase
TM0211 Glycine cleavage system Tprotein
TM0269 hypothetical protein
TM0271 hypothetical protein
TM0272 Phosphoenolpyruvate synthase/pyruvate phosphate dikinase
TM0273 Fructose/tagatose bisphosphate aldolase

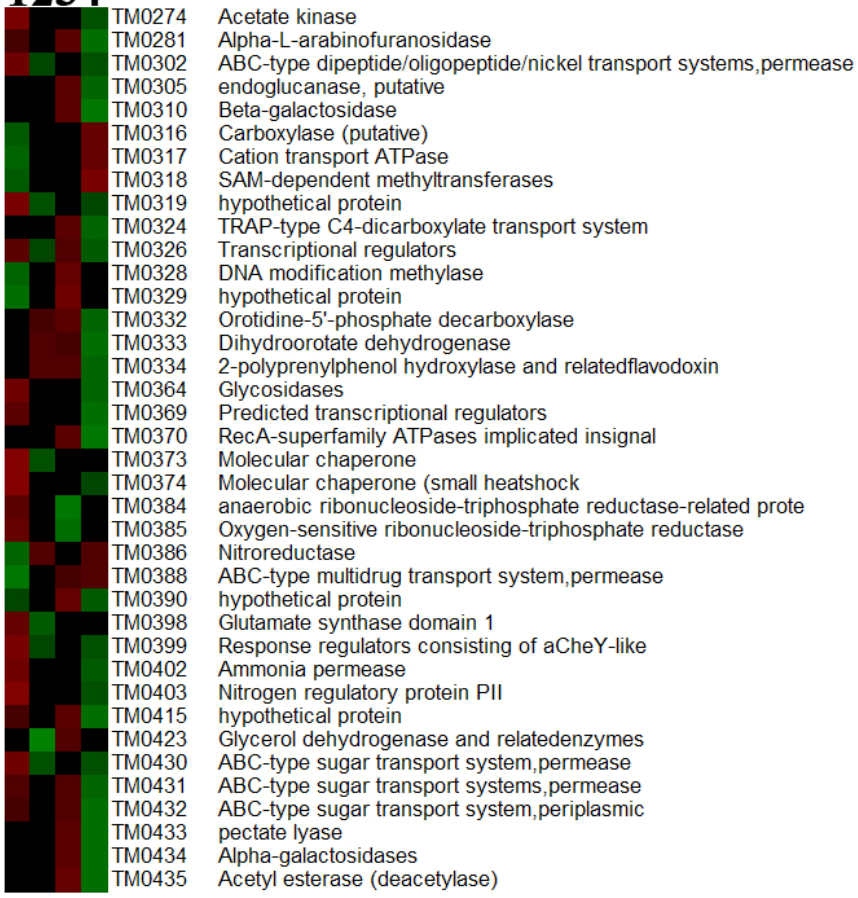
1234
TM0274 Acetate kinase
TM0281 Alpha-L-arabinofuranosidase
TM0302 ABC-type dipeptide/oligopeptide/nickel transport systems,permease
TM0305 endoglucanase, putative
TM0310 Beta-galactosidase
TM0316 Carboxylase (putative)
TM0317 Cation transport ATPase
TM0318 SAM-dependent methyltransferases
TM0319 hypothetical protein
TM0324 TRAP-type C4-dicarboxylate transport system
TM0326 Transcriptional regulators
TM0328 DNA modification methylase
TM0329 hypothetical protein
TM0332 Orotidine-5'-phosphate decarboxylase
TM0333 Dihydroorotate dehydrogenase
TM0334 2-polyprenylphenol hydroxylase and relatedflavodoxin
TM0364 Glycosidases
TM0369 Predicted transcriptional regulators
TM0370 RecA-superfamily ATPases implicated insignal
TM0373 Molecular chaperone
TM0374 Molecular chaperone (small heatshock
TM0384 anaerobic ribonucleoside-triphosphate reductase-related prote
TM0385 Oxygen-sensitive ribonucleoside-triphosphate reductase
TM0386 Nitroreductase
TM0388 ABC-type multidrug transport system,permease
TM0390 hypothetical protein
TM0398 Glutamate synthase domain 1
TM0399 Response regulators consisting of aCheY-like
TM0402 Ammonia permease
TM0403 Nitrogen regulatory protein PII
TM0415 hypothetical protein
TM0423 Glycerol dehydrogenase and relatedenzymes
TM0430 ABC-type sugar transport system,permease
TM0431 ABC-type sugar transport systems,permease
TM0432 ABC-type sugar transport system,periplasmic
TM0433 pectate lyase
TM0434 Alpha-galactosidases
TM0435 Acetyl esterase (deacetylase)

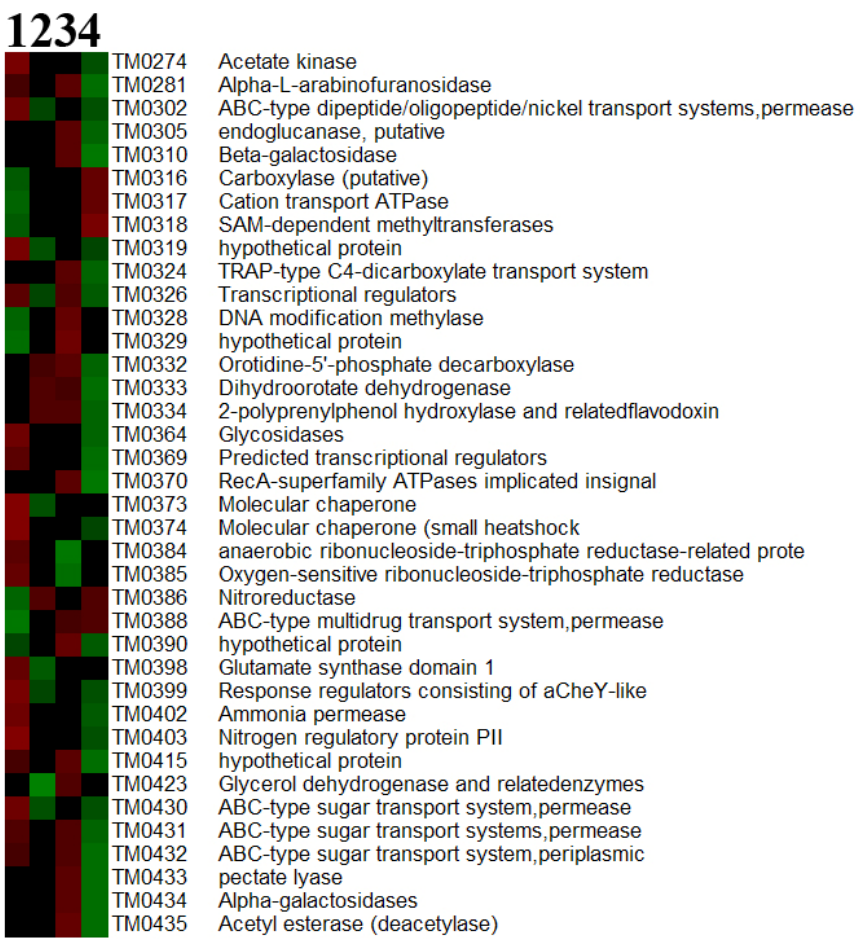
1234
TM0274 Acetate kinase
TM0281 Alpha-L-arabinofuranosidase
TM0302 ABC-type dipeptide/oligopeptide/nickel transport systems,permease
TM0305 endoglucanase, putative
TM0310 Beta-galactosidase
TM0316 Carboxylase (putative)
TM0317 Cation transport ATPase
TM0318 SAM-dependent methyltransferases
TM0319 hypothetical protein
TM0324 TRAP-type C4-dicarboxylate transport system
TM0326 Transcriptional regulators
TM0328 DNA modification methylase
TM0329 hypothetical protein
TM0332 Orotidine-5'-phosphate decarboxylase
TM0333 Dihydroorotate dehydrogenase
TM0334 2-polyprenylphenol hydroxylase and relatedflavodoxin
TM0364 Glycosidases
TM0369 Predicted transcriptional regulators
TM0370 RecA-superfamily ATPases implicated insignal
TM0373 Molecular chaperone
TM0374 Molecular chaperone (small heatshock
TM0384 anaerobic ribonucleoside-triphosphate reductase-related prote
TM0385 Oxygen-sensitive ribonucleoside-triphosphate reductase
TM0386 Nitroreductase
TM0388 ABC-type multidrug transport system,permease
TM0390 hypothetical protein
TM0398 Glutamate synthase domain 1
TM0399 Response regulators consisting of aCheY-like
TM0402 Ammonia permease
TM0403 Nitrogen regulatory protein PII
TM0415 hypothetical protein
TM0423 Glycerol dehydrogenase and relatedenzymes
TM0430 ABC-type sugar transport system,permease
TM0431 ABC-type sugar transport systems,permease
TM0432 ABC-type sugar transport system,periplasmic
TM0433 pectate lyase
TM0434 Alpha-galactosidases
TM0435 Acetyl esterase (deacetylase)

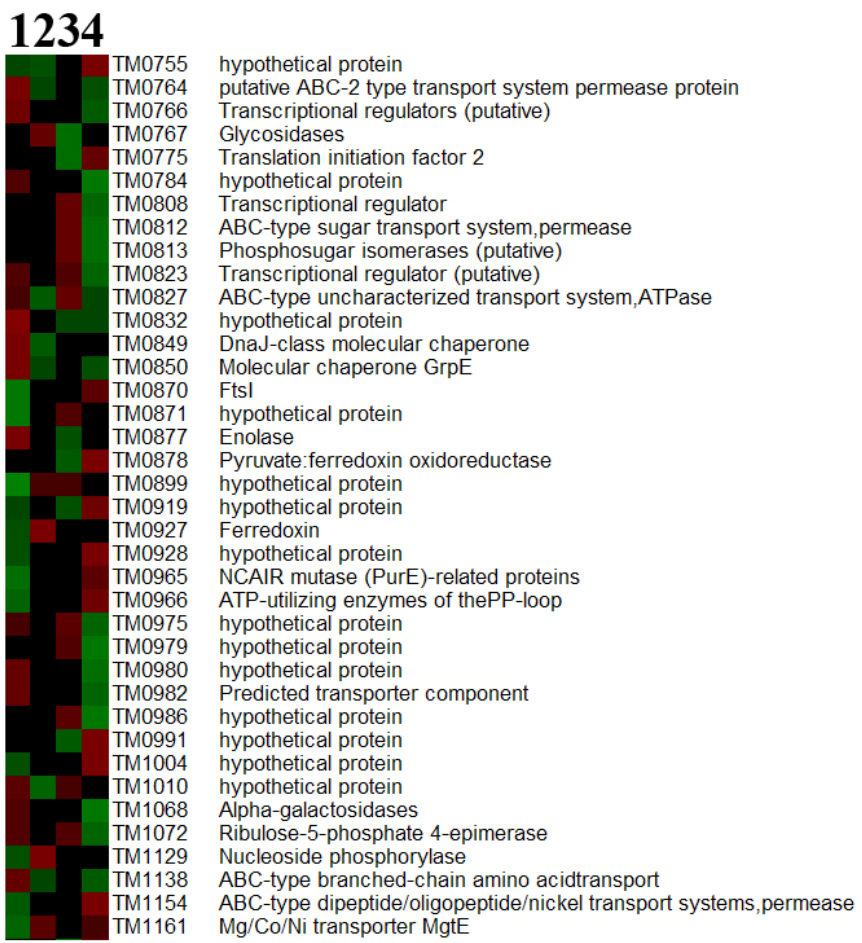
1234
TM0755 hypothetical protein
TM0764 putative ABC-2 type transport system permease protein
TM0766 Transcriptional regulators (putative)
TM0767 Glycosidases
TM0775 Translation initiation factor 2
TM0784 hypothetical protein
TM0808 Transcriptional regulator
TM0812 ABC-type sugar transport system,permease
TM0813 Phosphosugar isomerases (putative)
TM0823 Transcriptional regulator (putative)
TM0827 ABC-type uncharacterized transport system,ATPase
TM0832 hypothetical protein
TM0849 DnaJ-class molecular chaperone
TM0850 Molecular chaperone GrpE
TM0870 FtsI
TM0871 hypothetical protein
TM0877 Enolase
TM0878 Pyruvate:ferredoxin oxidoreductase
TM0899 hypothetical protein
TM0919 hypothetical protein
TM0927 Ferredoxin
TM0928 hypothetical protein
TM0965 NCAIR mutase (PurE)-related proteins
TM0966 ATP-utilizing enzymes of thePP-loop
TM0975 hypothetical protein
TM0979 hypothetical protein
TM0980 hypothetical protein
TM0982 Predicted transporter component
TM0986 hypothetical protein
TM0991 hypothetical protein
TM1004 hypothetical protein
TM1010 hypothetical protein
TM1068 Alpha-galactosidases
TM1072 Ribulose-5-phosphate 4-epimerase
TM1129 Nucleoside phosphorylase
TM1138 ABC-type branched-chain amino acidtransport
TM1154 ABC-type dipeptide/oligopeptide/nickel transport systems,permease
TM1161 Mg/Co/Ni transporter MgtE

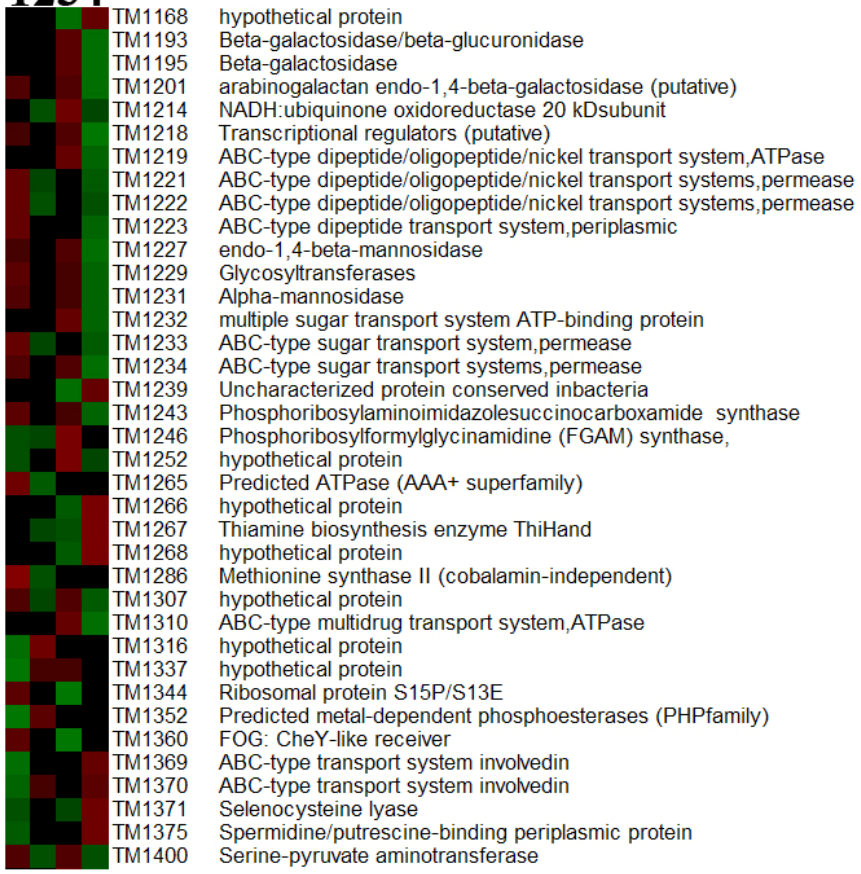
1234
TM1168 hypothetical protein
TM1193 Beta-galactosidase/beta-glucuronidase
TM1195 Beta-galactosidase
TM1201 arabinogalactan endo-1,4-beta-galactosidase (putative)
TM1214 NADH:ubiquinone oxidoreductase 20 kDsubunit
TM1218 Transcriptional regulators (putative)
TM1219 ABC-type dipeptide/oligopeptide/nickel transport system,ATPase
TM1221 ABC-type dipeptide/oligopeptide/nickel transport systems,permease
TM1222 ABC-type dipeptide/oligopeptide/nickel transport systems,permease
TM1223 ABC-type dipeptide transport system,periplasmic
TM1227 endo-1,4-beta-mannosidase
TM1229 Glycosyltransferases
TM1231 Alpha-mannosidase
TM1232 multiple sugar transport system ATP-binding protein
TM1233 ABC-type sugar transport system,permease
TM1234 ABC-type sugar transport systems,permease
TM1239 Uncharacterized protein conserved inbacteria
TM1243 Phosphoribosylaminoimidazolesuccinocarboxamide synthase
TM1246 Phosphoribosylformylglycinamidine (FGAM) synthase,
TM1252 hypothetical protein
TM1265 Predicted ATPase (AAA+ superfamily)
TM1266 hypothetical protein
TM1267 Thiamine biosynthesis enzyme ThiHand
TM1268 hypothetical protein
TM1286 Methionine synthase II (cobalamin-independent)
TM1307 hypothetical protein
TM1310 ABC-type multidrug transport system,ATPase
TM1316 hypothetical protein
TM1337 hypothetical protein
TM1344 Ribosomal protein S15P/S13E
TM1352 Predicted metal-dependent phosphoesterases (PHPfamily)
TM1360 FOG: CheY-like receiver
TM1369 ABC-type transport system involvedin
TM1370 ABC-type transport system involvedin
TM1371 Selenocysteine lyase
TM1375 Spermidine/putrescine-binding periplasmic protein
TM1400 Serine-pyruvate aminotransferase

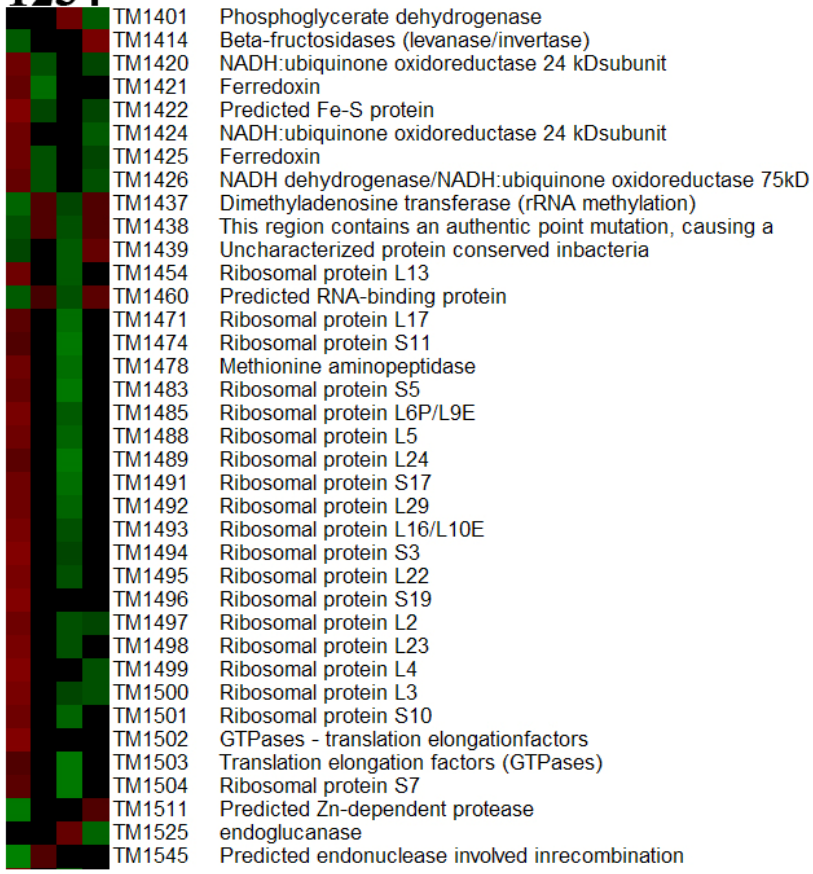
1234
TM1401 Phosphoglycerate dehydrogenase
TM1414 Beta-fructosidases (levanase/invertase)
TM1420 NADH:ubiquinone oxidoreductase 24 kDsubunit
TM1421 Ferredoxin
TM1422 Predicted Fe-S protein
TM1424 NADH:ubiquinone oxidoreductase 24 kDsubunit
TM1425 Ferredoxin
TM1426 NADH dehydrogenase/NADH:ubiquinone oxidoreductase 75kD
TM1437 Dimethyladenosine transferase (rRNA methylation)
TM1438 This region contains an authentic point mutation, causing a
TM1439 Uncharacterized protein conserved inbacteria
TM1454 Ribosomal protein L13
TM1460 Predicted RNA-binding protein
TM1471 Ribosomal protein L17
TM1474 Ribosomal protein S11
TM1478 Methionine aminopeptidase
TM1483 Ribosomal protein S5
TM1485 Ribosomal protein L6P/L9E
TM1488 Ribosomal protein L5
TM1489 Ribosomal protein L24
TM1491 Ribosomal protein S17
TM1492 Ribosomal protein L29
TM1493 Ribosomal protein L16/L10E
TM1494 Ribosomal protein S3
TM1495 Ribosomal protein L22
TM1496 Ribosomal protein S19
TM1497 Ribosomal protein L2
TM1498 Ribosomal protein L23
TM1499 Ribosomal protein L4
TM1500 Ribosomal protein L3
TM1501 Ribosomal protein S10
TM1502 GTPases - translation elongationfactors
TM1503 Translation elongation factors (GTPases)
TM1504 Ribosomal protein S7
TM1511 Predicted Zn-dependent protease
TM1525 endoglucanase
TM1545 Predicted endonuclease involved inrecombination

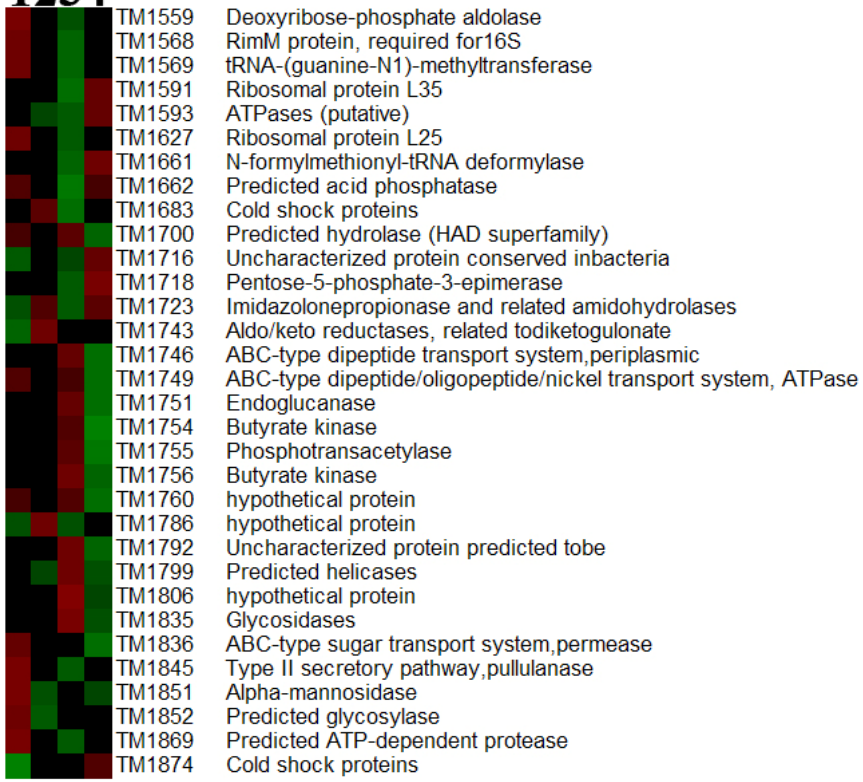
1234
TM1559 Deoxyribose-phosphate aldolase
TM1568 RimM protein, required for16S
TM1569 tRNA-(guanine-N1)-methyltransferase
TM1591 Ribosomal protein L35
TM1593 ATPases (putative)
TM1627 Ribosomal protein L25
TM1661 N-formylmethionyl-tRNA deformylase
TM1662 Predicted acid phosphatase
TM1683 Cold shock proteins
TM1700 Predicted hydrolase (HAD superfamily)
TM1716 Uncharacterized protein conserved inbacteria
TM1718 Pentose-5-phosphate-3-epimerase
TM1723 Imidazolonepropionase and related amidohydrolases
TM1743 Aldo/keto reductases, related todiketogulonate
TM1746 ABC-type dipeptide transport system,periplasmic
TM1749 ABC-type dipeptide/oligopeptide/nickel transport system, ATPase
TM1751 Endoglucanase
TM1754 Butyrate kinase
TM1755 Phosphotransacetylase
TM1756 Butyrate kinase
TM1760 hypothetical protein
TM1786 hypothetical protein
TM1792 Uncharacterized protein predicted tobe
TM1799 Predicted helicases
TM1806 hypothetical protein
TM1835 Glycosidases
TM1836 ABC-type sugar transport system,permease
TM1845 Type II secretory pathway,pullulanase
TM1851 Alpha-mannosidase
TM1852 Predicted glycosylase
TM1869 Predicted ATP-dependent protease
TM1874 Cold shock proteins